CHEMISTRY
A European Journal

Supporting Information

Modulation of the Physicochemical Properties of Donor–Spiro–Acceptor Derivatives through Donor Unit Planarisation: Phenylacridine versus Indoloacridine. New Hosts for Green and Blue Phosphorescent Organic Light-Emitting Diodes (PhOLEDs)

Sébastien Thiery,[a] Denis Tondelier,[c] Bernard Geffroy,[b, c] Olivier Jeannin,[a] Joëlle Rault-Berthelot,*[a] and Cyril Poriel*[a]

chem_201600652_sm_miscellaneous_information.pdf

Table of content

MATERIAL AND METHODS

All manipulations of oxygen- and moisture-sensitive materials were conducted with a standard Schlenk technique. Commercially available reagents and solvents were used without further purification other than those detailed below. THF was distilled from sodium/benzophenone prior to use. Light petroleum refers to the fraction with bp 40-60°C. 2.5M solutions of n-BuLi in hexanes or THF were purchased from Sigma Aldrich. 2,2'-dibromobiphenyl was purchased from Fluorochem. Reactions were stirred magnetically, unless otherwise indicated. Analytical thin layer chromatography was carried out using aluminum backed plates coated with Merck Kieselgel 60 GF254 and visualized under UV light (at 254 and 360 nm). Chromatography was carried out using Teledyne Isco CombiFlash® Rf 400 (UV detection 200-360nm), over standard silica cartridges (Redisep® Isco, GraceResolv™ Grace or Puriflash® columns Interchim). ^{1}H and ^{13}C NMR spectra were recorded using Bruker 300 MHz instruments (^{1}H frequency, corresponding ^{13}C frequency: 75 MHz); chemical shifts were recorded in ppm and J values in Hz. In the ^{13}C NMR spectra, signals corresponding to C, CH, CH_2 or Me groups, assigned from DEPT, are noted. The residual signals for the NMR solvents are: $CDCl_3$; 7.26 ppm for the proton and 77.00 ppm for the carbon, CD_2Cl_2; 5.32 ppm for the proton and 53.80 ppm for the carbon. The following abbreviations have been used for the NMR assignment: s for singlet, d for doublet, t for triplet and m for multiplet. High resolution mass spectra were recorded at the Centre Régional de Mesures Physiques de l'Ouest (Rennes) on (i) Bruker MicrO-Tof-Q II (Source: Atmospheric Pressure Chemical Ionization (APCI - direct introduction) (ASAP–Atmospheric Solids Analysis Probe) at a temperature of 30°C - positive mode) or on (ii) Waters Q-Tof II.

X-Ray :

Crystal was picked up with a cryoloop and then frozen at 150 K under a stream of dry N_2 on a APEX II Brucker AXS diffractometer for X-ray data collection (Mo Kα radiation, λ = 0.71073 Å).

The structures were solved by direct methods using the SIR97 program,[1] and then refined with full-matrix least-square methods based on F2 (SHELXL-97) with the aid of the WINGX[2] program. All non-

hydrogen atoms were refined with anisotropic atomic displacement parameters. H atoms were finally included in their calculated positions. Crystallographic data have been deposited with the Cambridge Crystallographic Data Centre as supplementary publication no. CCDC 1436575 (**SIA-F**) and 1436574 (**SIA-TXO$_2$**). Copies of the data can be obtained free of charge on application to CCDC, 12 Union Road, Cambridge CB2 1EZ, UK [fax: (+44) 1223-336-033; e-mail: deposit@ccdc.cam.ac.uk].

SIA-F :

(C_{31} H_{19} N); M = 405.47. APEXII, Bruker-AXS diffractometer, Mo-Kα radiation (λ = 0.71073 Å), T = 150(2) K; triclinic *P 1* (I.T.#1), a = 11.4724(8), b = 13.8188(11), c = 14.0714(11) Å, α = 91.414(4), β = 113.598(3), γ = 93.956(4) °, V = 2036.0(3) Å^3.Z = 4, d = 1.323 g.cm^{-3}, μ = 0.076 mm^{-1}. The structure was solved by direct methods using the *SIR97* program [1], and then refined with full-matrix least-square methods based on F^2 (*SHELXL-97*) [2] with the aid of the *WINGX* [3] program. All non-hydrogen atoms were refined with anisotropic atomic displacement parameters. H atoms were finally included in their calculated positions. A final refinement on F^2 with 14089 unique intensities and 1153 parameters converged at ω$R(F^2)$ = 0.2114 ($R(F)$ = 0.0806) for 10563 observed reflections with $I > 2\sigma(I)$.

SIATXO$_2$:

(C_{31} H_{19} N O_2 S); M = 469.53. APEXII, Bruker-AXS diffractometer, Mo-Kα radiation (λ = 0.71073 Å), T = 150(2) K; triclinic *P -1* (I.T.#2), a = 8.8559(10), b = 9.8766(11), c = 13.1084(15) Å, α = 77.196(4), β = 86.183(4), γ = 78.300(4) °, V = 1094.5(2) Å^3.Z = 2, d = 1.425 g.cm^{-3}, μ = 0.18 mm^{-1}. The structure was solved by direct methods using the *SIR97* program [1], and then refined with full-matrix least-square methods based on F^2 (*SHELXL-97*) [2] with the aid of the *WINGX* [3] program. All non-hydrogen atoms were refined with anisotropic atomic displacement parameters. H atoms were finally included in their calculated positions. A final refinement on F^2 with 4985 unique intensities and 316 parameters converged at ω$R(F^2)$ = 0.1063 ($R(F)$ = 0.0399) for 4384 observed reflections with $I > 2\sigma(I)$.

Figures were drawn using Mercury 3.3 (Build RC5).

Spectroscopic studies:

Cyclohexane (AnalaR NORMAPUR, VWR), Toluene (Spectrometric grade 99,7%, Alfa Aesar), Chloroform (AnalaR, NORMAPUR, VWR), Ethyl Acetate (for analysis, Carlo Erba) and Acetonitrile (Anhydrous for analysis, Carlo Erba). Standard 1N solution of sulfuric acid was purchased from Alfa Aesar. UV-visible spectra were recorded using an UV-Visible spectrophotometer SHIMADZU UV-1605. The energy gap was calculated from the absorption edge of the UV-vis absorption spectra in solution in cyclohexane, using the formula ΔEopt (eV) = hc/λ, λ being the ab¬sorption edge (in meter). With h = 6.6x10^{-34} J.s (1eV = 1.6x10^{-19} J) and c = 3.0x10^8 m.s-1, this equation may be simplified as: ΔE^{opt} (eV) = 1237.5/λ (in nm). Triplet energy level E_T was calculated from the maximum of the first phosphorescence emission peak, and conversion in electron volt was obtained with the previous formula. Emission spectra were recorded with a PTI spectrofluorimeter (PTI-814 PDS, MD 5020, LPS 220B) using a xenon lamp. Quantum yields in solution (øsol) were calculated relative to quinine sulfate (øsol = 0.546 in H_2SO_4 1N). øsol was determined according to the following equation,

$$\phi_{sol} = \phi_{ref} \times 100 \times \frac{(Ts \times Ar)}{(Tr \times As)} \left(\frac{n_s}{n_r} \right)^2 \quad (1)$$

where, subscripts s and r refer respectively to the sample and reference. The integrated area of the emission peak in arbitrary units is given as T, n is the refracting index of the solvent (n_s = 1.426 for cyclohexane) and A is the absorbance. Three solutions of different concentration of the substrate (A<0.1) and 3 solutions of the reference (quinine sulfate) were prepared. The quinine sulfate concentration was chosen so as the absorption of the reference and the substrate were the same at the excitation wavelength.

3 quantum yields were then calculated at this wavelength and the average value is reported. IR spectra were recorded on a Bruker Vertex 70 using a diamond crystal MIRacle ATR (Pike).

Lipper-Mataga-Ooshika formalism was used to estimate the excited state dipole moment.[3-5]

$$\Delta\nu = \frac{2(\Delta\mu)^2}{r^3 hc}\Delta f + C \quad \text{with} \quad \Delta f = \left(\frac{\varepsilon - 1}{2\varepsilon + 1} - \frac{n^2 - 1}{2n^2 + 1}\right)$$

With "Δν" (cm^{-1}) being the Stokes shift,[1] "Δμ" (D) the dipole moment difference between S_0 and S_1 states, "r" (cm) the radius of the solvatation sphere calculated from Xray structure, "h" Planck constant ($6{,}626.10^{-27}$erg.s^{-1}), "c" celerity ($2{,}998.10^{10}$ems.s^{-1}) "Δf" the orientation polarisability of the solvent calculated from its dielectric constant "ε" and its refractive index "n", and a constant C.

Experimentally, several points Δν/Δf were measured from absorption and emission spectra in several solvents (Cyclohexane, Toluene, Chloroform, Ethyl Acetate, and Acetonitrile). A slope is then calculated by a linear regression on these five points and the dipole moment difference (Δμ) is calculated with this equation:

$$\Delta\mu = \sqrt{\frac{r^3 hc.\,slope}{2}}$$

Excited state dipole moment μ* is then calculated from the ground state dipole moment μ estimated by DFT calculations.

Electrochemical studies

Electrochemical experiments were performed under argon atmosphere using a Pt disk electrode (diameter 1 mm), the counter electrode was a vitreous carbon rod and the reference electrode was a silver wire in a 0.1M $AgNO_3$ solution in CH_3CN. Ferrocene was added to the electrolyte solution at the end of a series of experiments. The ferrocene/ferrocenium (Fc/Fc^+) couple served as internal standard. The three electrodes cell was connected to a PAR Model 273 potentiostat/galvanostat (PAR, EG&G, USA) monitored with the ECHEM Software. Activated Al_2O_3 was added in the electrolytic solution to remove excess moisture. For a further comparison of the electrochemical and optical properties, all potentials are referred to the SCE electrode that was calibrated at –0.405 V vs. Fc/Fc^+ system. Following the work of Jenekhe, [6] we estimated the electron affinity (EA) or lowest unoccupied molecular orbital (LUMO) and the ionisation potential (IP) or highest occupied molecular orbital (HOMO) from the redox data. The LUMO level was calculated from: LUMO (eV)= -[E_{onset}^{red} (vs SCE) +4.4] and the HOMO level from: HOMO (eV) = -[E_{onset}^{ox} (vs SCE) + 4.4], based on an SCE energy level of 4.4 eV relative to the vacuum. The electrochemical gap was calculated from: ΔE^{el} = |HOMO-LUMO| (in eV).

Theoretical modeling

Full geometry optimization with Density functional theory (DFT)[7, 8] and Time-Dependent Density Functional Theory (TD-DFT) calculations were performed with the hybrid Becke-3 parameter exchange[9-11] functional and the Lee-Yang-Parr non-local correlation functional[12] (B3LYP) implemented in the Gaussian 09 (Revision B.01) program[13] using the 6-311G+(d,p) basis set and the default convergence criterion implemented in the program. The figures were generated with GaussView 5.0. The triplet state energy level (S_0 to T_1 energy transition E_T) of the different molecules was calculated from the difference between the total energy of the molecule in their respective optimized singlet and triplet states. Calculations were carried out under GENCI (project c2015085032).

[1] it should be mentioned that the Stokes shift has been evaluated using the band at the lowest energy, which is not the HOMO/LUMO transition (not experimentally observed)

Thermal analysis

Thermal Gravimetric Analysis (TGA) was carried out by using TA SDT Q600 instrument, at the Ecole Nationale Superieure de Chimie de Rennes or at the "Institut des Sciences Analytiques" (UMR CNRS 5280) of Villeurbanne. TGA curves were measured at 10°C/min from 0 to 600°C under nitrogen atmosphere. Differential scanning calorimetry (DSC) was carried out by using NETZSCH DSC 200 F3 instrument equipped with an intracooler. DSC traces were measured at 10°C/min. 2 heating/cooling cycles were successively carried out and the glass transition was determined from the 2nd heating cycle. The temperature of the transition were measured at the maxima of each transition peak.

Device fabrication and characterization

The structure of the device is the following: ITO/CuPc (10 nm)/NPB (40 nm)/TCTA (10 nm)/ Hosts:dopant (100 nm)/TPBi or TmPyPB (40 nm)/LiF (1.2 nm)/Al (100 nm). Devices have been fabricated onto patterned ITO coated glass substrates from XinYan Tech (thickness: 100 nm and sheet resistance: less of 20 W/m). At the exception of the host materials that are synthesized by us, all other materials were commercially available and used without purifications. The organic materials are deposited onto the ITO anode by sublimation under high vacuum (< 10^{-6} Torr) at a rate of 0.2 – 0.3 nm/s. The entire device is fabricated in the same run without breaking the vacuum. In this study, the thicknesses of the different organic layers were kept constant for all the devices. The active area of the devices defined by the overlap of the ITO anode and the metallic cathode was 0.3 cm^2. The current-voltage-luminance (I-V-L) characteristics of the devices were measured with a regulated power supply (Laboratory Power Supply EA-PS 3032-10B) combined with a multimeter and a 1 cm^2 area silicon calibrated photodiode (Hamamatsu). The spectral emission was recorded with a SpectraScan PR650 spectrophotometer. All the measurements were performed at room temperature and at ambient atmosphere with no further encapsulation of devices.

SYNTHESIS

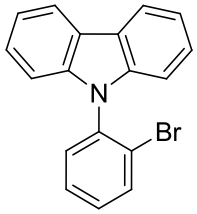

9-(2-bromophenyl)-9H-carbazole (1)

Carbazole (5.007 g, 29.945 mmol), 1,2-dibromobenzene (12.500 g, 52.988 mmol, 1.77 eq), potassium phosphate tribasic (31.514 g, 0.148 mmol, 4.94 eq), copper (I) oxide (0.869 g, 6.073 mmol, 0.20 eq) and DMEDA (1.097 g, 12.445 mmol, 0.42 eq) were dissolved in xylenes (50 mL) under argon. The mixture was heated at 130°C for two days. Then, the mixture was allowed to cool down to room temperature, and water (100 mL) was poured in. The crude was extracted three times with dichloromethane (3X50 mL). The combined organic extracts were dried over magnesium sulfate, filtered, and concentrated under reduced pressure. The residue was purified by flash chromatography on silica gel (light petroleum/dichloromethane) (9 / 1), and after recrystallized from ethanol to give colorless needles (5.596 g, 17.368 mmol). Yield: 58%. mp: 77 °C. ^{1}H NMR (300 MHz, CD_2Cl_2): δ 8.16 (ddd, J = 7.7, 1.2, 0.7 Hz, 2H, ArH), 7.92 – 7.86 (m, 1H, ArH), 7.62 – 7.37 (m, 5H, ArH), 7.30 (ddd, J = 7.7, 7.2, 1.1 Hz, 2H, ArH), 7.10 – 7.04 (m, 2H, ArH). ^{13}C NMR (75 MHz, CD_2Cl_2): δ 141.4 (C), 137.0 (C), 134.7 (CH), 131.7 (CH), 130.9 (CH), 129.5 (CH), 126.5 (CH), 124.2 (C), 123.6 (C), 120.8 (CH), 120.5 (CH), 110.5 (CH). HRMS calculated for $C_{18}H_{13}NBr$ 322.0231 $[M+H]^+$, found: 322.0227.

General procedure for lithiated reaction

9-(2-bromophenyl)-9H-carbazole **(1)** (1 eq) was dissolved in dry THF under argon atmosphere, cooled at -78 °C and stirred during 10 minutes at this temperature. A 2.5M *n*-BuLi solution (1.1 eq) in THF was then slowly injected via a syringe, at -78 °C. The resulting mixture was stirred at the same temperature for 30 min. The corresponding ketone (1.15 eq) dissolved in dry THF was then added dropwise, the mixture was stirred for another 30 minutes at -78°C, and allowed warming up to room temperature gradually overnight. Absolute ethanol (10 mL) was added and the mixture was concentrated under reduced pressure.

Without other purification, the crude was dissolved in methanesulfonic acid and heated up. Then, the mixture was poured onto water/ice (200 mL) and the solution was extracted three times with dichloromethane. The combined organic extracts were dried over magnesium sulfate, filtered, and concentrated under reduced pressure. The residue was purified by flash chromatography on silica gel.

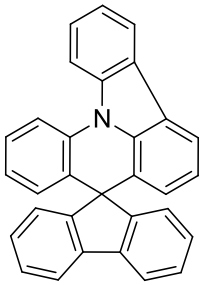

Spiro[fluorene-9,8'-indolo[3,2,1-de]acridine] (SIA-F)

Spiro[fluorene-9,8'-indolo[3,2,1-de]acridine] was synthesized following the general procedure using 9-(2-bromophenyl)-9H-carbazole **(1)** (0.86 g, 2.67 mmol), 9-fluorenone (0.55 g, 3.05 mmol, 1.14 eq) and 2.5M *n*-BuLi solution (1.16 mL, 2.9 mmol, 1.09 eq). Recrystallized from a mixture of dichloromethane/methanol (1:1) giving a colorless powder (0.56 g, 1.39 mmol). Yield: 52 % m.p: 233 °C. ^{1}H NMR (300 MHz, CD_2Cl_2): δ 8.31 (d, *J* = 8.5 Hz, 1H, ArH), 8.26 (dd, *J* = 8.3, 1.1 Hz, 1H, ArH), 8.21 (ddd, *J* = 7.8, 1.3, 0.7 Hz, 1H, ArH), 7.93 – 7.85 (m, 3H, ArH), 7.66 (ddd, *J* = 8.5, 7.3, 1.4 Hz, 1H, ArH), 7.47 – 7.33 (m, 4H, ArH), 7.19 (td, *J* = 7.4, 1.1 Hz, 2H, ArH), 7.12 (ddd, *J* = 7.6, 1.3, 0.7 Hz, 2H, ArH), 7.08 (t, *J* = 7.6 Hz, 1H, ArH), 6.86 (ddd, *J* = 7.9, 7.3, 1.2 Hz, 1H, ArH), 6.59 (dd, *J* = 7.9, 1.5 Hz, 1H, ArH), 6.49 (dd, *J* = 7.5, 1.0 Hz, 1H, ArH). ^{13}C NMR (75 MHz, CD_2Cl_2): δ 155.9 (C), 140.1 (C), 139.1 (C), 137.6 (C), 137.3 (C), 129.9 (C), 129.6 (CH), 128.9 (CH), 128.5 (CH), 128.4 (CH), 127.3 (CH), 126.8 (C), 125.9 (CH), 125.1, 123.8 (CH), 123.5 (CH), 123.2 (C), 123.1 (CH), 121.7 (CH), 121.6 (CH), 120.7 (CH), 118.6 (CH), 115.1 (CH), 114.3 (CH), 57.4 (C spiro). HRMS calculated for $C_{31}H_{20}N$ 406.1595 $[M+H]^+$, found: 406.1594. IR (ATR, cm^{-1}): ν = 553, 619, 644, 654, 675, 721, 742, 798, 904, 933, 970, 1005, 1026, 1062, 1120, 1159, 1190, 1238, 1257, 1271, 1319, 1340, 1402, 1432, 1446, 1456, 1477, 1495, 1599, 3012, 3045.

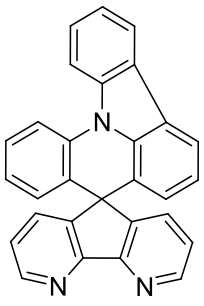

Spiro[cyclopenta[1,2-b:5,4-b']dipyridine-5,8'-indolo[3,2,1-de]acridine] (SIA-DAF)

Spiro[cyclopenta[1,2-b:5,4-b']dipyridine-5,8'-indolo[3,2,1-de]acridine] was synthesized following the general procedure using 9-(2-bromophenyl)-9H-carbazole **(1)** (1.00 g, 3.10 mmol), 5H-cyclopenta[1,2-

b:5,4-b']dipyridin-5-one (0.65 g, 3.57 mmol, 1.15 eq), and 2.5M *n*-BuLi solution (1.37 mL, 3.43 mmol, 1.11 eq). Recrystallized from a mixture of dichloromethane/methanol (1:1) giving a beige powder (0.52 g, 0.13 mmol). Yield: 41 %. m.p: 298 °C ^{1}H NMR (300 MHz, CD_2Cl_2): δ 8.65 (dd, *J* = 4.8, 1.5 Hz, 2H, ArH), 8.26 – 8.16 (m, 2H, ArH), 8.13 (ddd, *J* = 7.8, 1.3, 0.6 Hz, 1H, ArH), 7.85 (dd, *J* = 7.7, 0.9 Hz, 1H, ArH), 7.58 (ddd, *J* = 8.5, 7.3, 1.3 Hz, 1H, ArH), 7.43 (dd, *J* = 7.8, 1.5 Hz, 2H, ArH), 7.38 – 7.28 (m, 2H, ArH), 7.11 (dd, *J* = 7.8, 4.8 Hz, 2H, ArH), 7.01 (t, *J* = 7.6 Hz, 1H, ArH), 6.79 (ddd, *J* = 7.9, 7.3, 1.1 Hz, 1H, ArH), 6.51 (dd, *J* = 7.9, 1.5 Hz, 1H, ArH), 6.42 (dd, *J* = 7.6, 0.9 Hz, 1H, ArH); ^{13}C NMR (75 MHz, CD_2Cl_2): δ 157.8 (C), 151.0 (CH), 150.1 (C), 139.1 (C), 137.9 (C), 137.5 (C), 133.6 (CH), 129.3 (CH), 129.2 (CH), 127.5 (CH), 127.3 (C), 126.7 (C), 124.6 (CH), 124.0 (CH), 123.5 (C), 123.3 (CH), 123.2 (CH), 122.6 (C), 121.9 (CH), 121.8 (CH), 119.3 (CH), 115.3 (CH), 114.4 (CH), 53.4 (C spiro). HRMS calculated for $C_{29}H_{18}N_3$ 408.1500 $[M+H]^+$, found: 408.1500. IR (ATR, cm^{-1}): ν = 577, 623, 631, 650, 673, 681, 737, 744, 754, 768, 787, 816, 908, 1024, 1059, 1076, 1092, 1110, 1132, 1161, 1188, 1230, 1257, 1336, 1402, 1433, 1454, 1475, 1495, 1562, 1585, 1595, 1907, 1927, 3055, 3120.

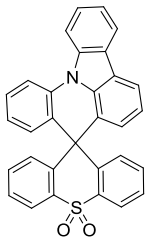

Spiro[indolo[3,2,1-de]acridine-8,9'-thioxanthene] 10',10'-dioxide (SIA-TXO$_2$)

Spiro[indolo[3,2,1-de]acridine-8,9'-thioxanthene] 10',10'-dioxide was synthesized according to the general procedure using 9-(2-bromophenyl)-9H-carbazole (1.002 g, 3.110 mmol, 1 eq), 9H-thioxanthen-9-one 10,10-dioxide (1.664 g, 6.812 mmol, 2.19 eq) and 2.5M solution of *n*-BuLi (1.37 mL, 3.425 mmol, 1.10 eq). Recrystallized from a mixture of dichloromethane/methanol (1:1) giving a colorless powder. Yield: 44 %. m.p: over 320 °C. ^{1}H NMR (300 MHz, $CDCl_3$) δ 8.29 (t, *J* = 8.0 Hz, 2H, ArH), 8.20 (dd, *J* = 8.0, 1.1 Hz, 3H, ArH), 7.89 (dd, *J* = 7.6, 0.9 Hz, 1H, ArH), 7.66 (ddd, *J* = 8.5, 7.3, 1.3 Hz, 1H, ArH), 7.48 – 7.35 (m, 4H, ArH), 7.31 (ddd, *J* = 8.6, 7.3, 1.4 Hz, 2H, ArH), 7.16 (t, *J* = 7.7 Hz, 1H, ArH), 7.06 (dd, *J* = 8.2, 0.9 Hz, 2H, ArH), 7.04 – 6.91 (m, 3H, ArH). ^{13}C NMR (75 MHz, $CDCl_3$) δ 145.0 (C), 138.4 (C), 135.7 (C), 134.2 (C), 133.9 (C), 133.7 (CH), 133.2 (CH), 133.1 (CH), 132.6 (C), 128.6 (CH), 128.1 (CH), 127.3 (CH), 126.9 (C), 126.6 (CH), 126.2 (C), 124.1 (CH), 123.5 (CH), 122.9 (C), 122.5 (CH), 121.5 (CH), 121.4 (CH), 118.6 (CH), 114.6 (CH), 113.5 (CH), 48.8 (C Spiro). HRMS calculated for $C_{31}H_{19}NO_2NaS$ 492.1034 $[M+Na]^+$, found 492.1032. Elemental analysis calculated for $C_{31}H_{19}NO_2S$: C, 79.29 %; H, 4.08 %; N, 2.98 %. Found: C 78.90 %; H 3.89 %; N, 2.70%. IR (ATR, cm^{-1}): ν = 536, 550, 567, 580, 604, 648, 719, 750, 795, 933, 966, 1026, 1059, 1115, 1140, 115, 1230, 1257, 1294, 1338, 1435, 1456, 1479, 1497, 1591, 3010, 3024, 3055.

STRUCTURAL PROPERTIES

Table 1 Crystal data and structure refinement for **SIA-F**

Empirical formula	$C_{31}H_{19}N$
Formula weight	405.47
Temperature	150(2) K
Wavelength	0.71073 Å
Crystal system, space group	triclinic, P 1
Unit cell dimensions	a = 11.4724(8) Å, α = 91.414(4) °
	b = 13.8188(11) Å, β = 113.598(3) °
	c = 14.0714(11) Å, γ = 93.956(4) °
Volume	2036.0(3) $Å^3$
Z, Calculated density	4, 1.323 ($g.cm^{-3}$)
Absorption coefficient	0.076 mm^{-1}
F(000)	848
Crystal size	0.32 x 0.25 x 0.02 mm
Crystal color	colorless
Theta range for data collection	1.48 to 27.42 °
h_min, h_max	-14, 14
k_min, k_max	-17, 16
l_min, l_max	-17, 18
Reflections collected / unique	18516 / 14089 [R(int) = 0.032]
Reflections [I>2σ]	10563
Completeness to theta_max	0.974
Absorption correction type	multi-scan
Max. and min. transmission	0.998 , 0.977
Refinement method	Full-matrix least-squares on F^2
Data / restraints / parameters	14089 / 3 / 1153
bGoodness-of-fit	1.067
Final R indices [I>2σ]	R1 = 0.0806, wR2 = 0.2114
R indices (all data)	R1 = 0.1098, wR2 = 0.2348
Largest diff. peak and hole	0.496 and -0.464 $e^-.Å^{-3}$

SIA-F X-Ray structure: Molecule 1

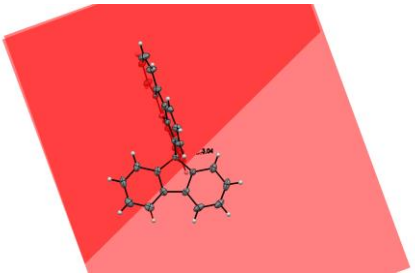

S 1 Fluorene deformation: angle between the mean planes of the two phenyl units (6 and 8) of the fluorenyl fragment in **SIA-F molecule 1**: 3.04 °

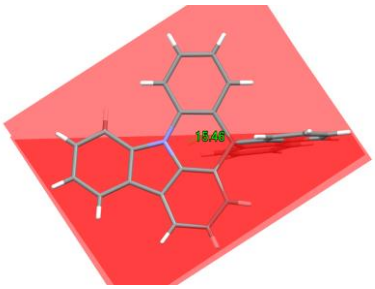

S 2 Indoloacridine deformation: angle between mean planes of rings 1 and 5 in SIA-F molecule 1: 15.46 °

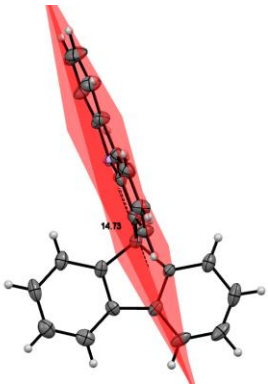

S 3 Acridine deformation: angle between the two phenyl units (3 and 5) of the acridine fragment in **SIA-F molecule 1**: 14.73 °

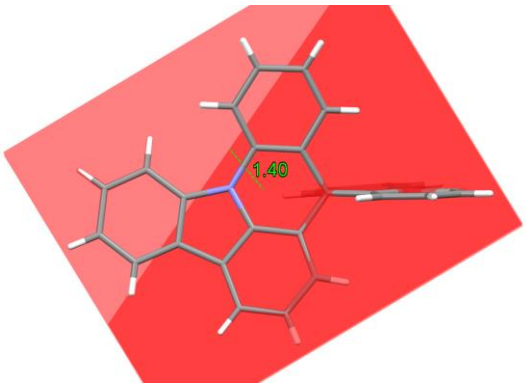

S 4 Carbazole deformation: angle between the two phenyl units (1 and 3) of the carbazole fragment in **SIA-F molecule 1**: 1.40 °

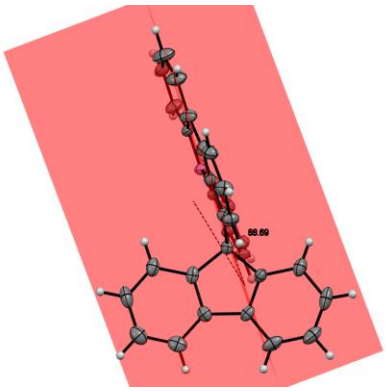

S 5 Spiro angle: angle between the mean plane of cyclohexadiene in fluorene fragment and the mean plane of cyclohexadiene in acridine fragment in **SIA-F molecule 1**: 88.69 °

SIA-F X-Ray structure: Molecule 2

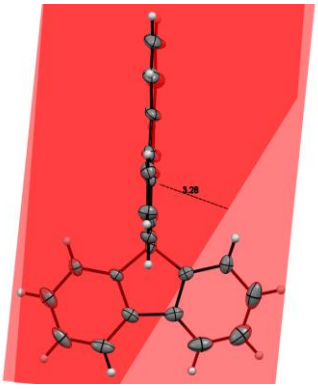

S 6 Fluorene deformation: angle between the two phenyl units (6 and 8) of the fluorenyl fragment in **SIA-F molecule 2**: 3.28 °

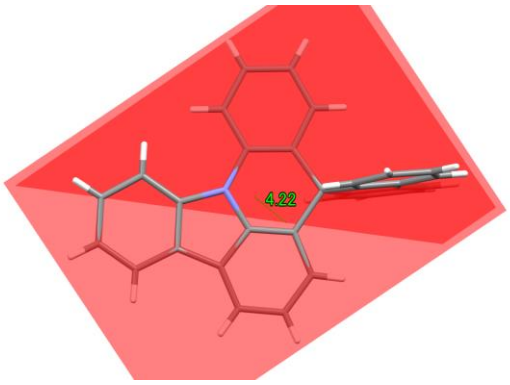

S 7 Indoloacridine deformation: angle between mean planes of rings 1 and 5 in **SIA-F molecule 2**: 4.22 °

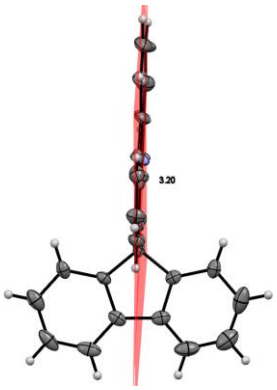

S 8 Acridine deformation: angle between the two phenyl units (1 and 5) of the acridine fragment in **SIA-F molecule 2**: 3.20 °

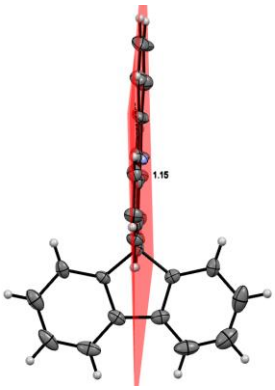

S 9 Carbazole deformation: angle between the two phenyl units (1 and 3) of the carbazole fragment in **SIA-F molecule 2**: 1.15 °

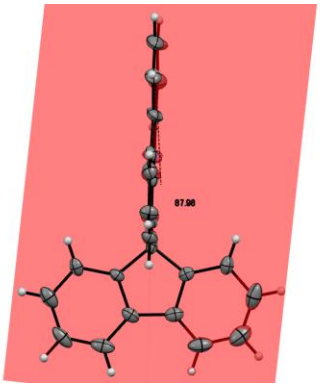

S 10 Spiro angle: angle between the mean plane of cyclohexadiene in fluorene fragment and the mean plane of cyclohexadiene in acridine fragment in **SIA-F molecule 2**: 87.98 °

SIA-F X-Ray structure: Molecule 3

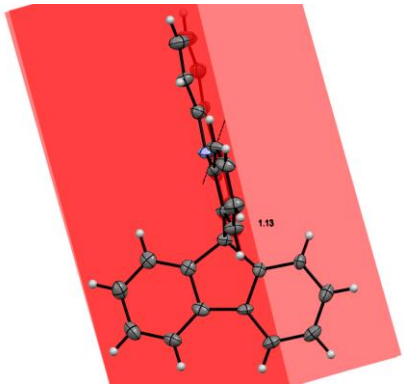

S 11 Fluorene deformation: angle between the two phenyl units (6 and 8) of the fluorene fragment in **SIA-F molecule 3**: 1.13 °

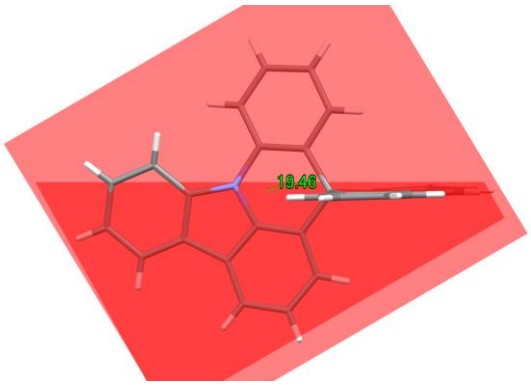

S 12 Indoloacridine deformation: angle between mean planes of rings (1 and 5) in **SIA-F molecule 3**: 4.22 °

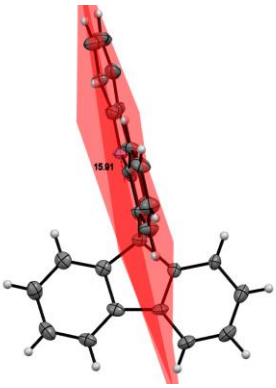

S 13 Acridine deformation: angle between the two phenyl units (3 and 5) of the acridine fragment in **SIA-F molecule 3**: 15.91 °

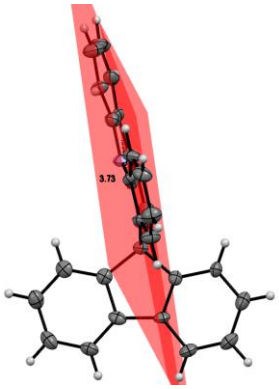

S 14 Carbazole deformation: angle between the two phenyl units (1 and 3) of the carbazole fragment in **SIA-F molecule 3**: 3.73 °

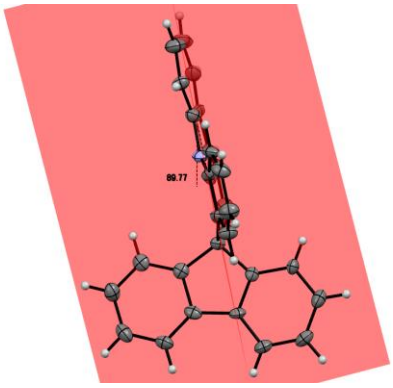

S 15 Spiro angle: angle between the mean plane of cyclohexadiene in fluorene fragment and the mean plane of cyclohexadiene in acridine fragment in **SIA-F molecule 3**: 89.77 °

SIA-F X-Ray structure: Molecule 4

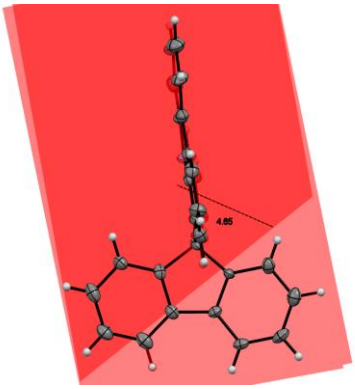

S 16 Fluorene deformation: angle between the two phenyl units (6 and 8) of the fluorene fragment in **SIA-F molecule 4**: 4.65 °

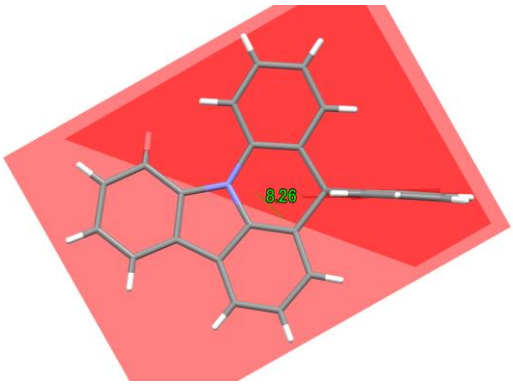

S 17 Indoloacridine deformation: angle between mean planes of rings 1 and 5 in **SIA-F molecule 4**: 8.26 °

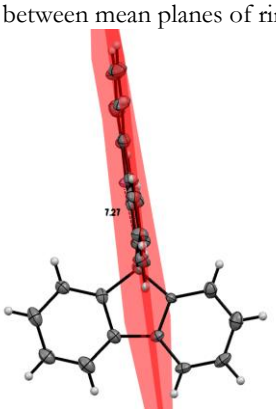

S 18 Acridine deformation: angle between the two phenyl units (3 and 5) of the acridine fragment in **SIA-F molecule 4**: 7.27 °

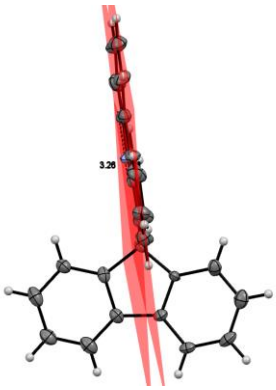

S 19 Carbazole deformation: angle between the two phenyl units (1 and 3) of the carbazole fragment in **SIA-F molecule 4**: 3.26 °

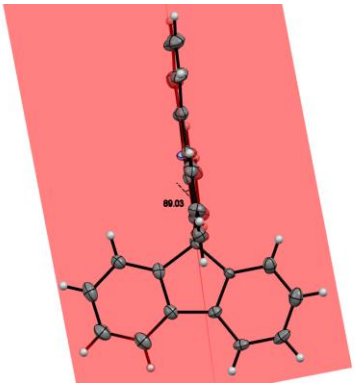

S 20 Spiro angle: angle between the mean plane of cyclohexadiene in fluorene fragment and the mean plane of cyclohexadiene in acridine fragment in **SIA-F molecule 4**: 89.03 °

Table 2 Crystal data and structure refinement for **SIA-TXO$_2$**

Empirical formula	$C_{31}H_{19}NO_2S$
Formula weight	469.53
Temperature	150(2) K
Wavelength	0.71073 Å
Crystal system, space group	triclinic, P *-1*
Unit cell dimensions	a = 8.8559(10) Å, α = 77.196(4) ° b = 9.8766(11) Å, β = 86.183(4) ° c = 13.1084(15) Å, γ = 78.300(4) °
Volume	1094.5(2) Å^3
Z, Calculated density	2, 1.425 (g.cm^{-3})
Absorption coefficient	0.18 mm^{-1}
F(000)	488
Crystal size	0.26 x 0.25 x 0.11 mm
Crystal color	colorless
Theta range for data collection	1.59 to 27.49 °
h_min, h_max	-11, 11
k_min, k_max	-9, 12
l_min, l_max	-16, 17
Reflections collected / unique	17980 / 4985 [R(int) = 0.0258]
Reflections [I>2σ]	4384
Completeness to theta_max	0.992
Absorption correction type	multi-scan
Max. and min. transmission	0.98 , 0.954
Refinement method	Full-matrix least-squares on F^2
Data / restraints / parameters	4985 / 0 / 316
Goodness-of-fit	1.112
Final *R* indices [I>2σ]	R1 = 0.0399, *w*R2 = 0.1063
R indices (all data)	R1 = 0.0473, *w*R2 = 0.1203
Largest diff. peak and hole	0.412 and -0.396 e$^-$.Å^{-3}

SIA-TXO$_2$ X-Ray structure

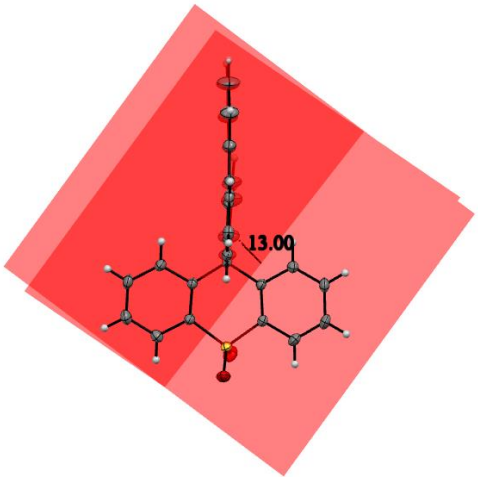

S 21 TXO$_2$ deformation: angle between the two phenyl units (8 and 6) of the dioxothioxanthene fragment in: 13.00 °

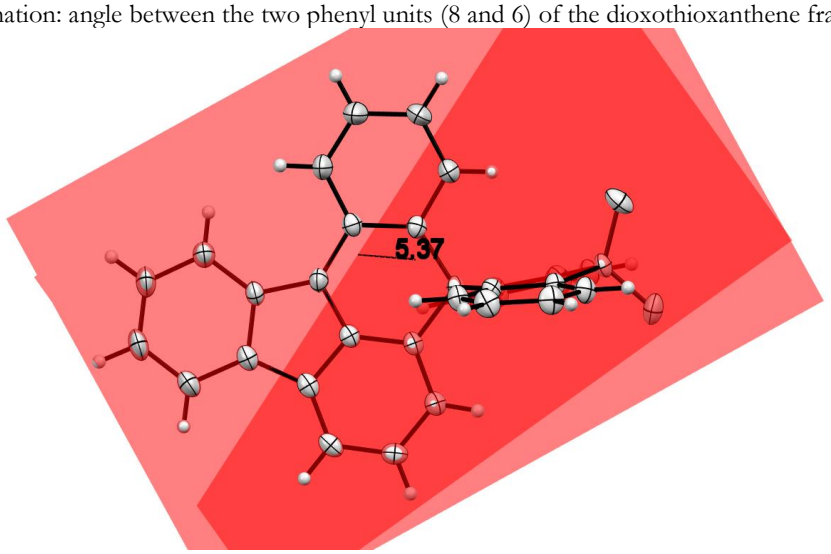

S 22 Indoloacridine deformation: angle between mean planes of rings 1 and 5 in **SIA-TXO$_2$**: 5.37 °

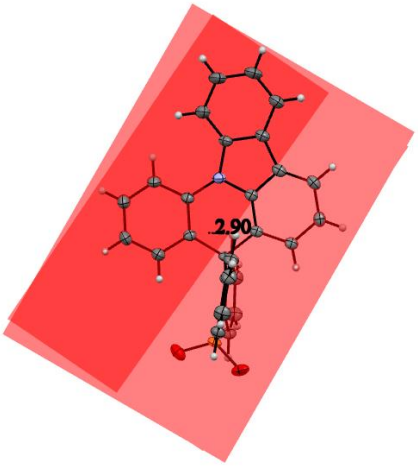

S 23 Acridine deformation: angle between the two phenyl units (3 and 5) of the acridine fragment in **SIA-TXO$_2$**: 2.90 °

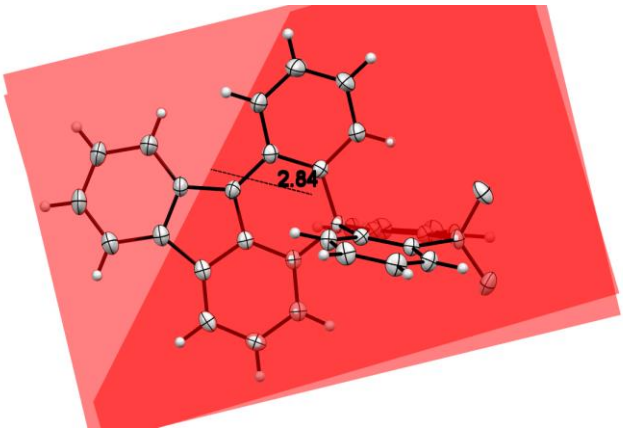

S 24 Carbazole deformation: angle between the two phenyl units (1 and 3) of the carbazole fragment in **SIA-TXO$_2$**: 2.84 °

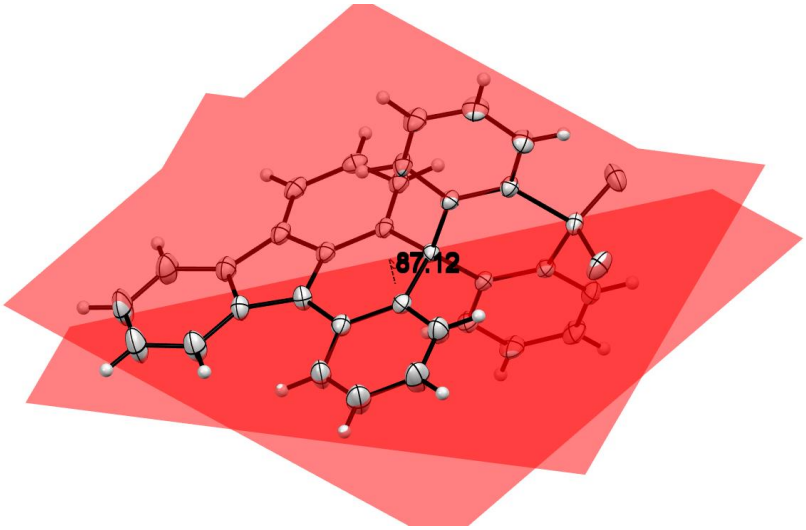

S 25 Spiro angle: angle between the mean plane of cyclohexadiene in dioxothioxanthene fragment and the mean plane of cyclohexadiene in acridine fragment in **SIA-TXO$_2$**: 87.12 °

THERMAL PROPERTIES

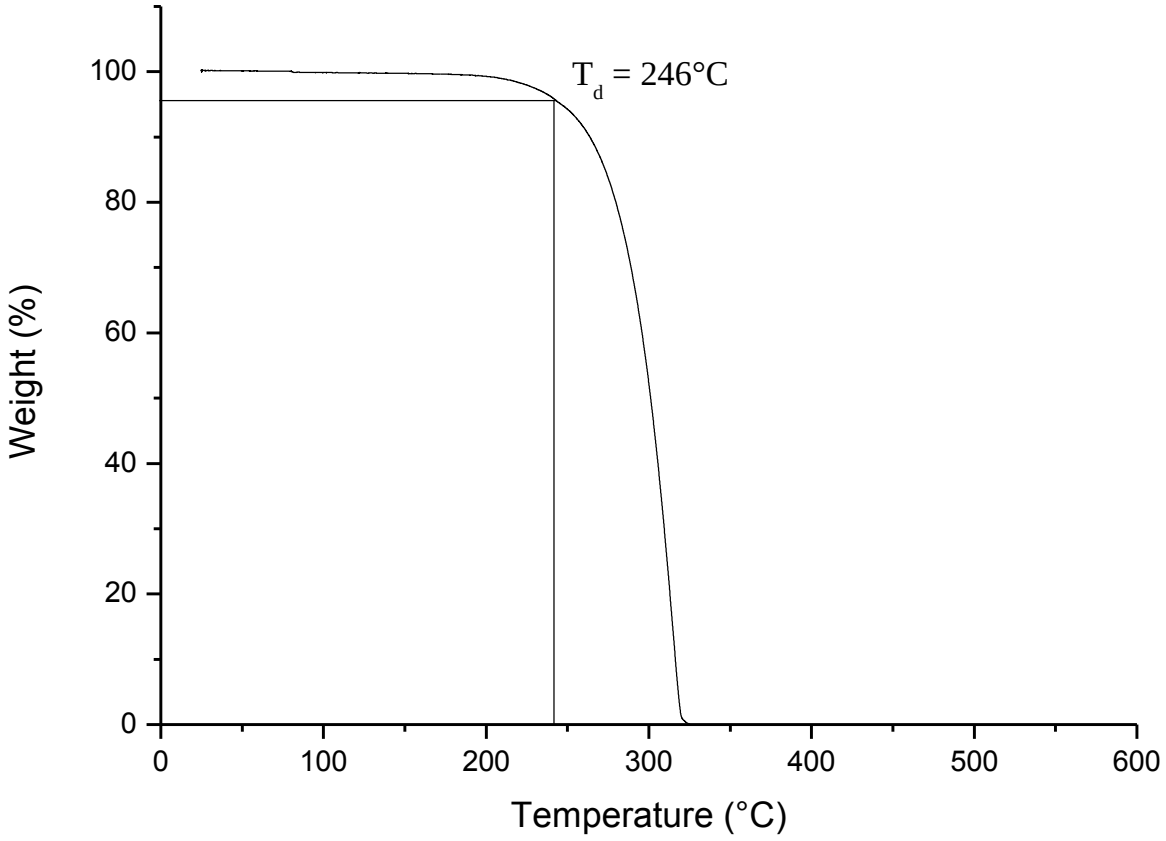

S 26 TGA curve of SIA-F

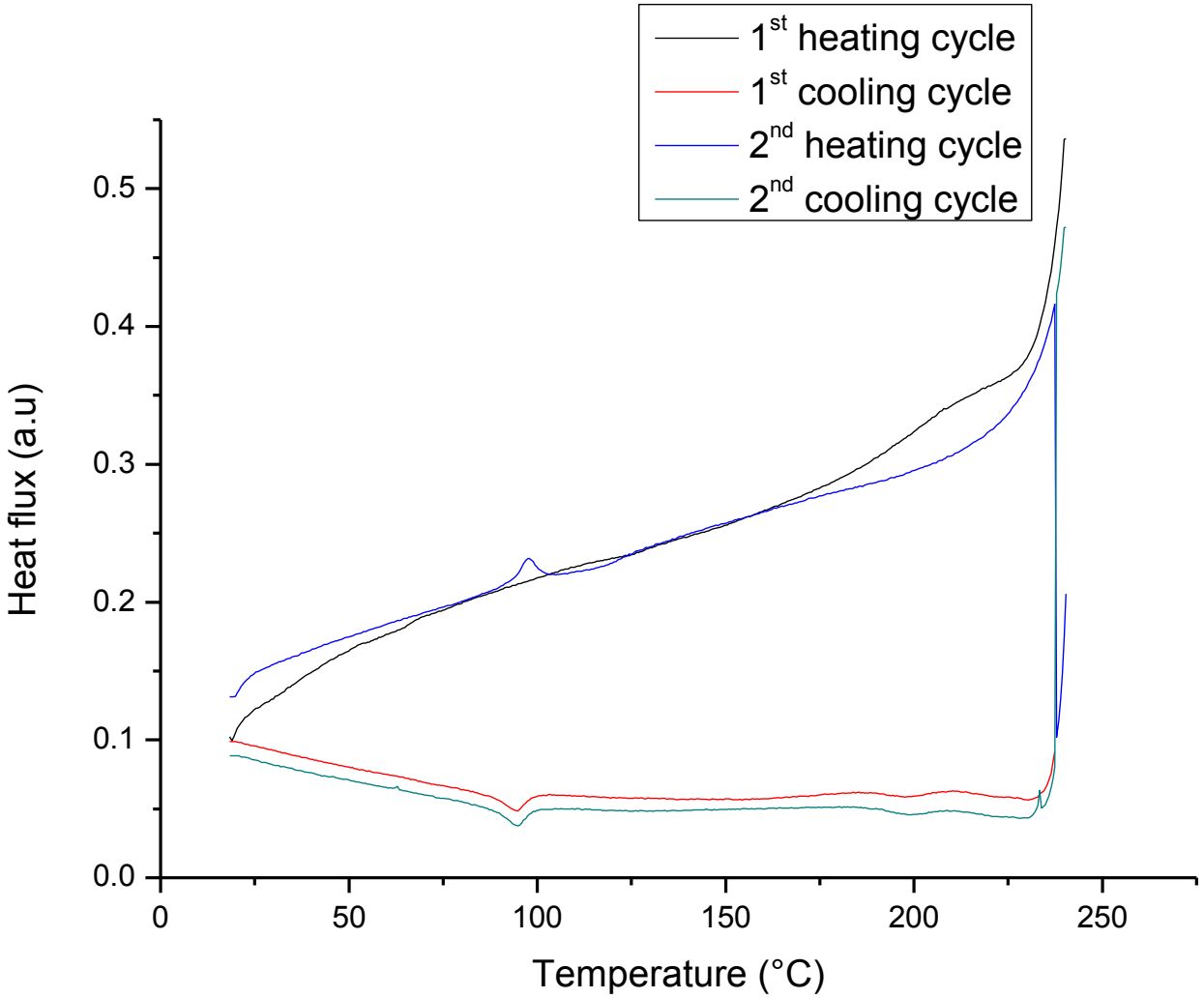

S 27 DSC curves of SIA-F

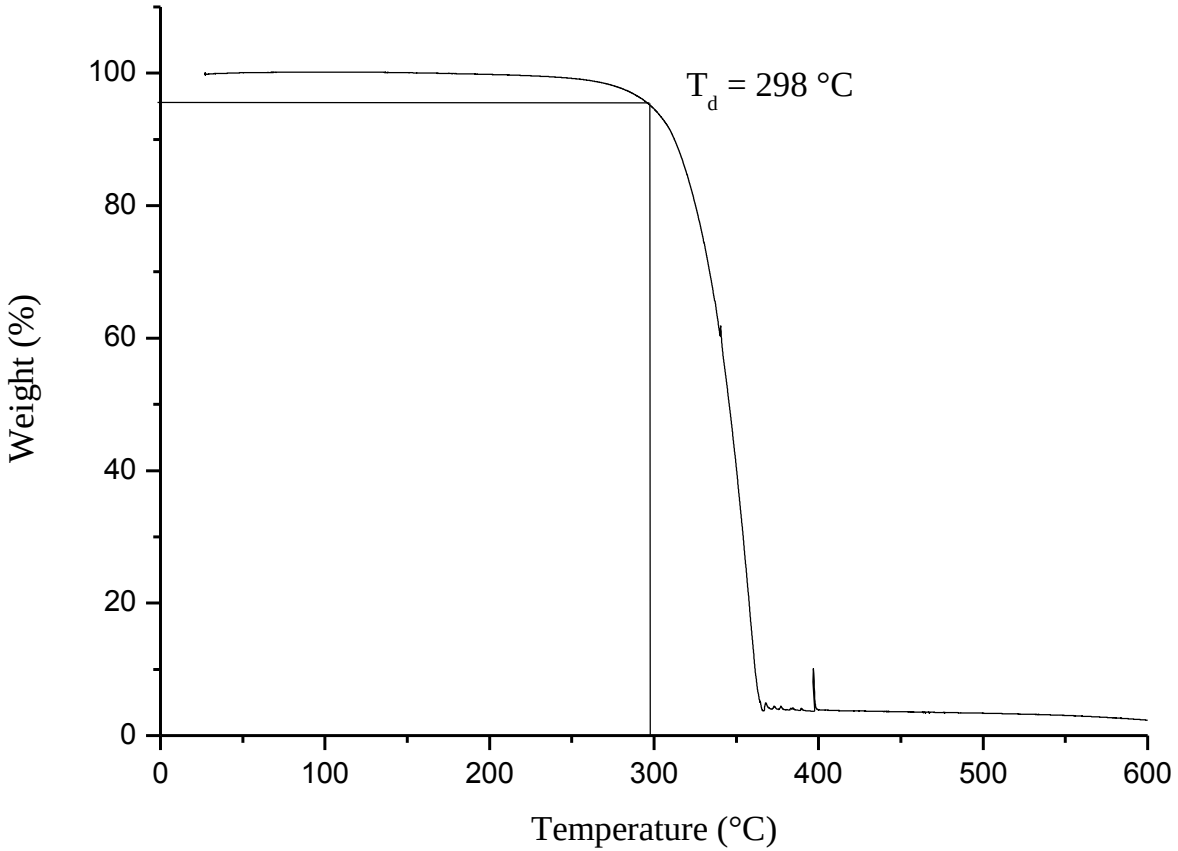

S 28 TGA curve of SIA-DAF

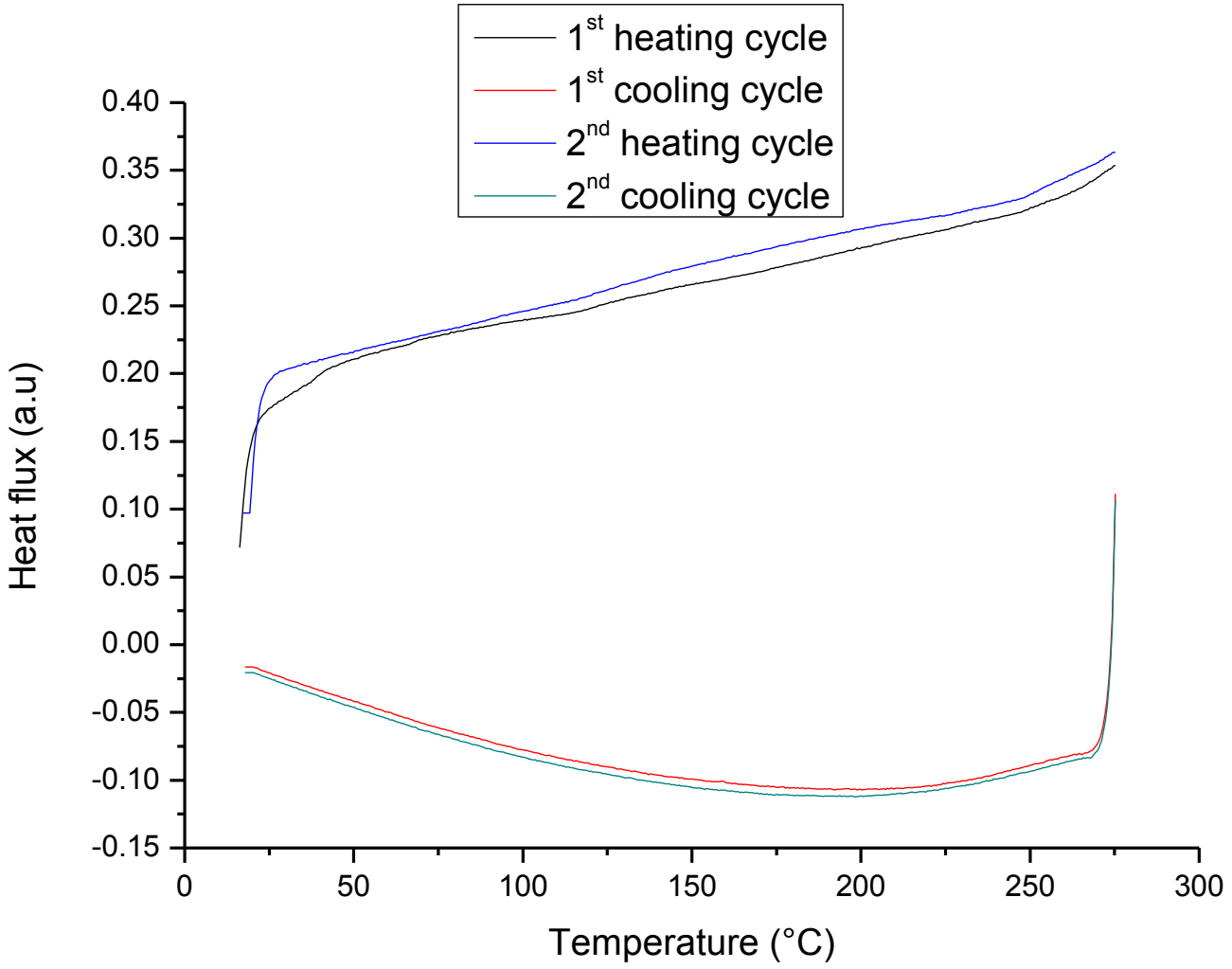

S 29 DSC curve of SIA-DAF

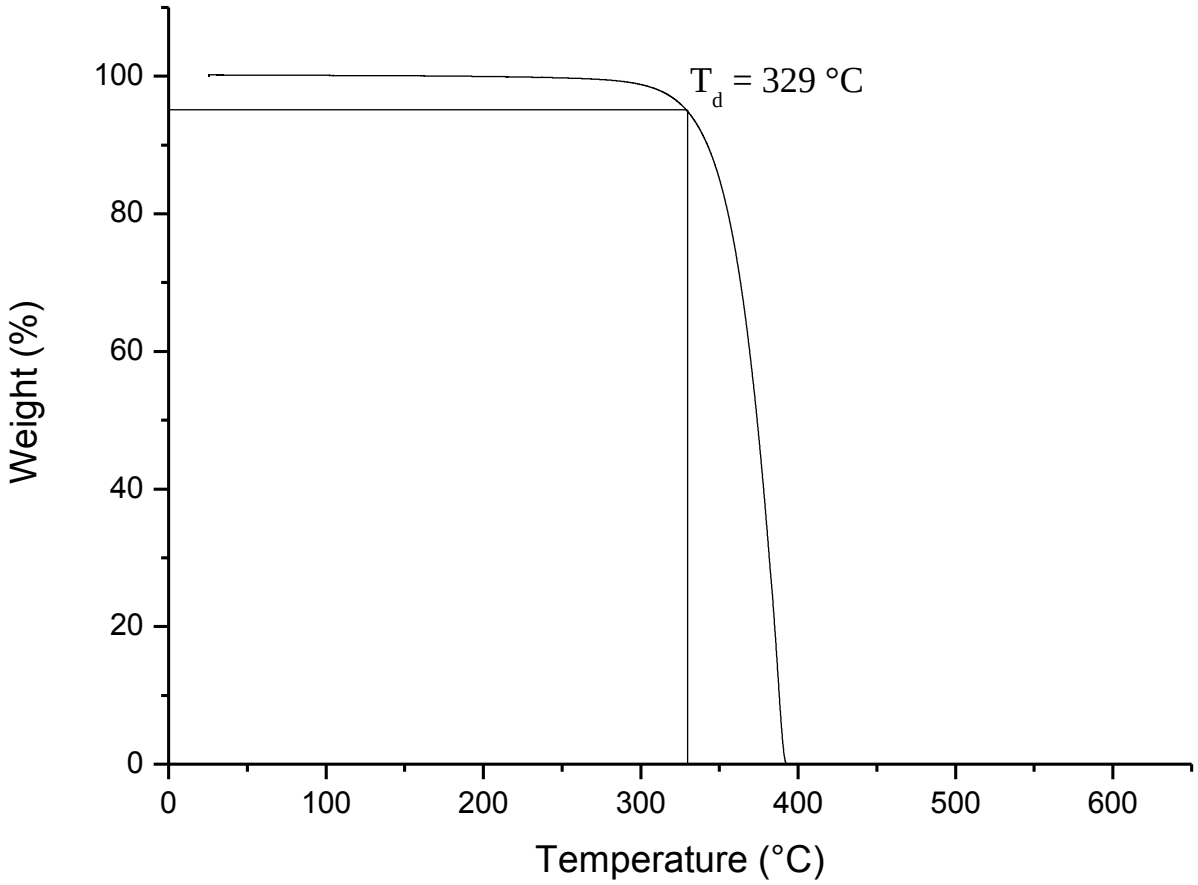

S 30 TGA curve of SIA-TXO_2

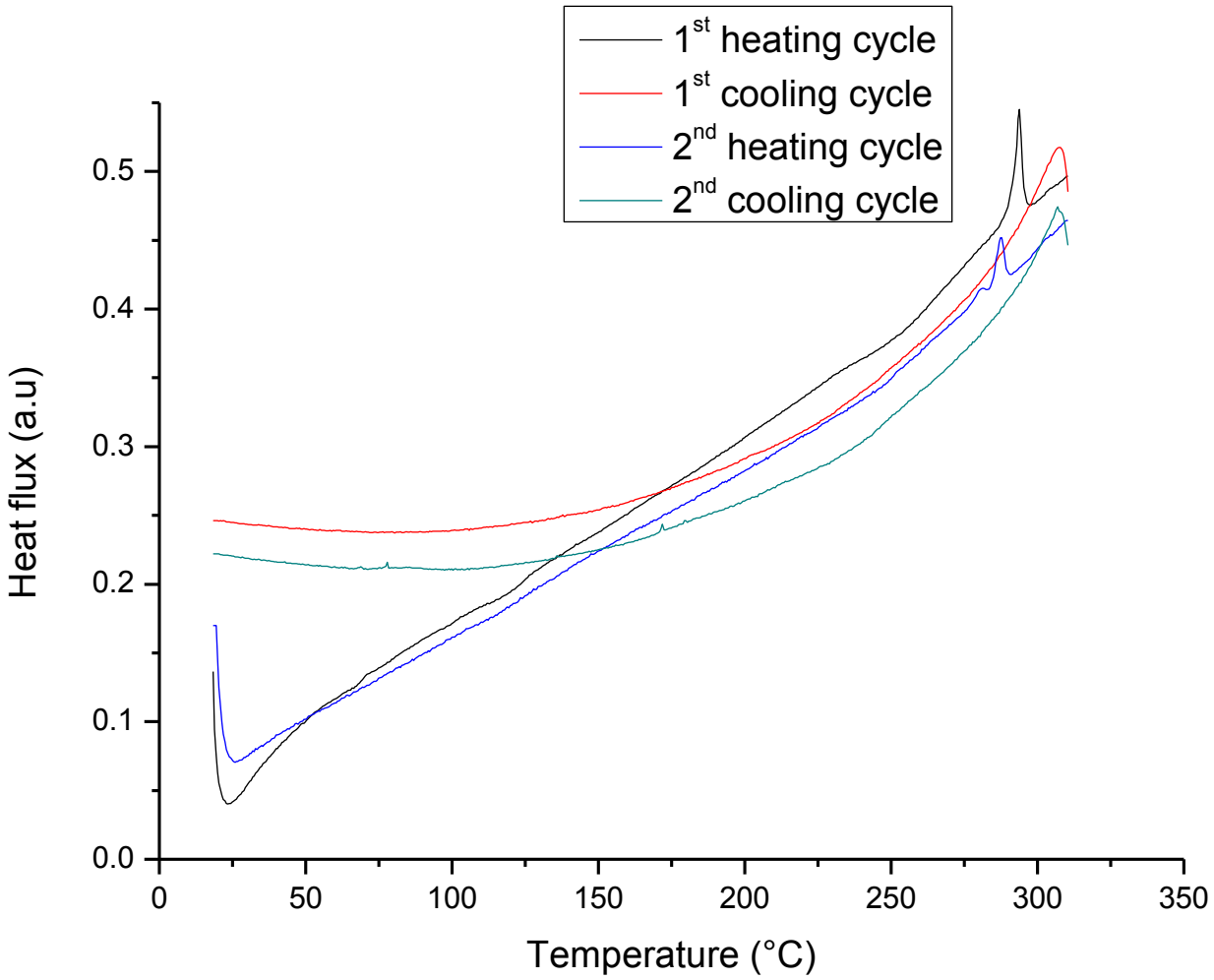

S 31 DSC curve of SIA-TXO_2

PHOTOPHYSICAL PROPERTIES

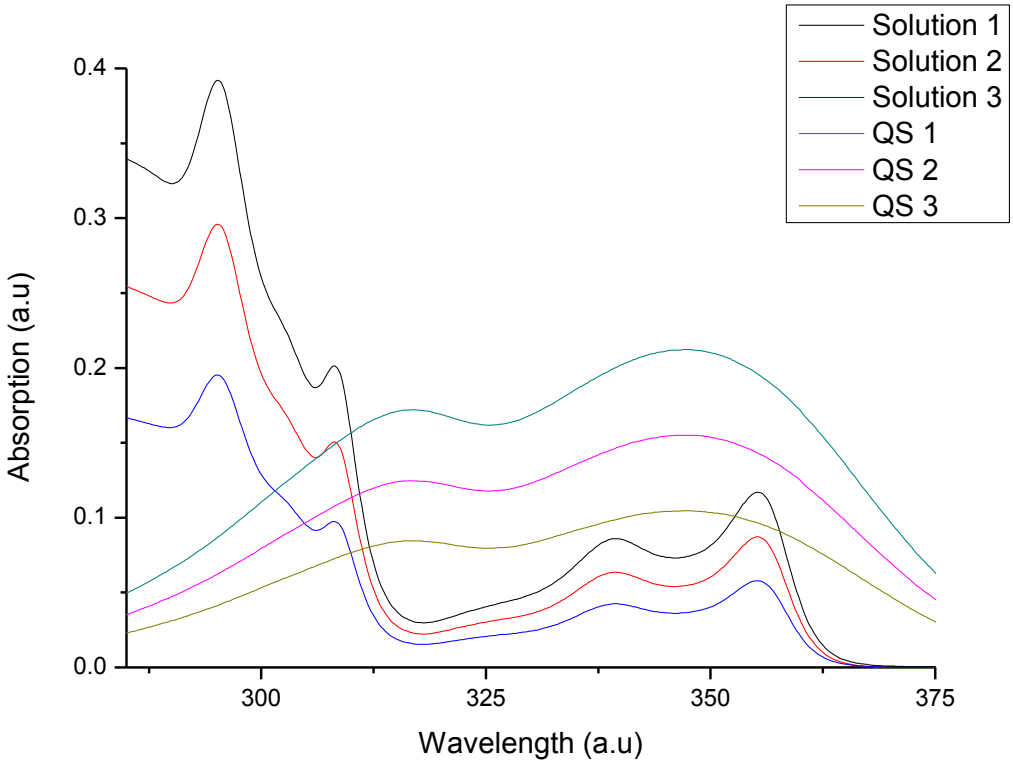

S 32 Quantum yield measurements: Absorption of solutions of **SIA-F** in cyclohexane and quinine sulfate (QS) in H_2SO_4 1N

Table 3 Quantum yield calculation of **SIA-F**

Solution	λ (nm)	A	T_S	T_{QS}	n_D^{25} (cyclohexane)	n_D^{25} (H_2SO_4 1N)	φ (%)
1	310	0.1565	24084.7	45750.8	1.42662	1.3325	33
2	310	0.1133	19309.1	35802.2	1.42662	1.3325	34
3	310	0.0763	13992	26308.4	1.42662	1.3325	33

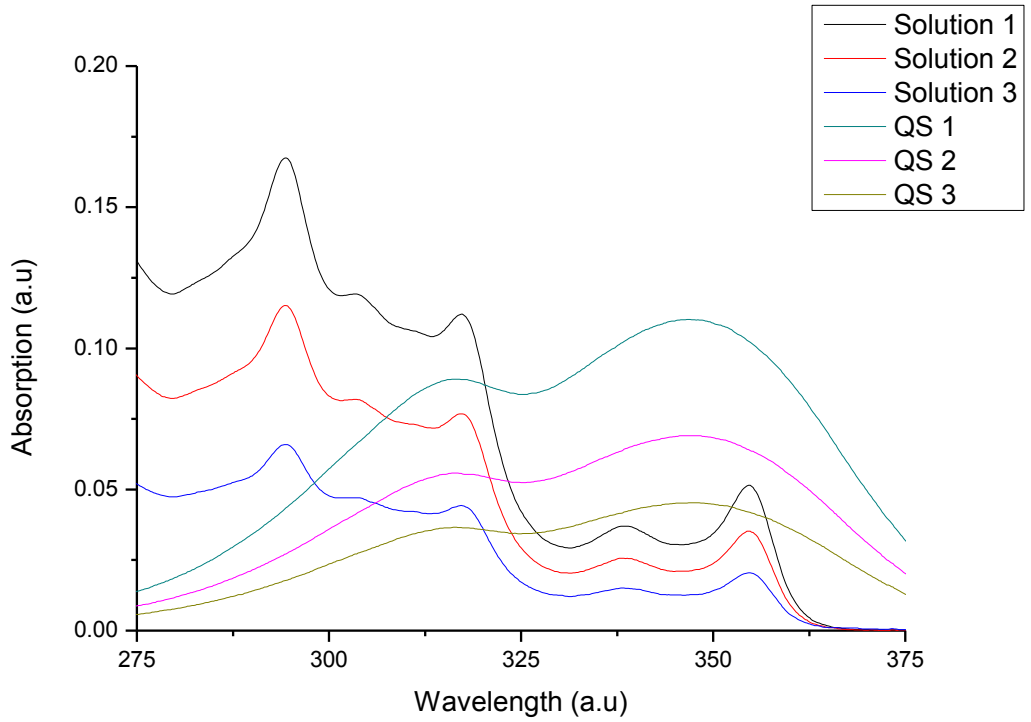

S 33 Quantum yield measurements: Absorption of solutions of **SIA-DAF** in cyclohexane and quinine sulfate (QS) in H_2SO_4 1N

Table 4 Quantum yield calculation of SIA-DAF

Solution	λ (nm)	A	T_S	T_{QS}	n_D^{25} (cyclohexane)	n_D^{25} (H_2SO_4 1N)	φ (%)
1	320	0.087	20848.5	37518.5	1.42662	1.3325	35
2	321	0.0541	15451.1	25325.6	1.42662	1.3325	38
3	320	0.0352	11779.3	17566.7	1.42662	1.3325	42

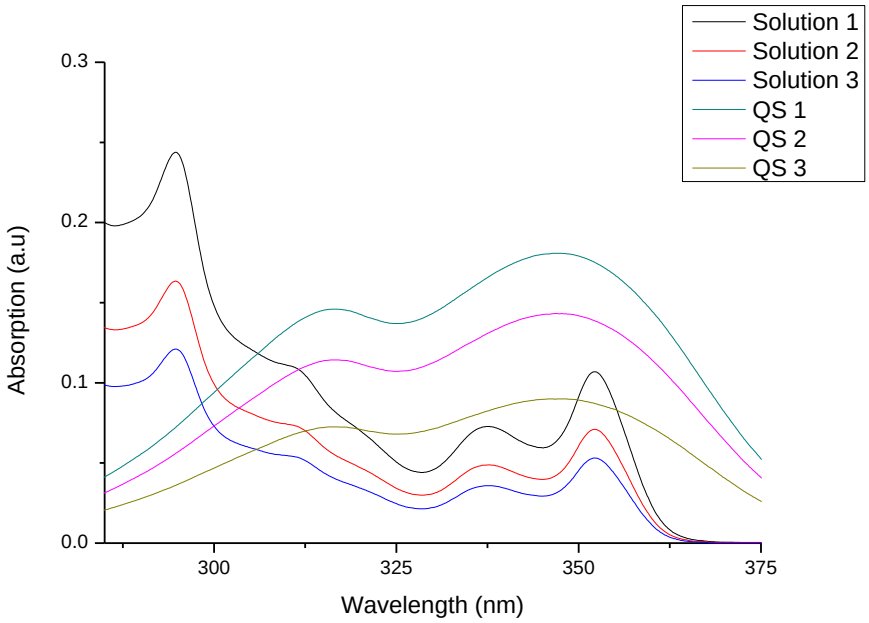

S 34 Quantum yield measurements: Absorption of solutions of **SIA-TXO$_2$** in cyclohexane and quinine sulfate (QS) in H_2SO_4 1N

Table 5 Quantum yield calculation of SIA-TXO_2

Solution	λ (nm)	A	T_S	T_{QS}	n_D^{25} (cyclohexane)	n_D^{25} (H_2SO_4 1N)	φ (%)
1	306	0.1187	97797	155771	1.42662	1.3325	39
2	303.5	0.0841	79751.6	132411	1.42662	1.3325	38
3	305.5	0.0585	67062.7	100789	1.42662	1.3325	42

Table 6 Quantum yields measured in various solvents of **SIA-F**, **SIA-DAF** and **SIA-TXO$_2$**

	Quantum Yield				
	Cyclohexane	Toluene	THF	EtOAc	MeCN
SIA-F	33.3%	31.1%	32.5%	28.8%	31.8%
SIA-DAF	38.3%	4.9%	0.9%	1.5%	0.8%
SIA-TXO$_2$	39.5%	27.5%	27.2%	19.6%	19.9%

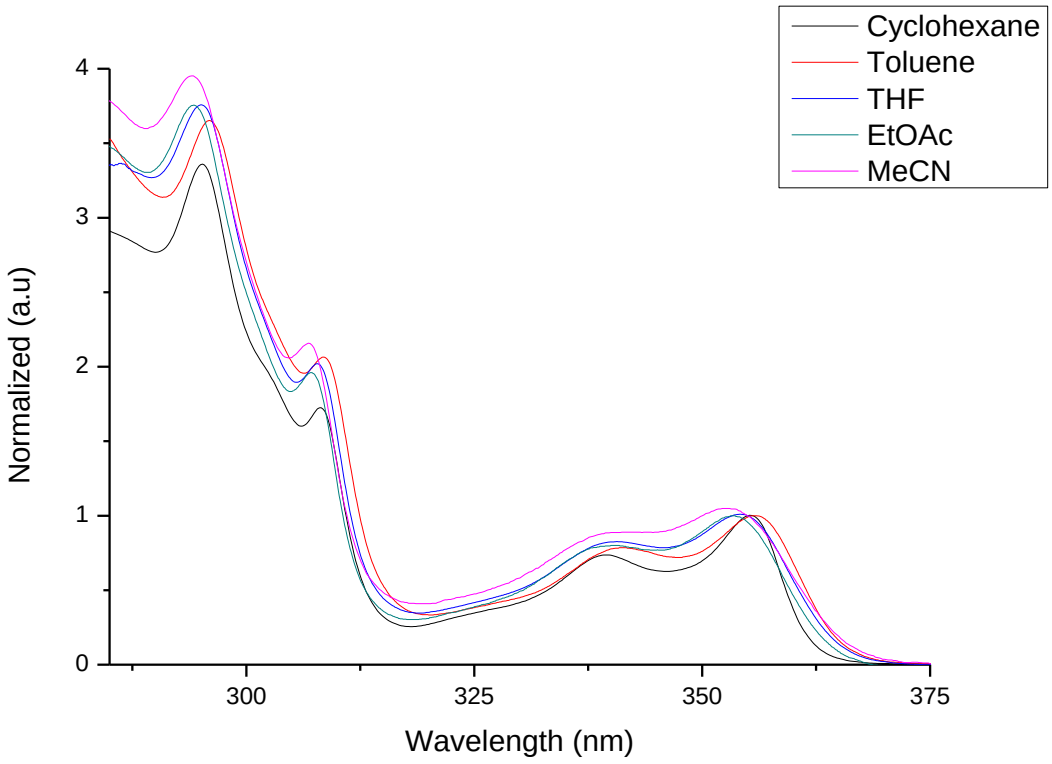

S 35 UV-Vis absorption of **SIA-F** in various solvents

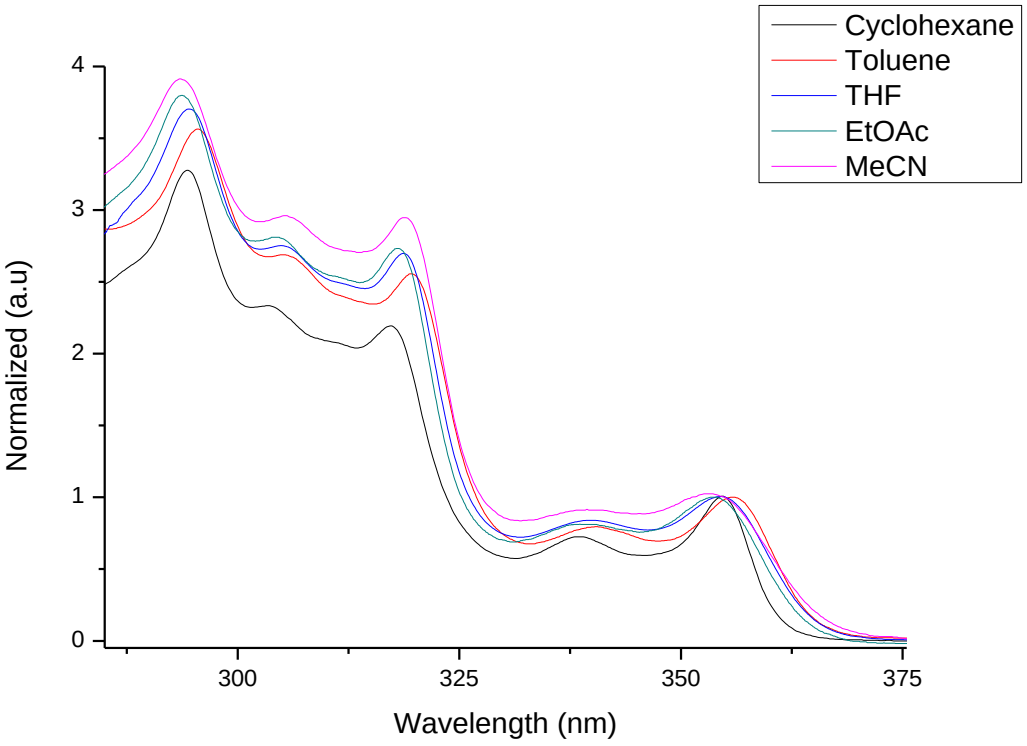

S 36 UV-Vis absorption of **SIA-DAF** in various solvents

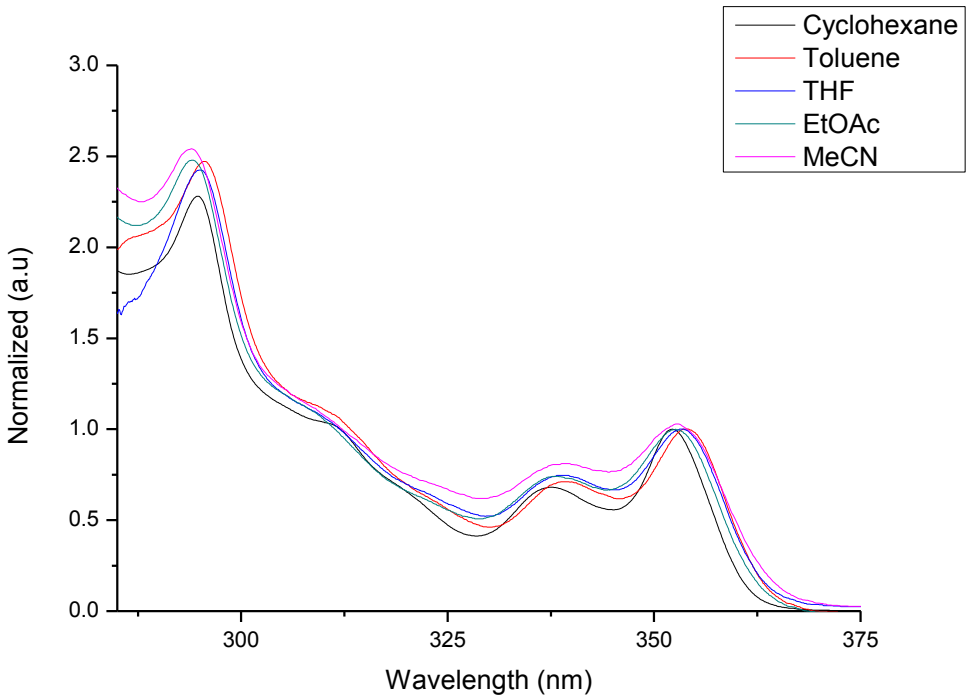

S 37 UV-Vis absorption of **SIA-TXO$_2$** in various solvents

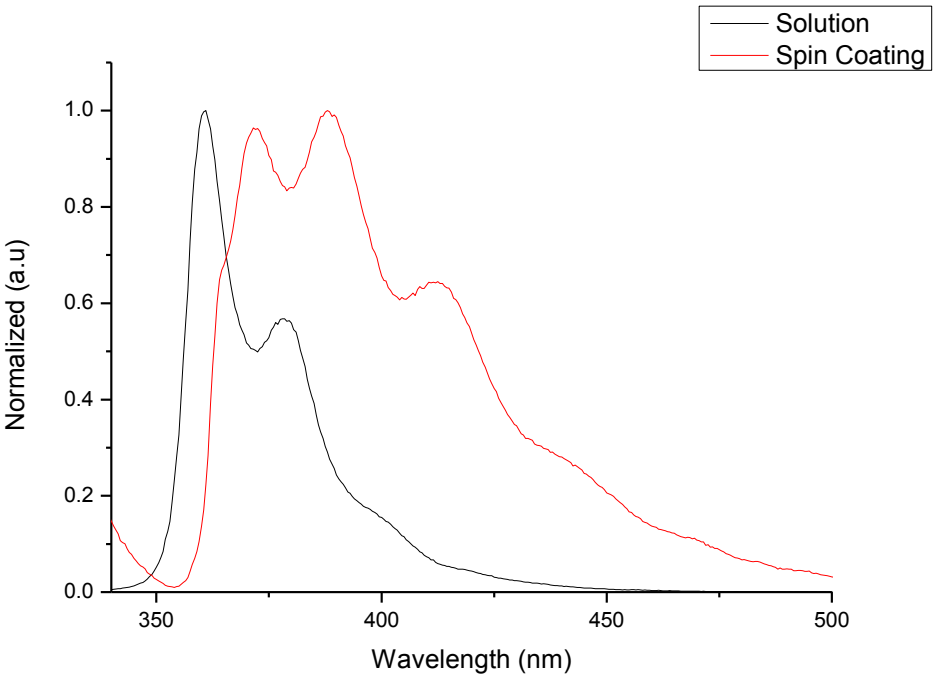

S 38 Fluorescence spectrum of **SIA-F** in cyclohexane solution (λ_{exc} = 295 nm) and in thin film (λ_{exc} = 300 nm)

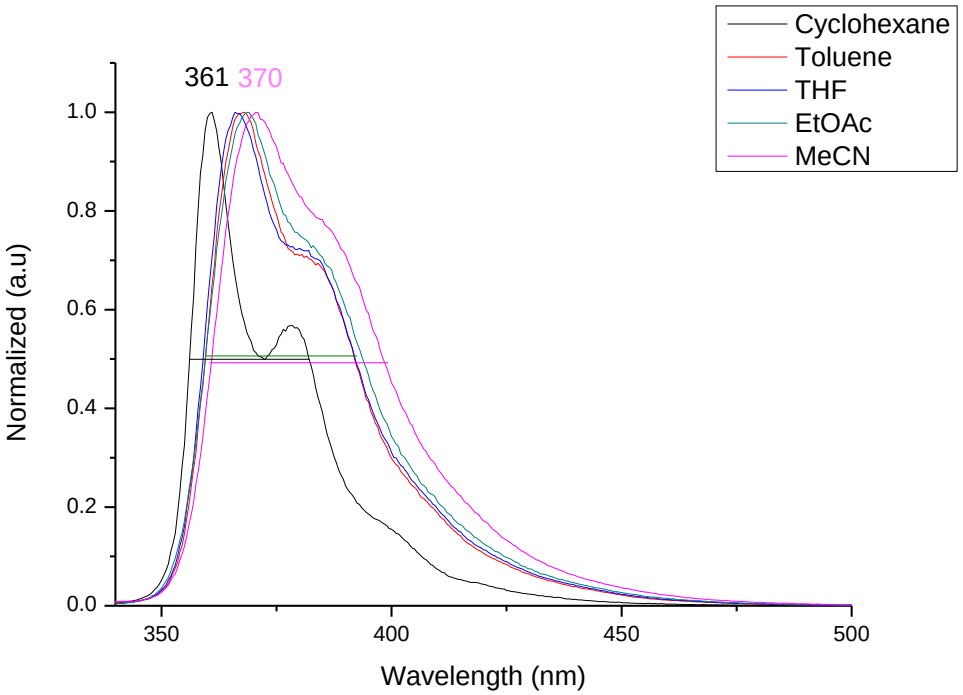

S 39 Fluorescence spectra of **SIA-F** in various solvents (λ_{ex} Cyclohexane: 295 nm, Toluene: 305.5 nm, THF: 305 nm, EtOAc: 300 nm, MeCN: 308.5 nm)

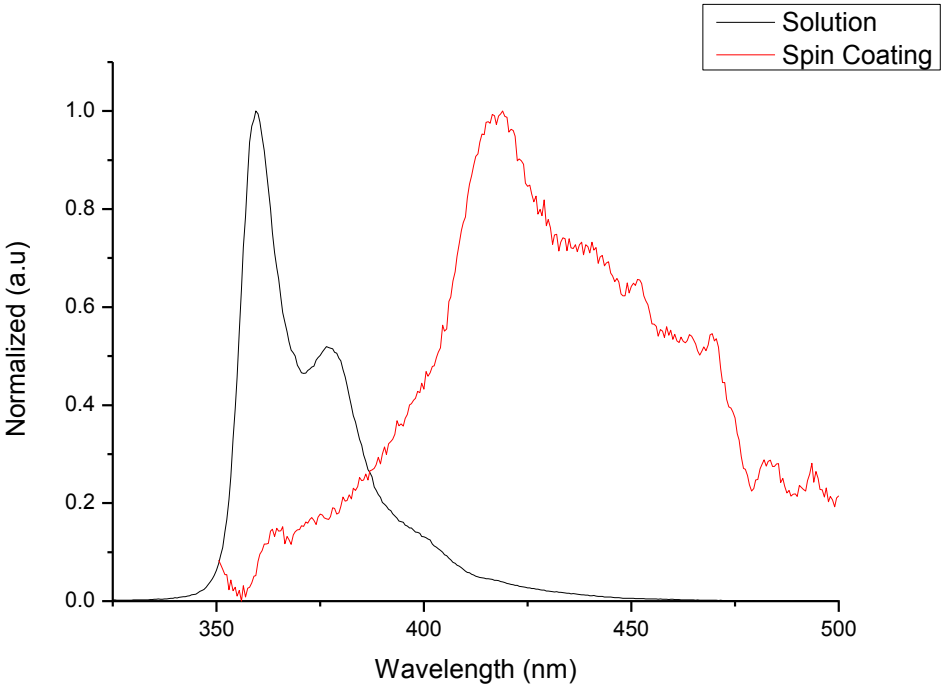

S 40 Fluorescence spectrum of **SIA-DAF** in cyclohexane solution (λ_{exc} = 294 nm) and in thin film (λ_{exc} = 280 nm)

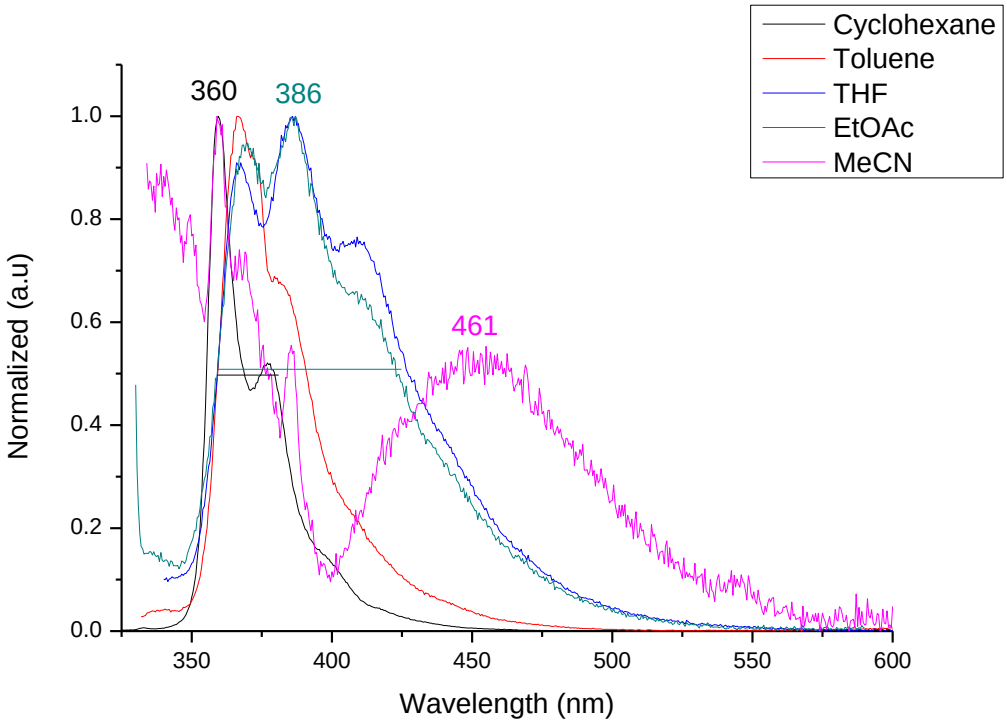

S 41 Fluorescence spectrum of **SIA-DAF** in various solvents (λ_{ex} Cyclohexane: 303 nm, Toluene: 305 nm, THF: 320 nm, EtOAc: 319 nm, MeCN: 323.5 nm)

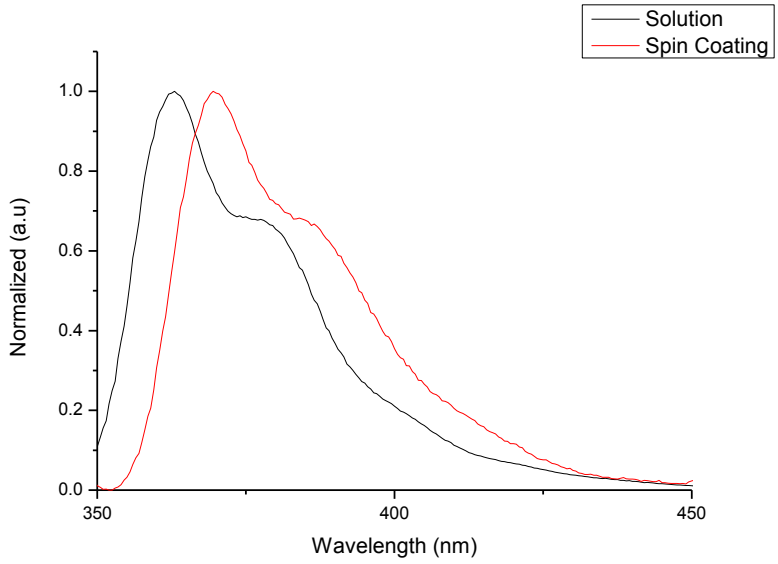

S 42 Fluorescence spectrum of **SIA-TXO$_2$** in cyclohexane solution (λ_{exc} = 306 nm) and in thin film (λ_{exc} = 280 nm)

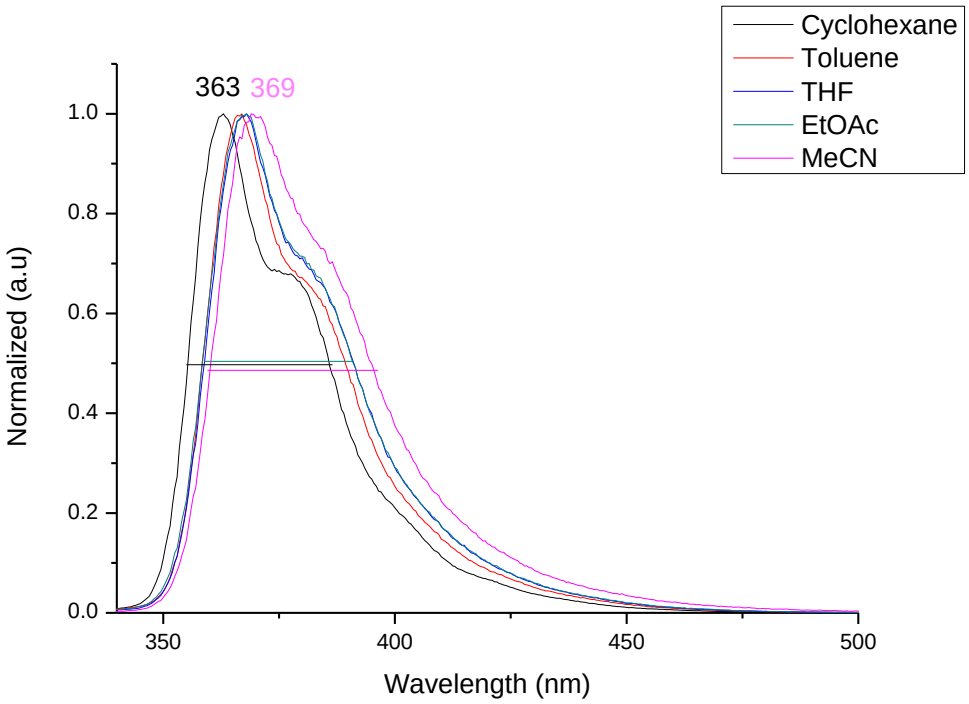

S 43 Fluorescence spectrum of **SIA-TXO$_2$** in various solvents (λ_{ex} Cyclohexane: 306 nm, Toluene: 297.5 nm, THF: 298 nm, EtOAc: 299.5 nm, MeCN: 296.5 nm)

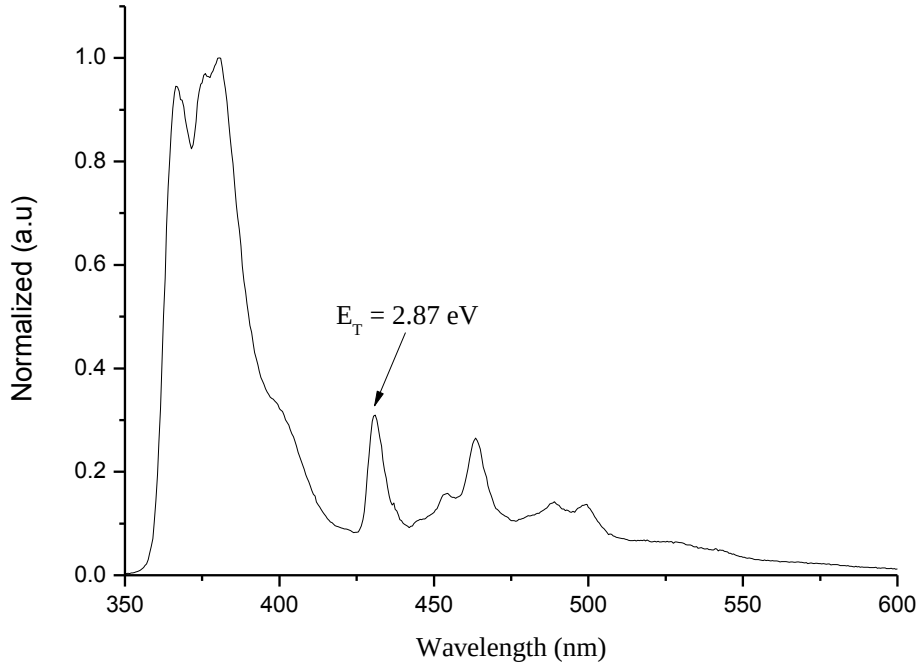

S 44 Emission spectrum of **SIA-F**, fluorescence and phosphorescence contributions recorded in a frozen matrix of 2-methyltetrahydrofuran at 77 K, λexc = 310 nm

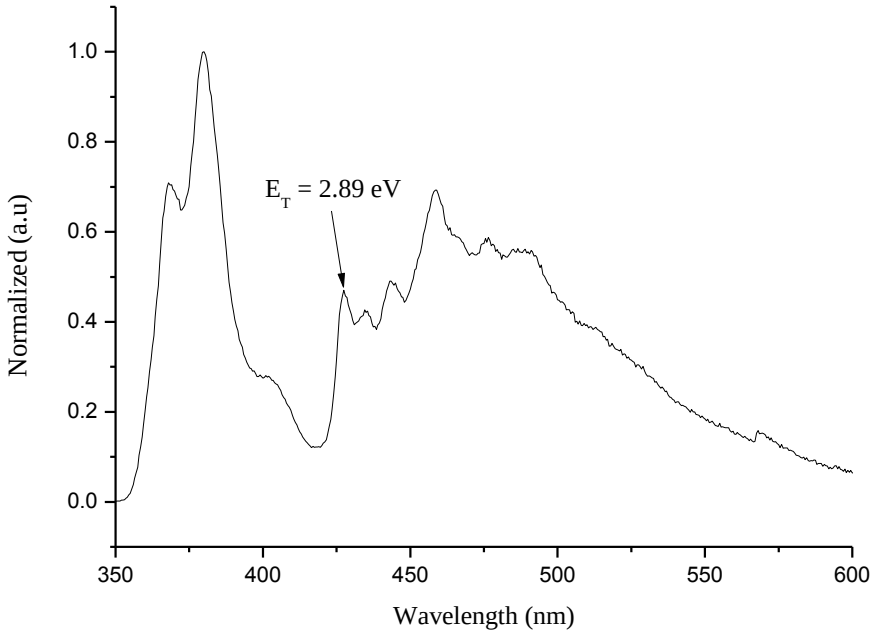

S 45 Emission spectrum of **SIA-DAF**, fluorescence and phosphorescence contributions recorded in a frozen matrix of 2-methyltetrahydrofuran at 77 K, λexc = 315 nm

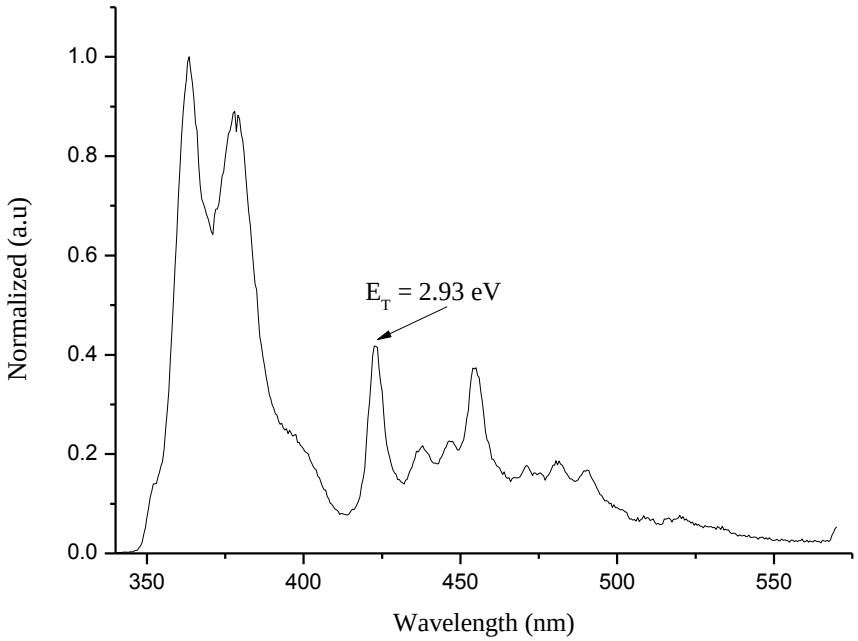

S 46 Emission spectrum of **SIA-TXO$_2$**, fluorescence and phosphorescence contributions recorded in a frozen matrix of 2-methyltetrahydrofuran at 77 K, λexc = 285 nm

ELECTROCHEMICAL PROPERTIES

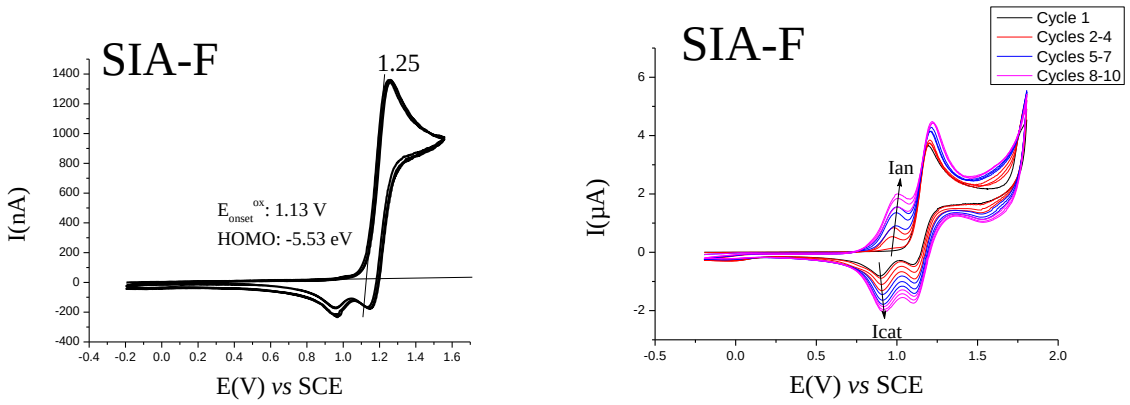

S 47 Cyclic voltammetry at 100 mV s^{-1} in CH_2Cl_2/[NBu_4] [PF_6] 0.2 M in presence of **SIA-F** (5 10^{-3} M).
Left three recurrent sweeps on the first oxidation wave showing the irreversibility of the redox process.
Right ten recurrent sweeps including the first and second oxidation waves showing a polymerization process.
Platinum disk working electrode (diameter 1 mm).

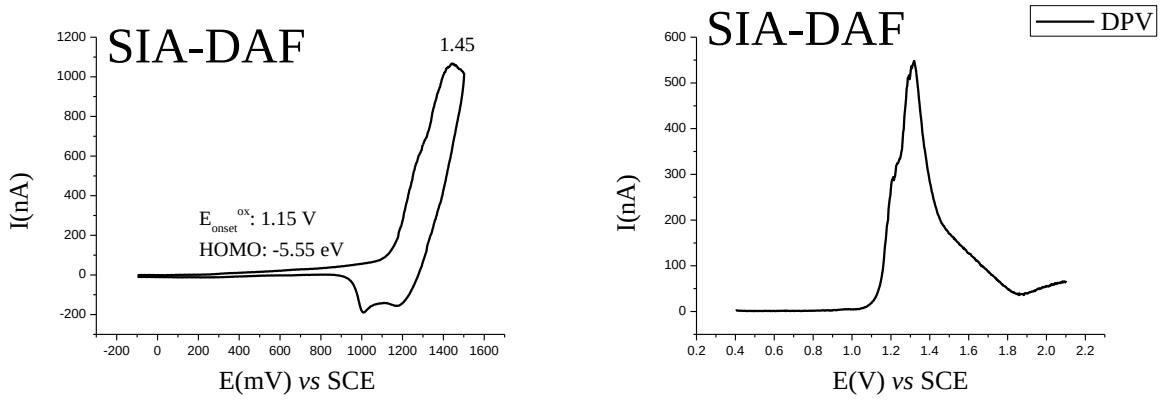

S 48 Cyclic voltammetry at 100 mV s^{-1} in CH_2Cl_2/[NBu_4] [PF_6] 0.2 M in presence of **SIA-DAF** (5 10^{-3} M).
Left one sweep on the two first irreversible oxidation waves.
Right Differential Pulse Voltammetry on the two first oxidation waves
Platinum disk working electrode (diameter 1 mm).

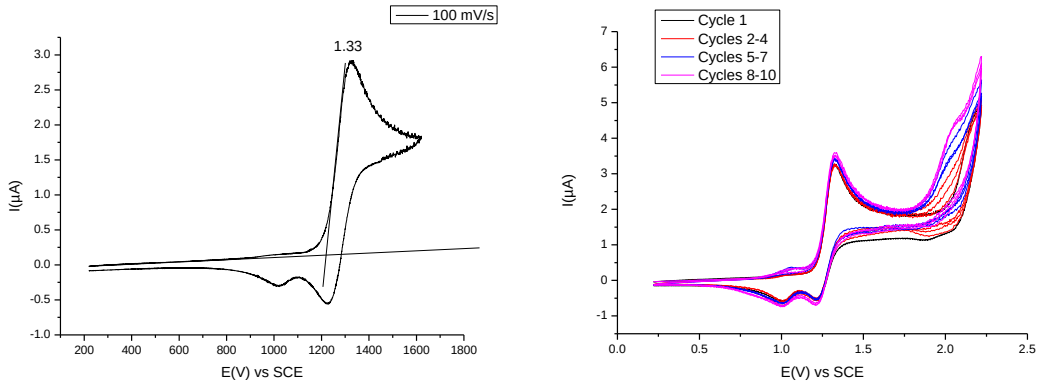

S 49 Cyclic voltammetry at 100 mV s^{-1} in CH_2Cl_2/[NBu_4] [PF_6] 0.2 M in presence of **SIA-TXO$_2$** (5 10^{-3} M). Left three recurrent sweeps on the first oxidation wave showing the irreversibility of the redox process.
Right ten recurrent sweeps including the first and second oxidation waves showing a very weak polymerization process.
Platinum disk working electrode (diameter 1 mm).

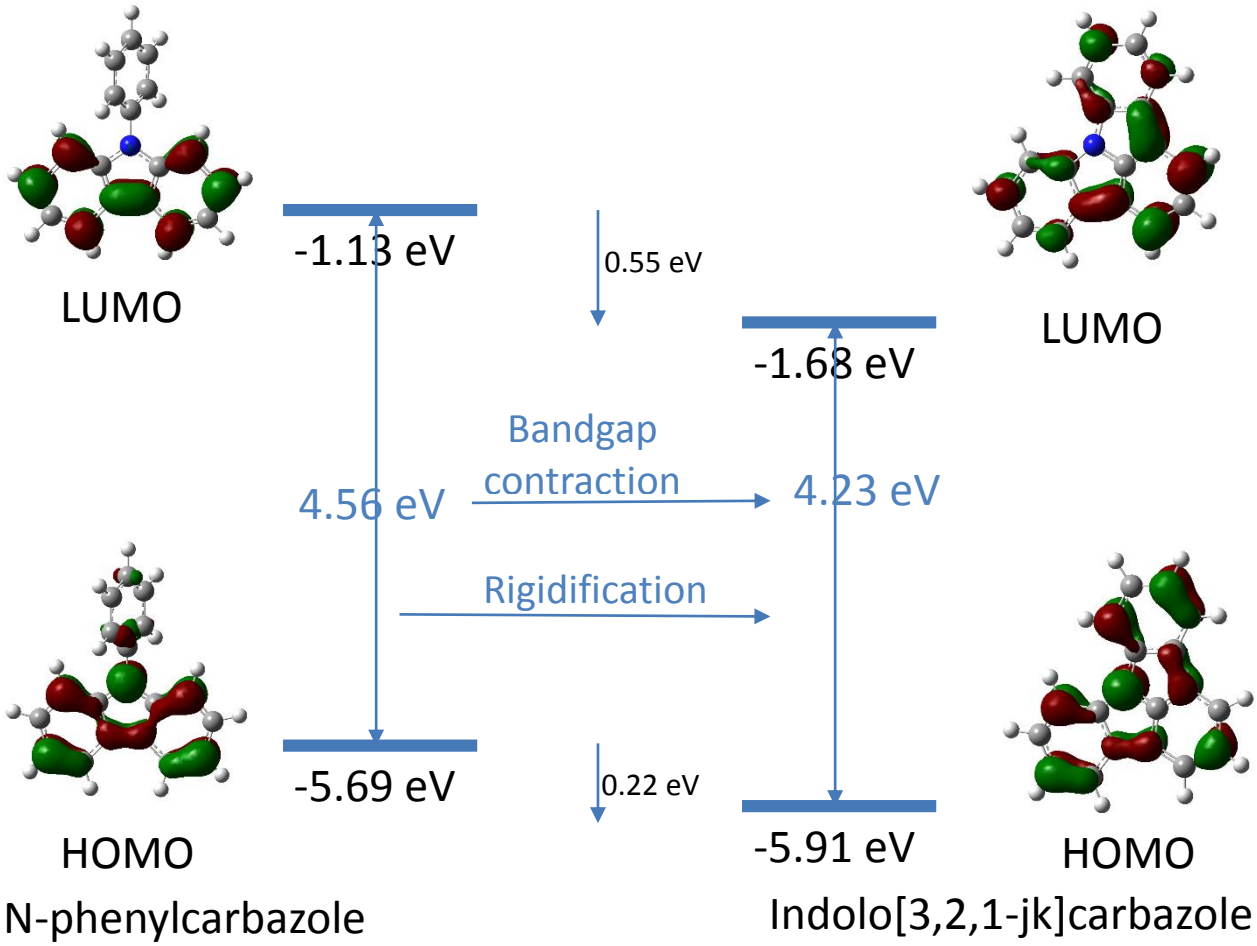

S 50 Calculated frontier molecular orbitals by DFT of N-Phenylcarbazole and Indolo[3,2,1-jk]carbazole after geometry optimization with DFT B3LYP/6-311G+(d,p), show with an isovalue of 0.04

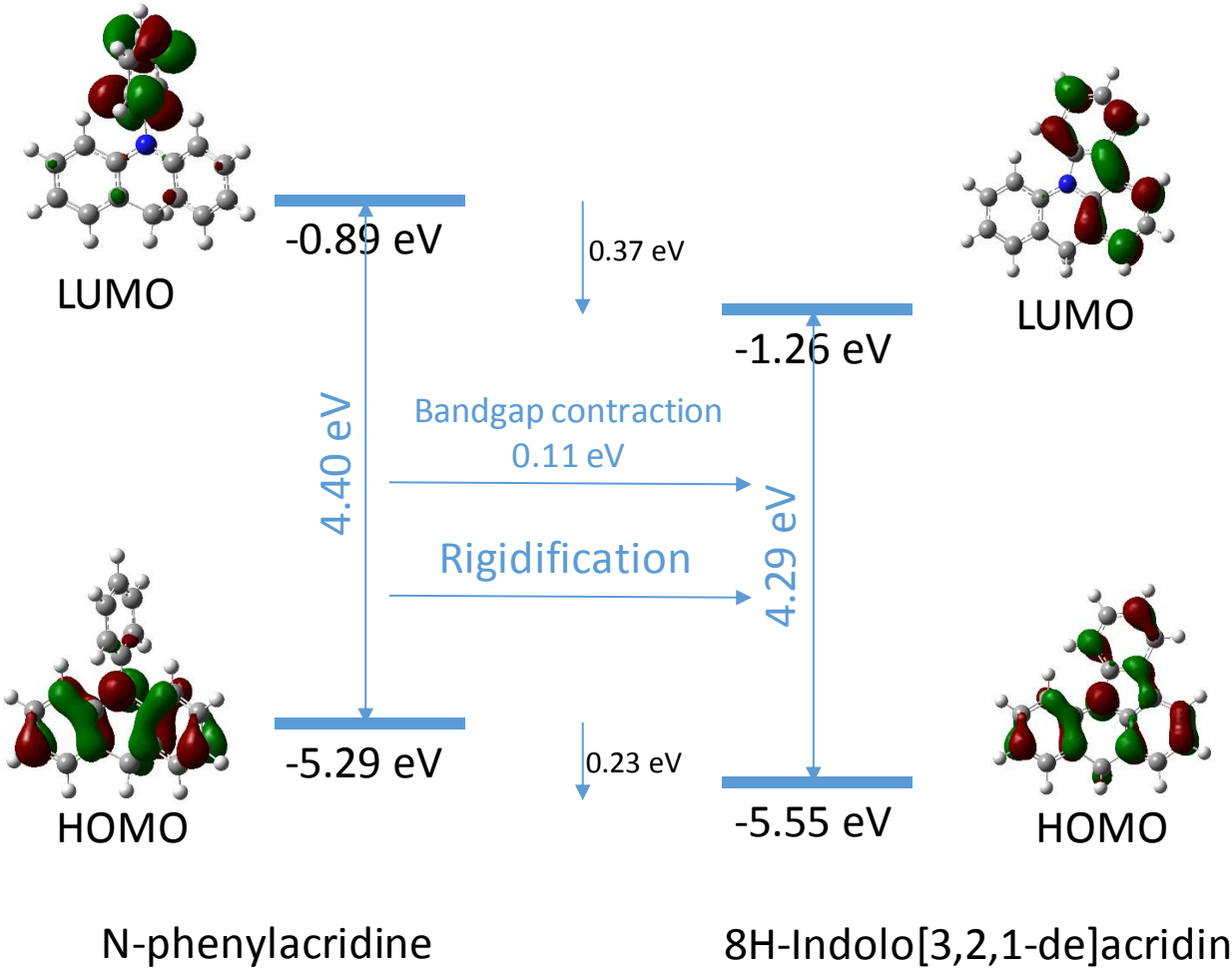

S 51 Calculated frontier molecular orbitals by DFT of N-phenylacridine and 8H-indolo[3,2,1-de]acridine after geometry optimization with DFT B3LYP/6-311G+(d,p), show with an isovalue of 0.04

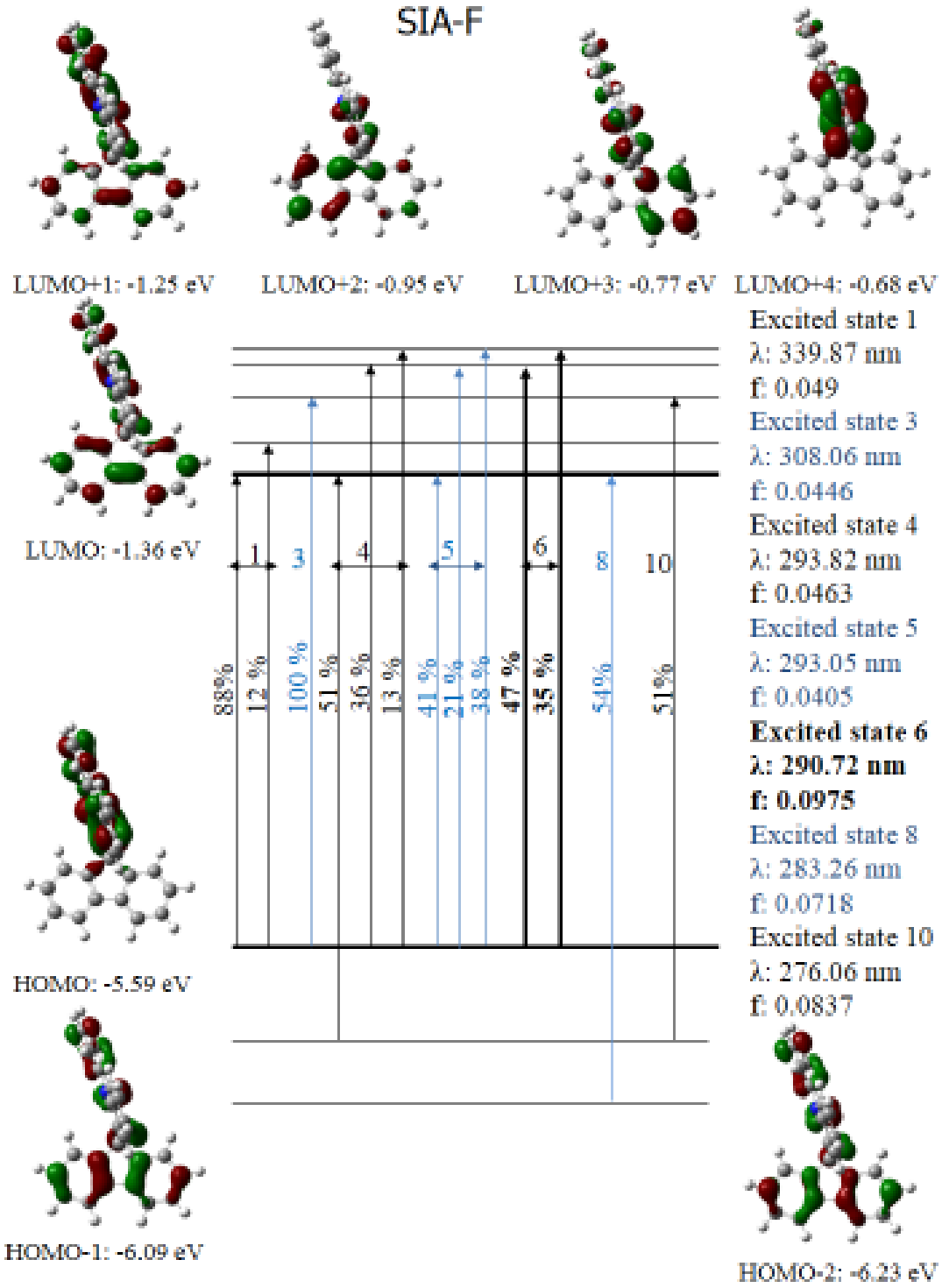

S 52 Calculated frontier molecular orbitals by DFT and the 10th first calculated electronic transitions by TD-DFT of **SIA-F**, after geometry optimization with DFT B3LYP/6-311G+(d,p), show with an isovalue of 0.04

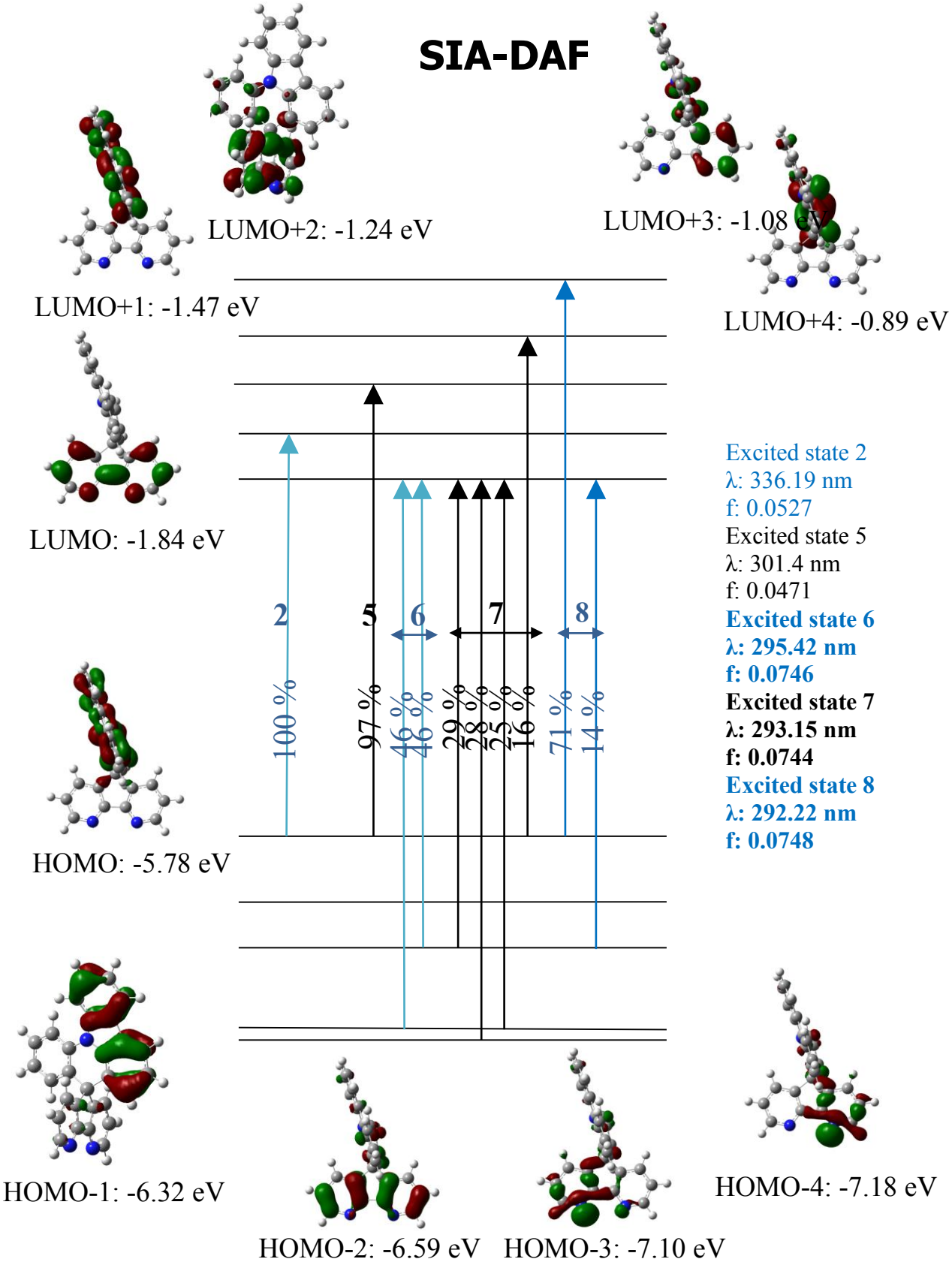

S 53 Calculated frontier molecular orbitals by DFT and the 10th first calculated electronic transitions by TD-DFT of **SIA-DAF**, after geometry optimization with DFT B3LYP/6-311G+(d,p), show with an isovalue of 0.04

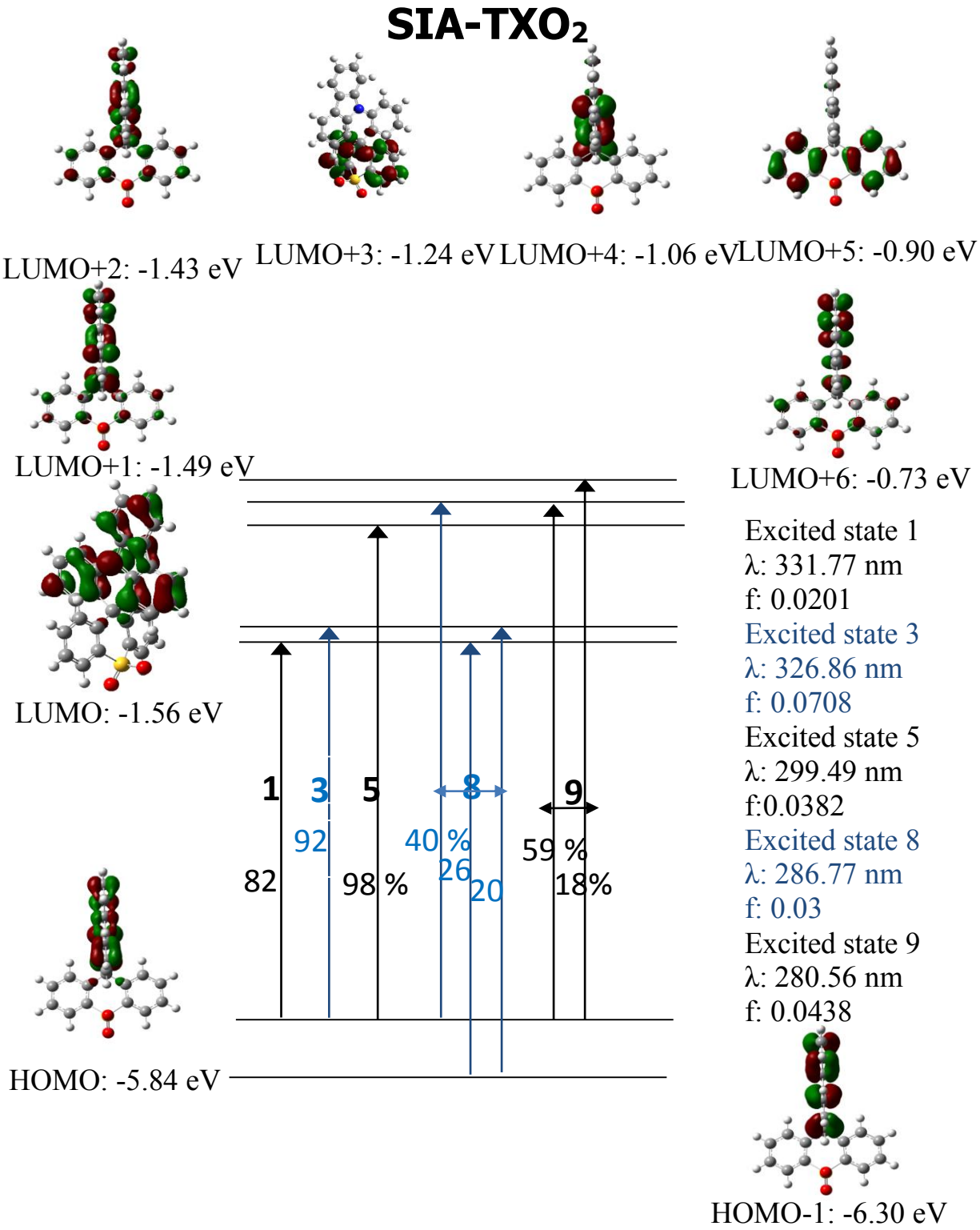

S 54 Calculated frontier molecular orbitals by DFT and the 12th first calculated electronic transitions by TD-DFT of **SIA-TXO$_2$**, after geometry optimization with DFT B3LYP/6-311G+(d,p), show with an isovalue of 0.04

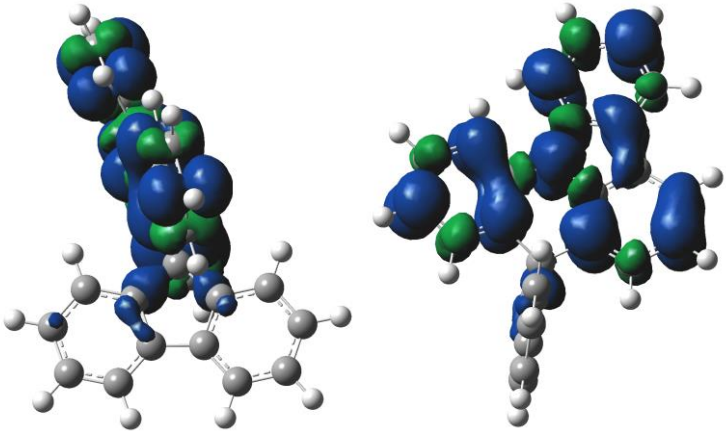

S 55 Spin density of the cation radical of SIA-F (**SIA-F**$^{\cdot+}$) shown with the fluorene in plane (left) and with the indoloacridine in plane (right) with an isovalue of 0.01 [e bohr^{-3}]$^{1/2}$

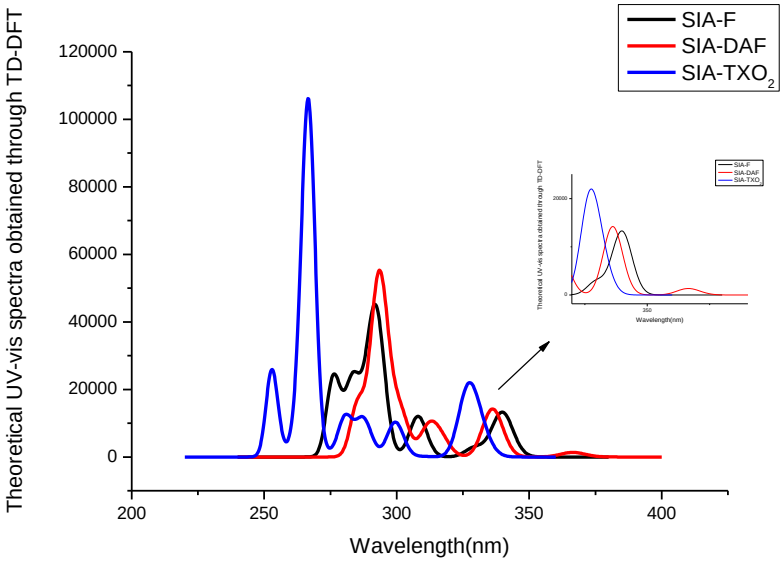

S 56 Predicted UV-vis spectra from TD-DFT energy calculations of **SIA-F**, **SIA-DAF** and **SIA-TXO$_2$**, after geometry optimization with DFT B3LYP/6-311G+(d,p). Inset a zoom between 320 and 385 nm.

GREEN DEVICES PERFORMANCES

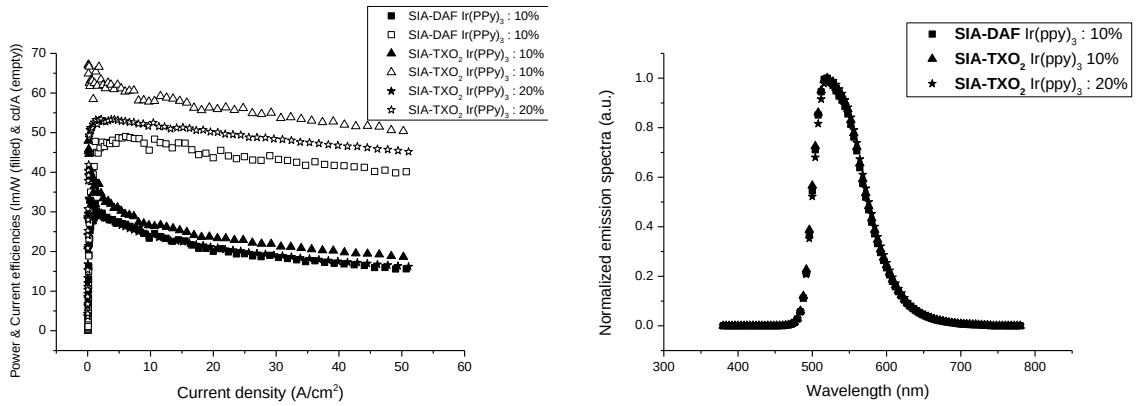

S 57 Current (empty symbol) and power efficiencies (filled symbol) versus current density of the green devices using **SIA-DAF** doped with $Ir(ppy)_3$ 10 % or **SIA-TXO$_2$** doped with $Ir(ppy)_3$ 10 or 20 % in mass as emitting layer (left). Corresponding EL spectra recorded at 10 mA/cm^2 (right).

BLUE DEVICES PERFORMANCES

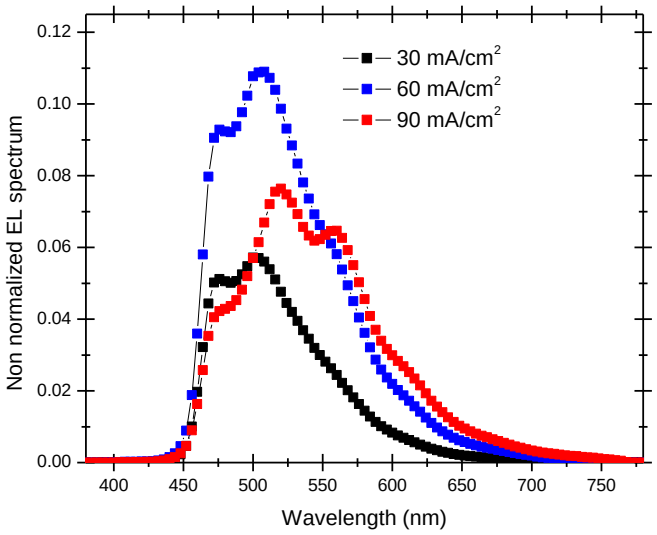

S 58 Non-normalized EL spectra of **SIA-DAF** + 10% FIrpic recorded at different current densities: 30 mA/cm^2 (black line), 60 mA/cm^2 (blue line) and 90 mA/cm^2 (red line).

COPIES OF NMR SPECTRA

^{1}H-**(1)**-CD_2Cl_2

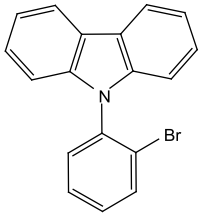

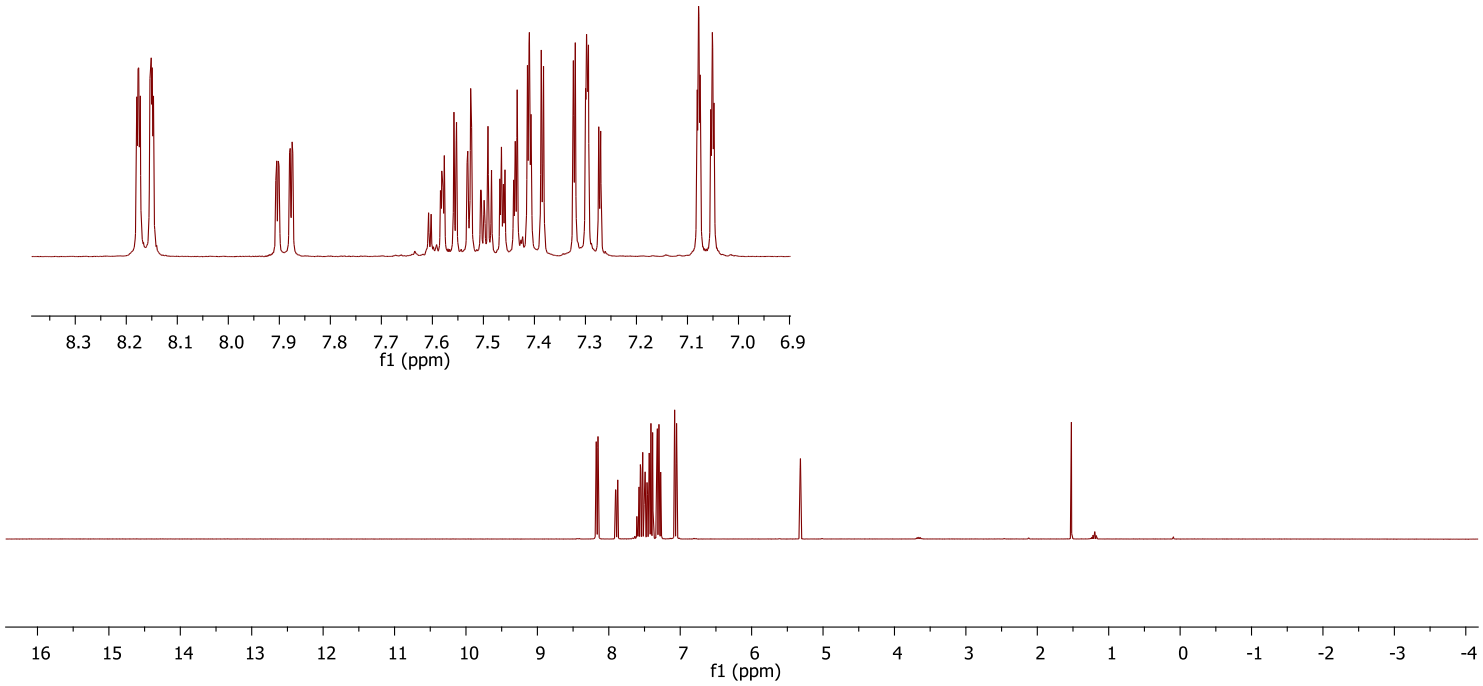

^{13}C-**(1)**-CD_2Cl_2

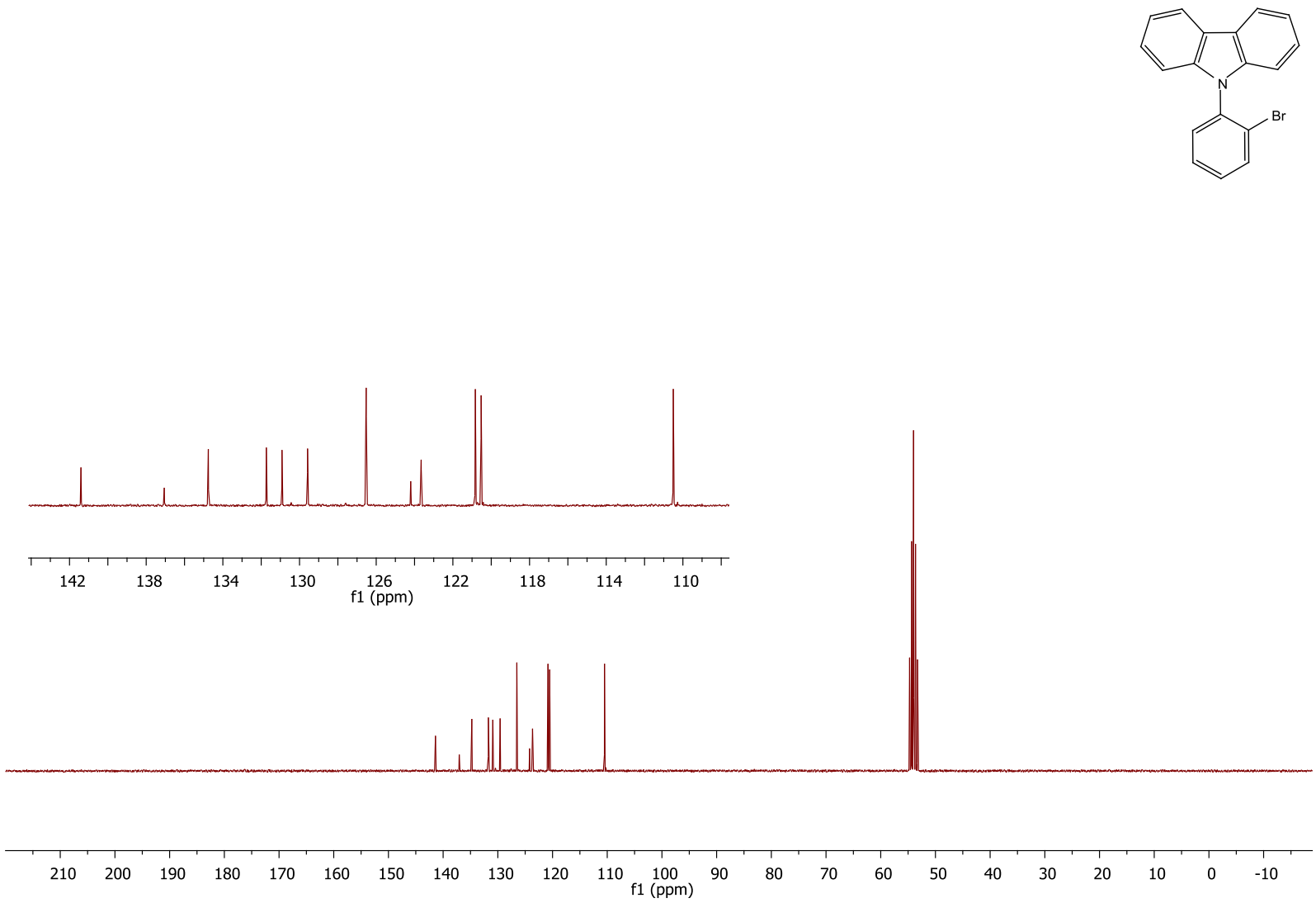
N
Br
142
138
134
130
126
122
118
114
110
f1 (ppm)
210
200
190
180
170
160
150
140
130
120
110
100
90
80
70
60
50
40
30
20
10
0
-10
f1 (ppm)

DEPT-**(1)**-CD_2Cl_2

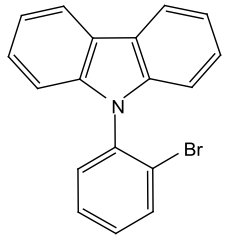

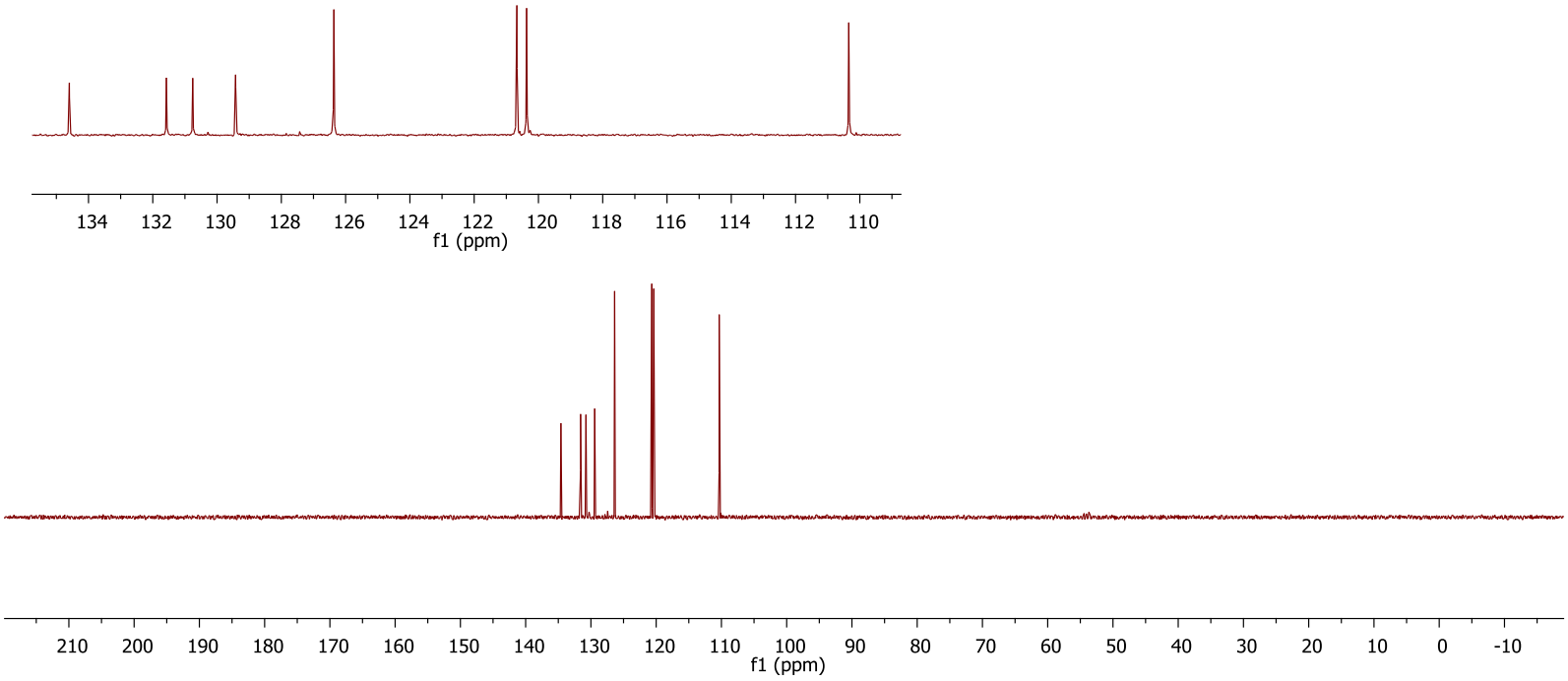

^{1}H-**(2)**-CD_2Cl_2

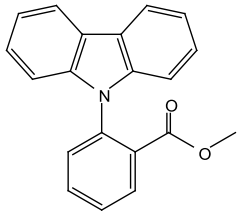
N
O
O

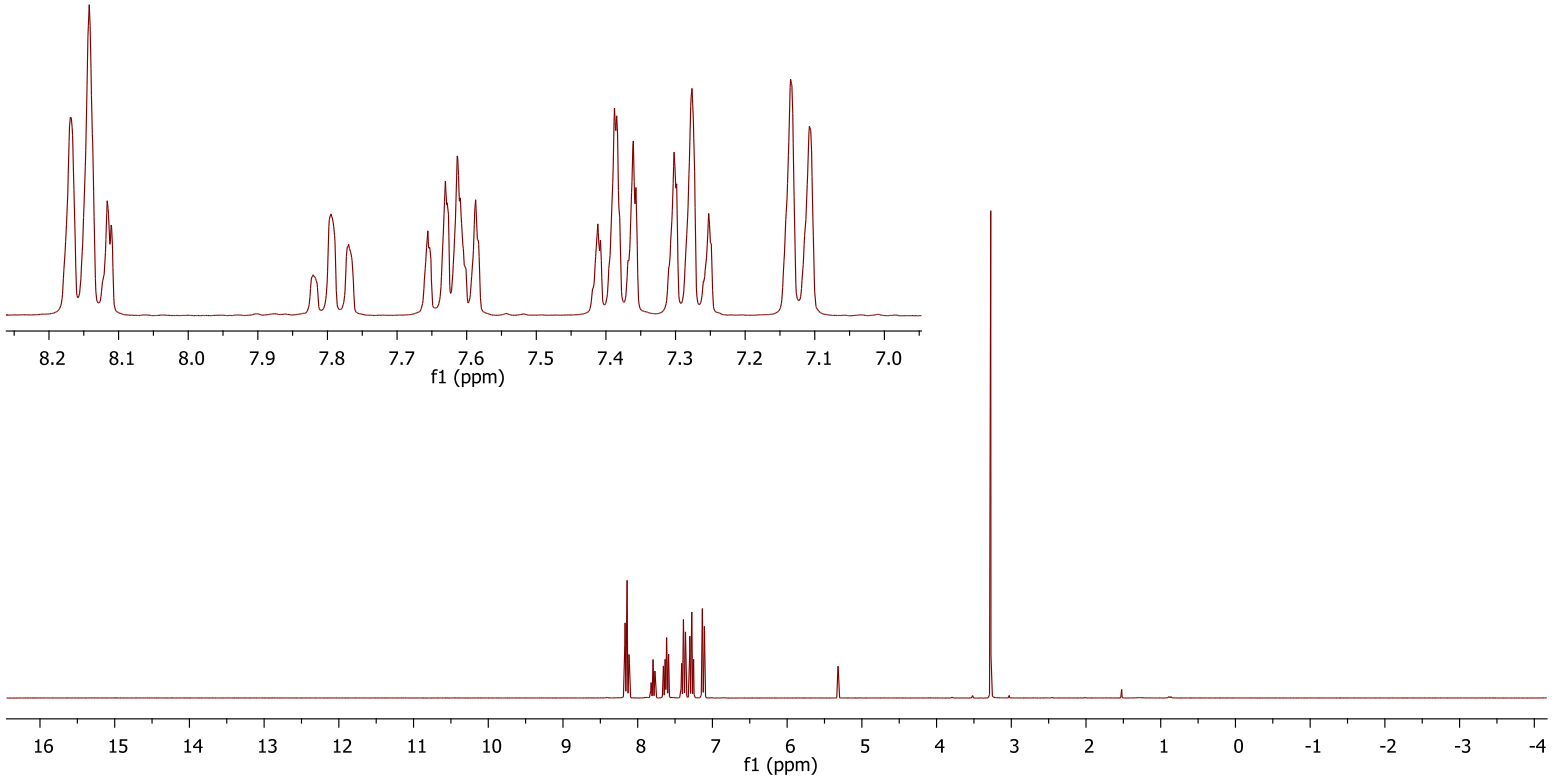
8.2
8.1
8.0
7.9
7.8
7.7
7.6
7.5
7.4
7.3
7.2
7.1
7.0
f1 (ppm)
16
15
14
13
12
11
10
9
8
7
6
5
4
3
2
1
0
-1
-2
-3
-4
f1 (ppm)

^{13}C-**(2)**-CD_2Cl_2

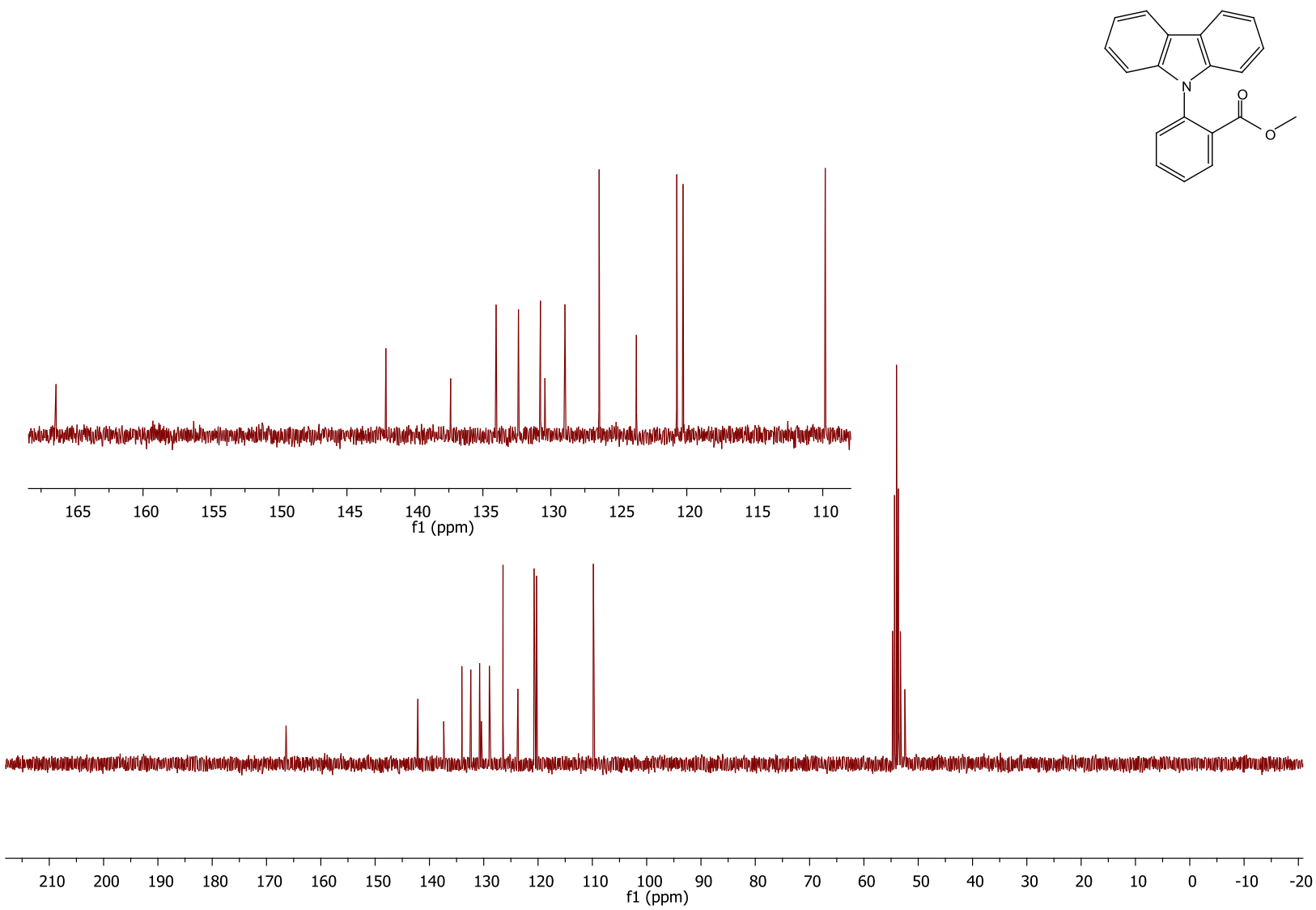
N
O
O
165 160 155 150 145 140 135 130 125 120 115 110
f1 (ppm)
210 200 190 180 170 160 150 140 130 120 110 100 90 80 70 60 50 40 30 20 10 0 -10 -20
f1 (ppm)

DEPT-**(2)**-CD_2Cl_2

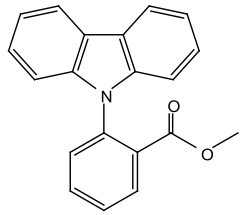

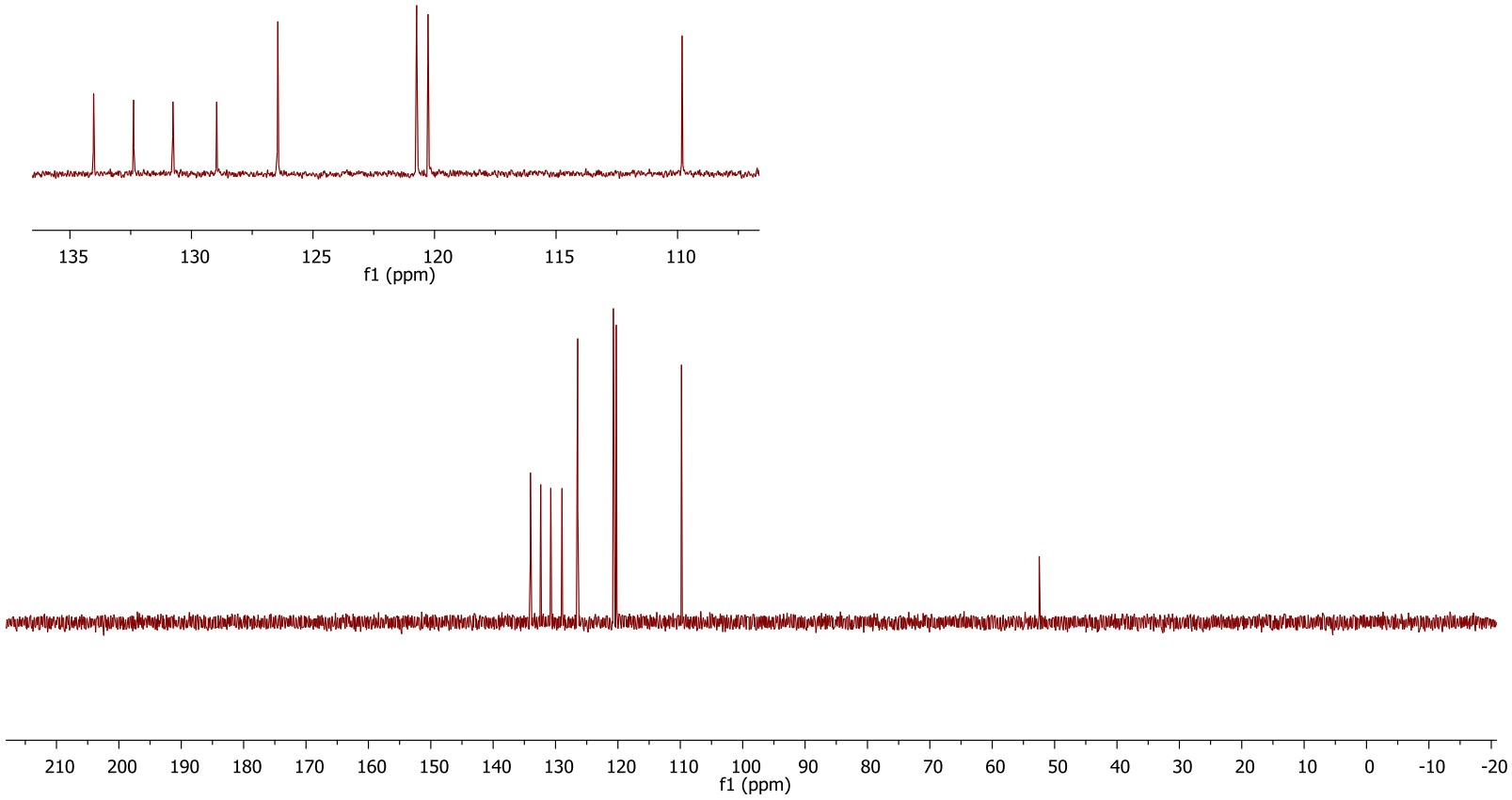

^{1}H-**(3)**-CD_2Cl_2

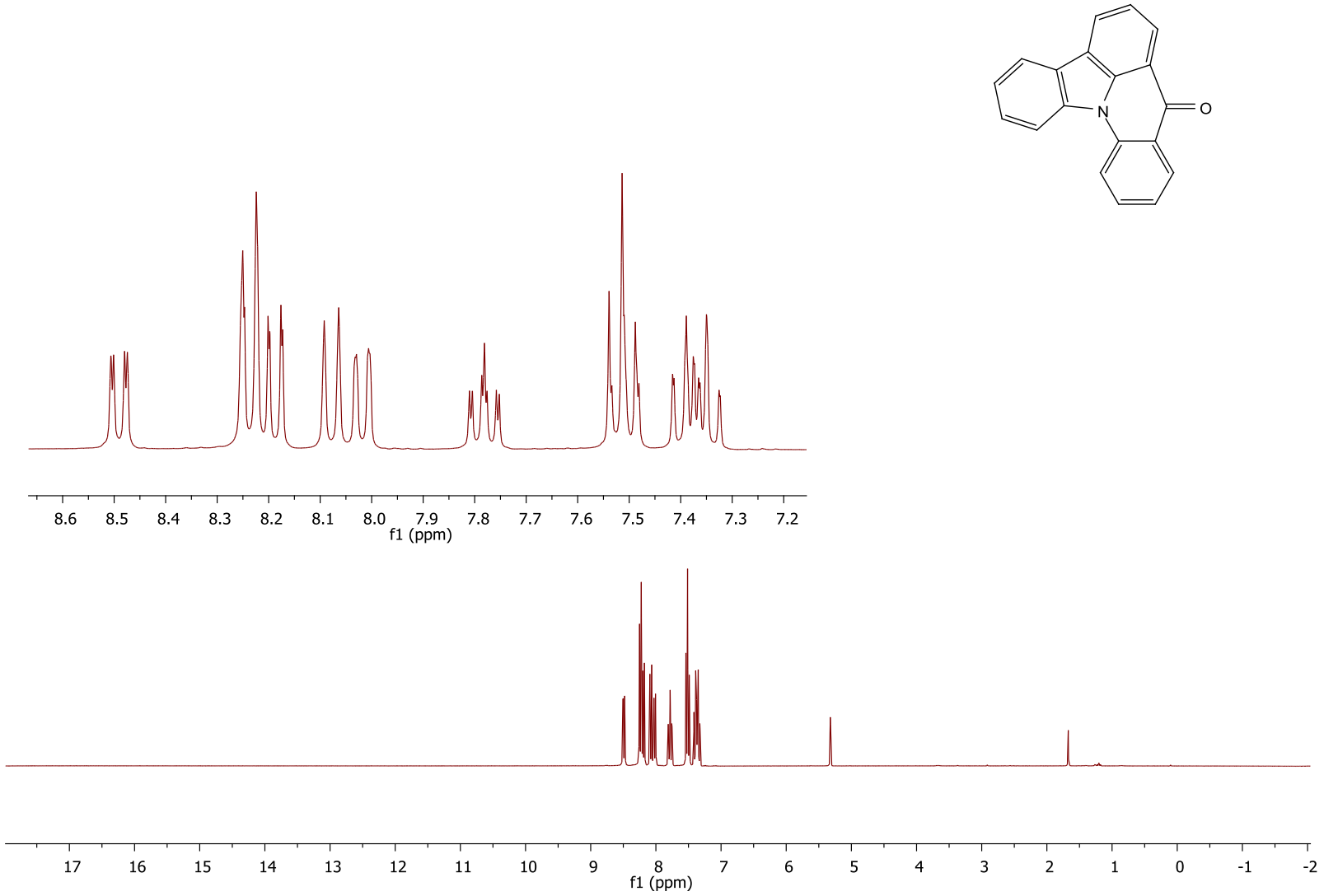
N
O
8.6
8.5
8.4
8.3
8.2
8.1
8.0
7.9
7.8
7.7
7.6
7.5
7.4
7.3
7.2
f1 (ppm)
17
16
15
14
13
12
11
10
9
8
7
6
5
4
3
2
1
0
-1
-2
f1 (ppm)

^{13}C-**(3)**-CD_2Cl_2

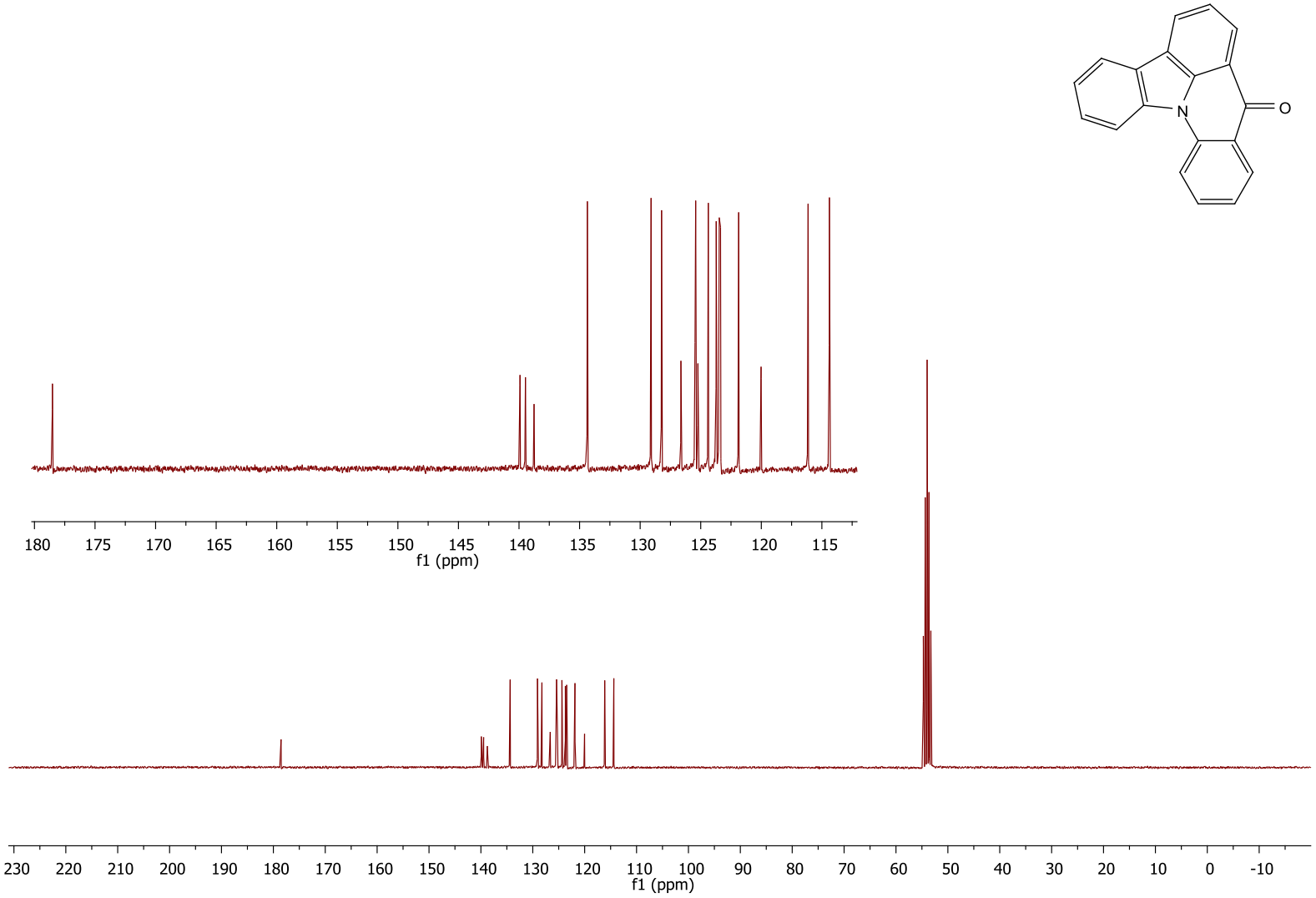
N
O
180 175 170 165 160 155 150 145 140 135 130 125 120 115
f1 (ppm)
230 220 210 200 190 180 170 160 150 140 130 120 110 100 90 80 70 60 50 40 30 20 10 0 -10
f1 (ppm)

DEPT-**(3)**-CD_2Cl_2

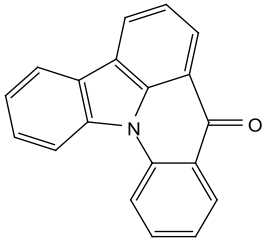

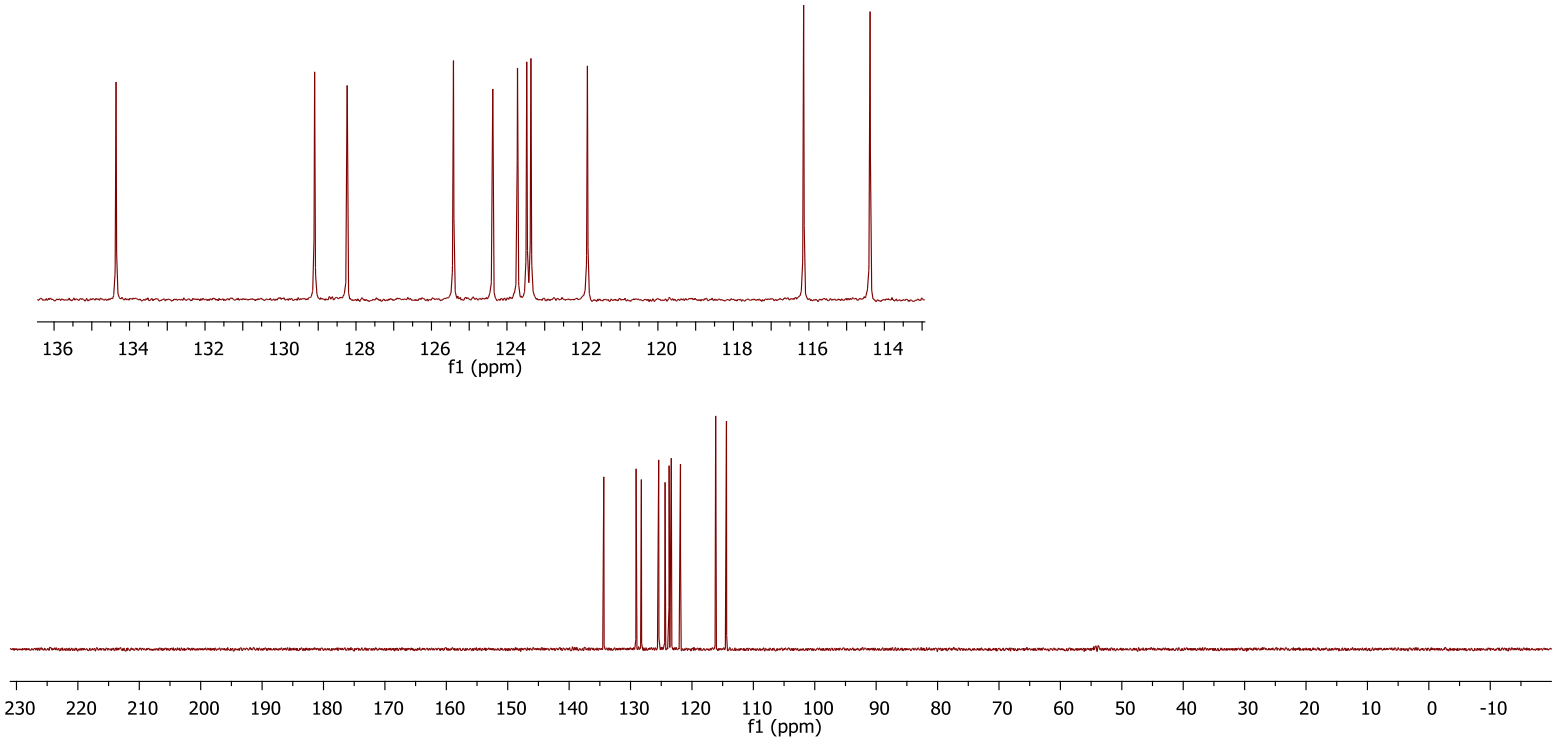

^{1}H-**(SIA-F)**-CD_2Cl_2

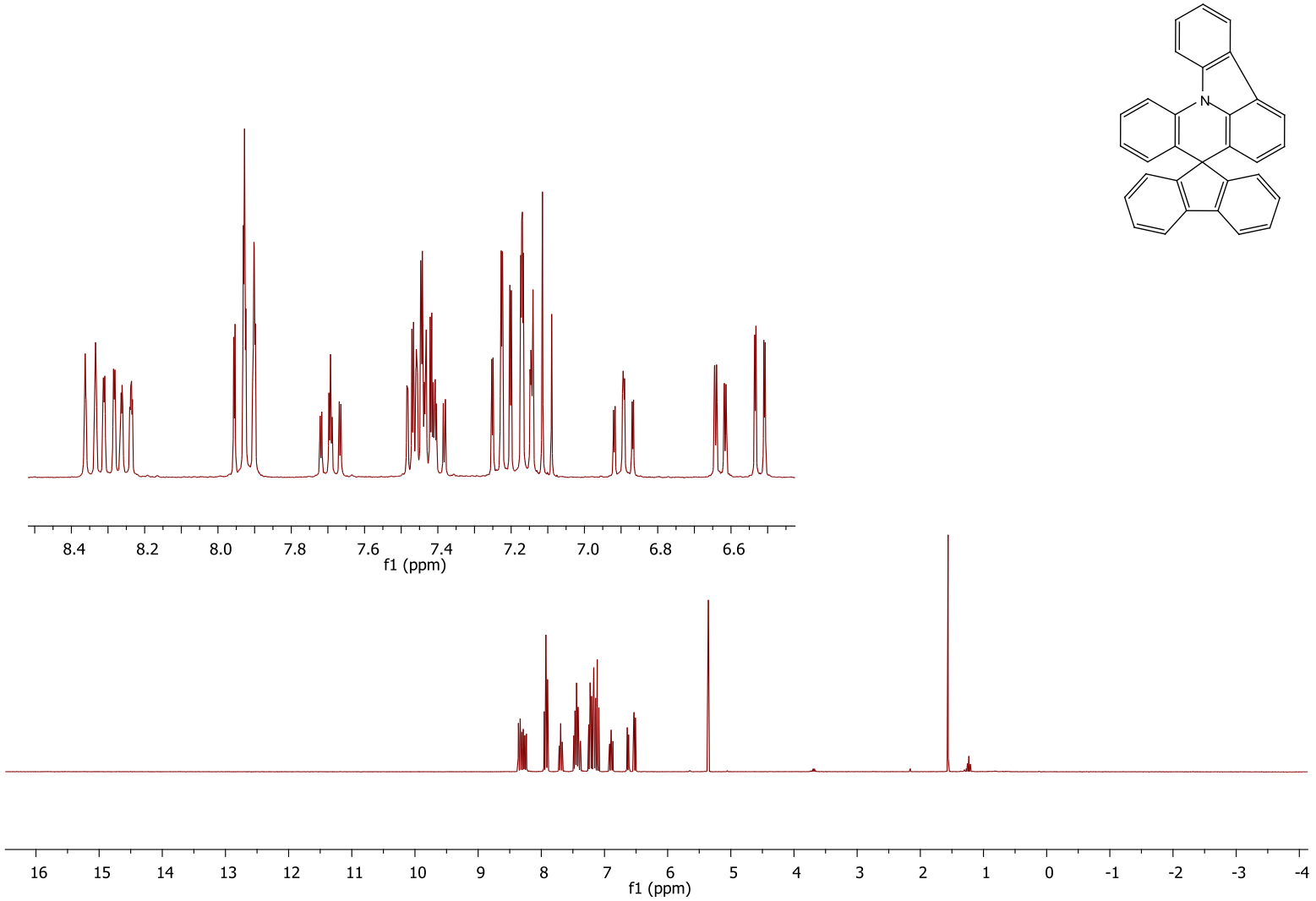

^{13}C-**(SIA-F)**-CD_2Cl_2

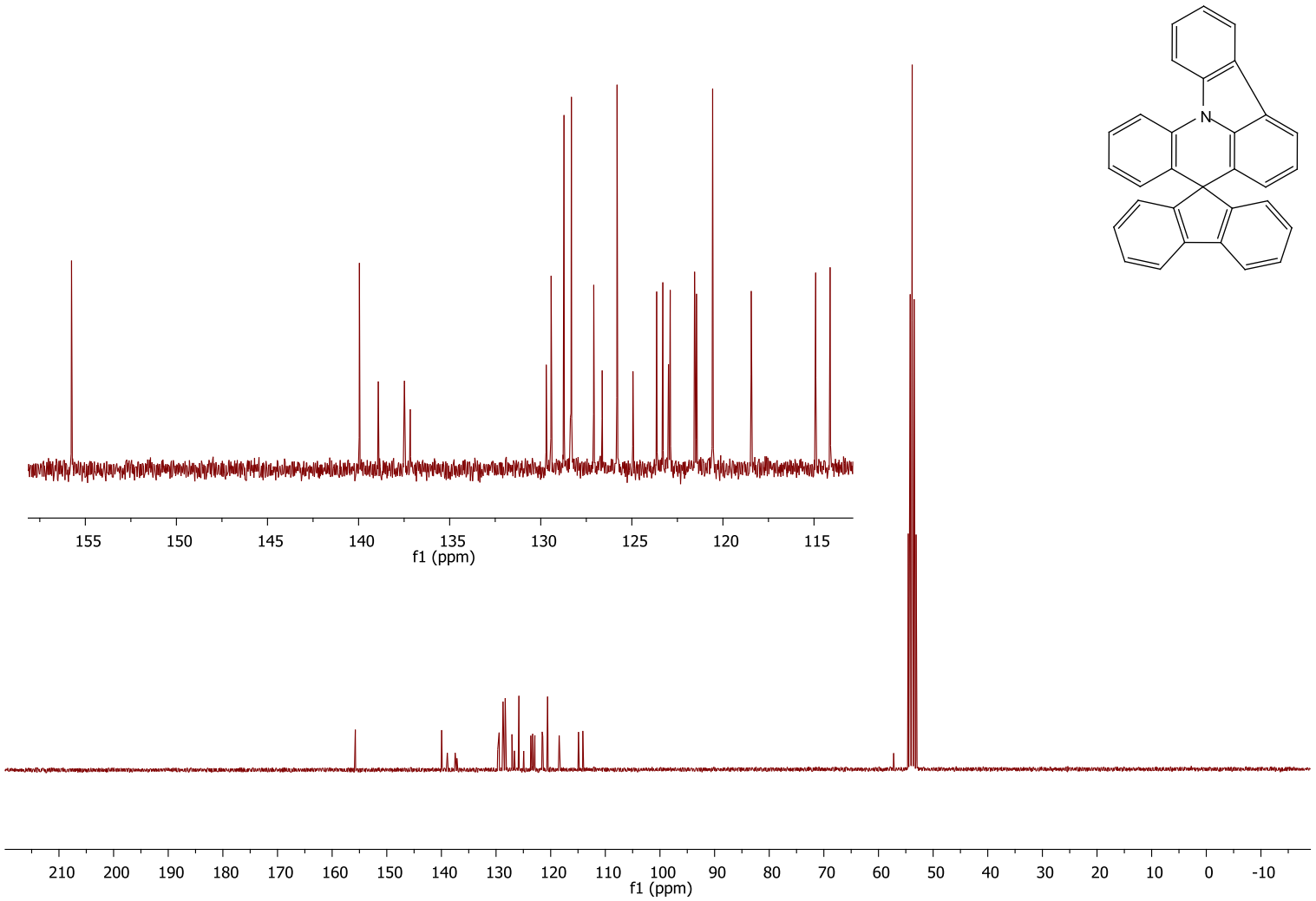

DEPT-**(SIA-F)**-CD_2Cl_2

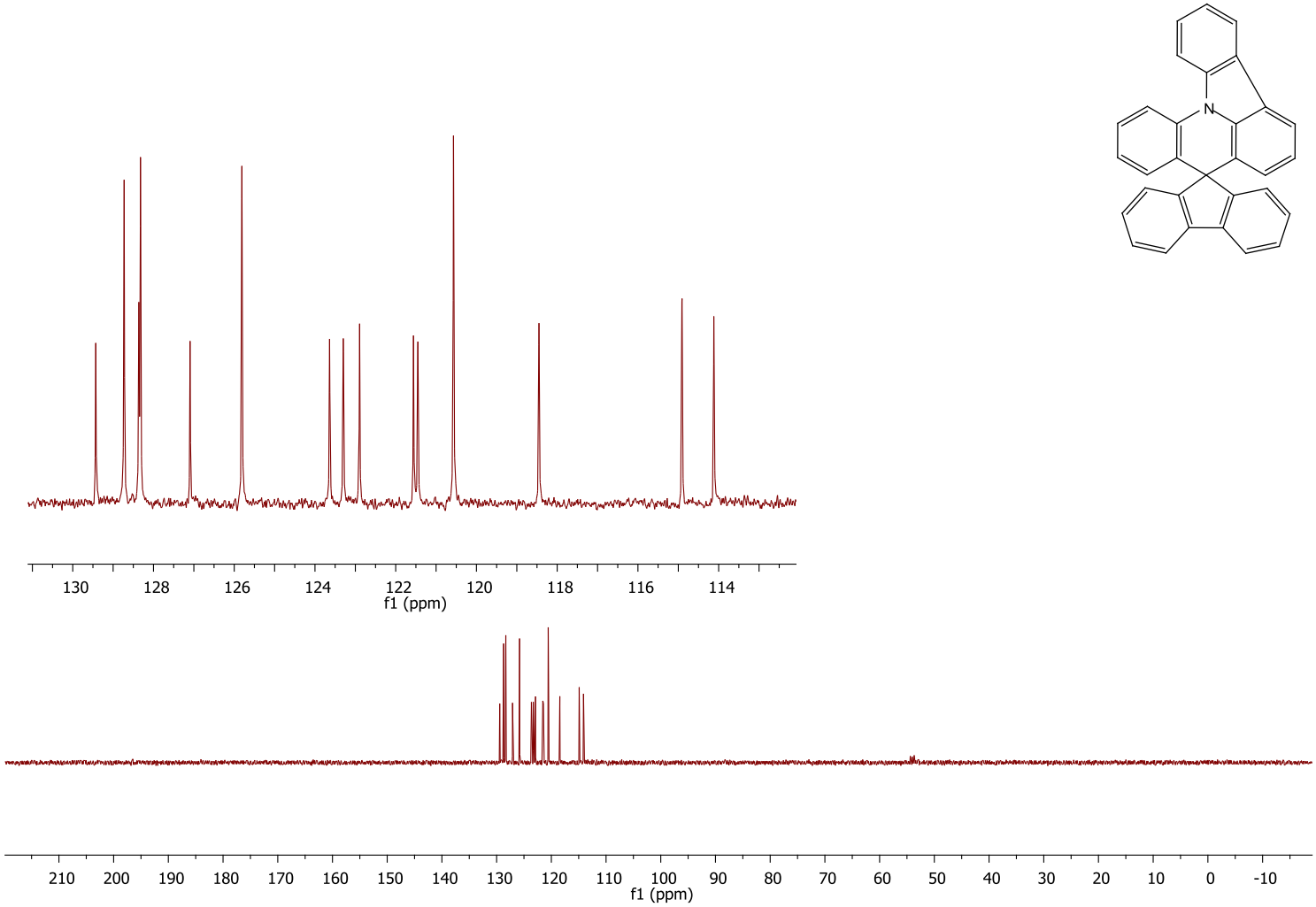

^{1}H-**(SIA-DAF)**-CD_2Cl_2

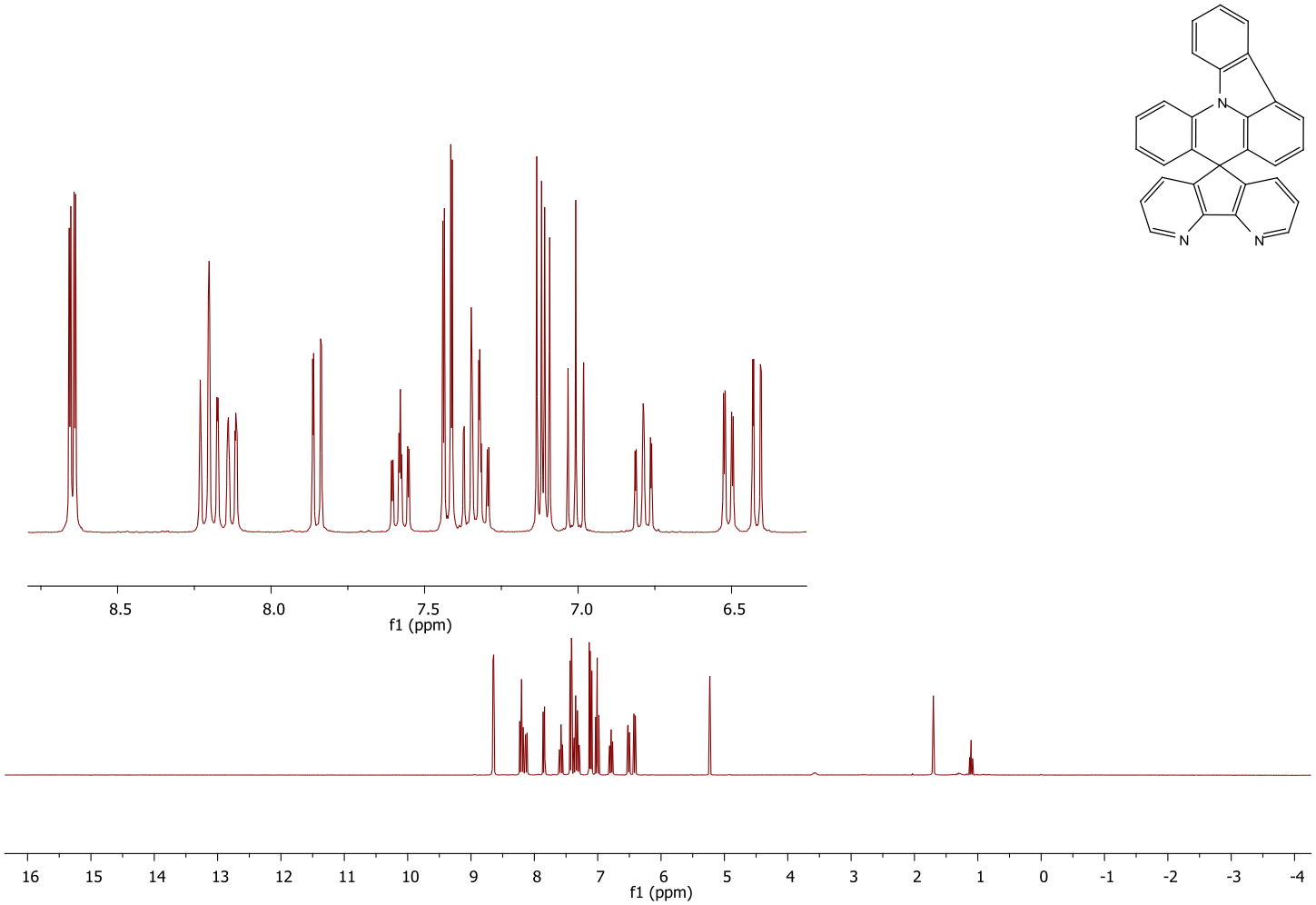

^{13}C-**(SIA-DAF)**-CD_2Cl_2

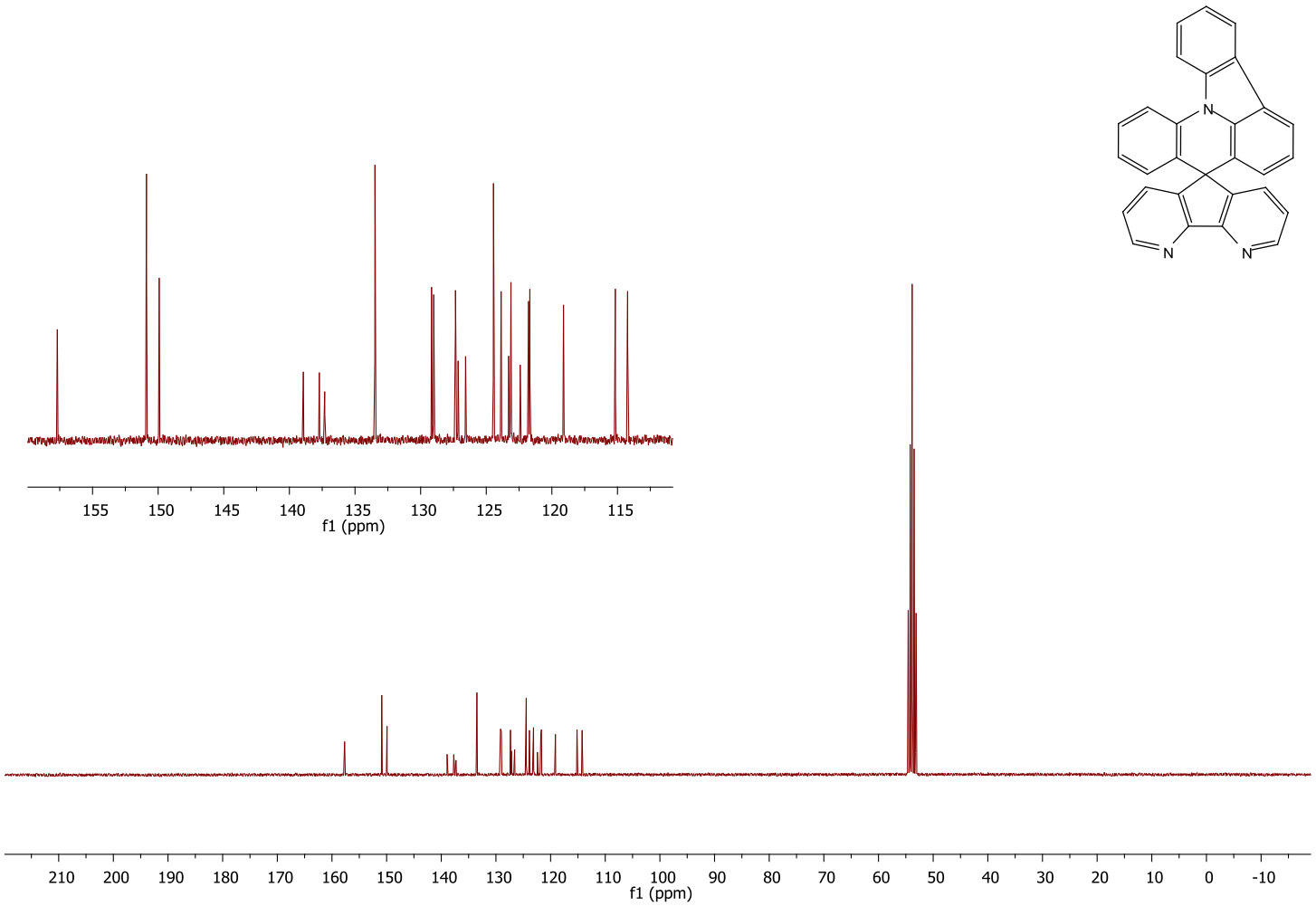

DEPT-**(SIA-DAF)**-CD_2Cl_2

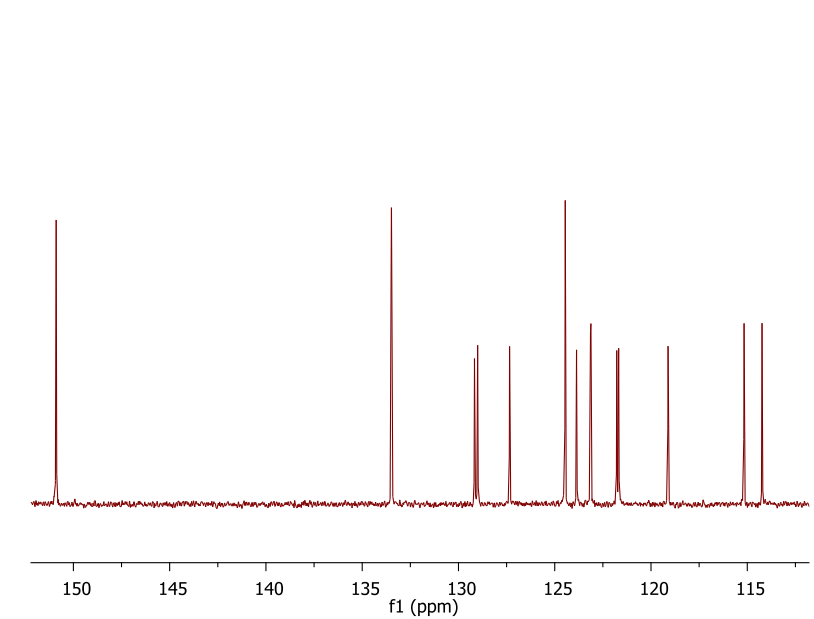

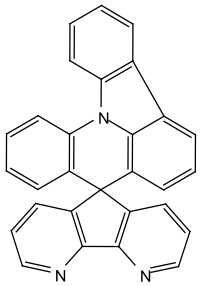

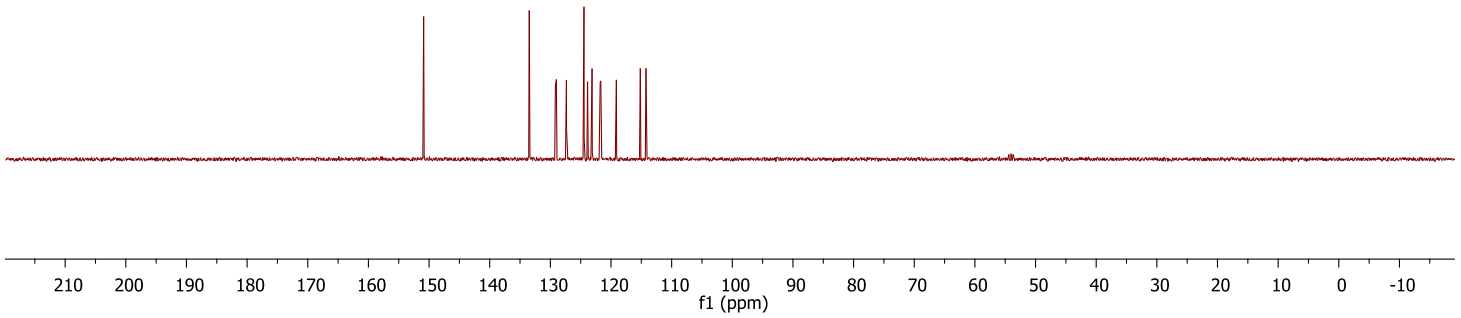

^{1}H-(**SIA-TXO$_2$**)-$CDCl_3$-

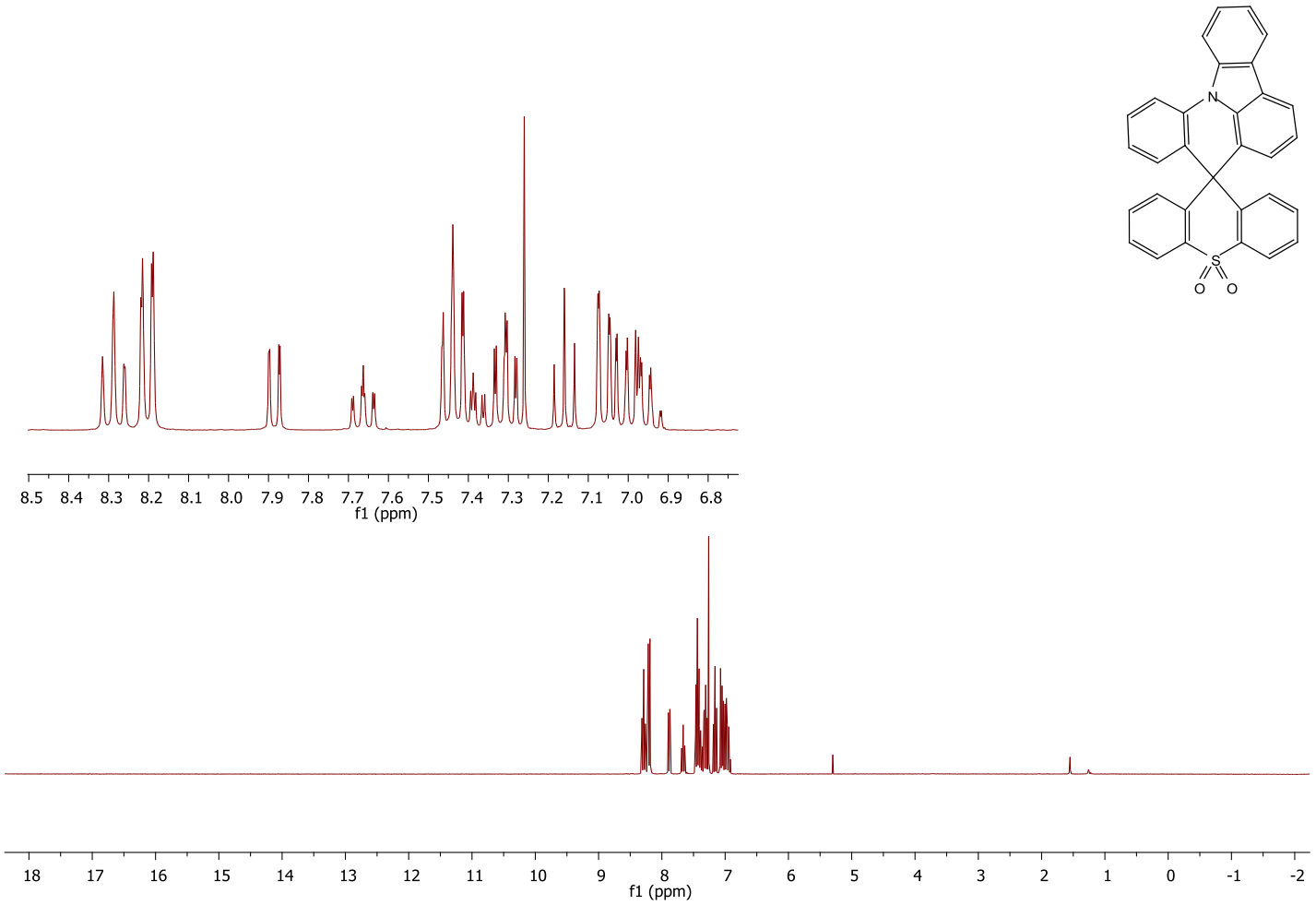

^{13}C-(**SIA-TXO$_2$**)-$CDCl_3$

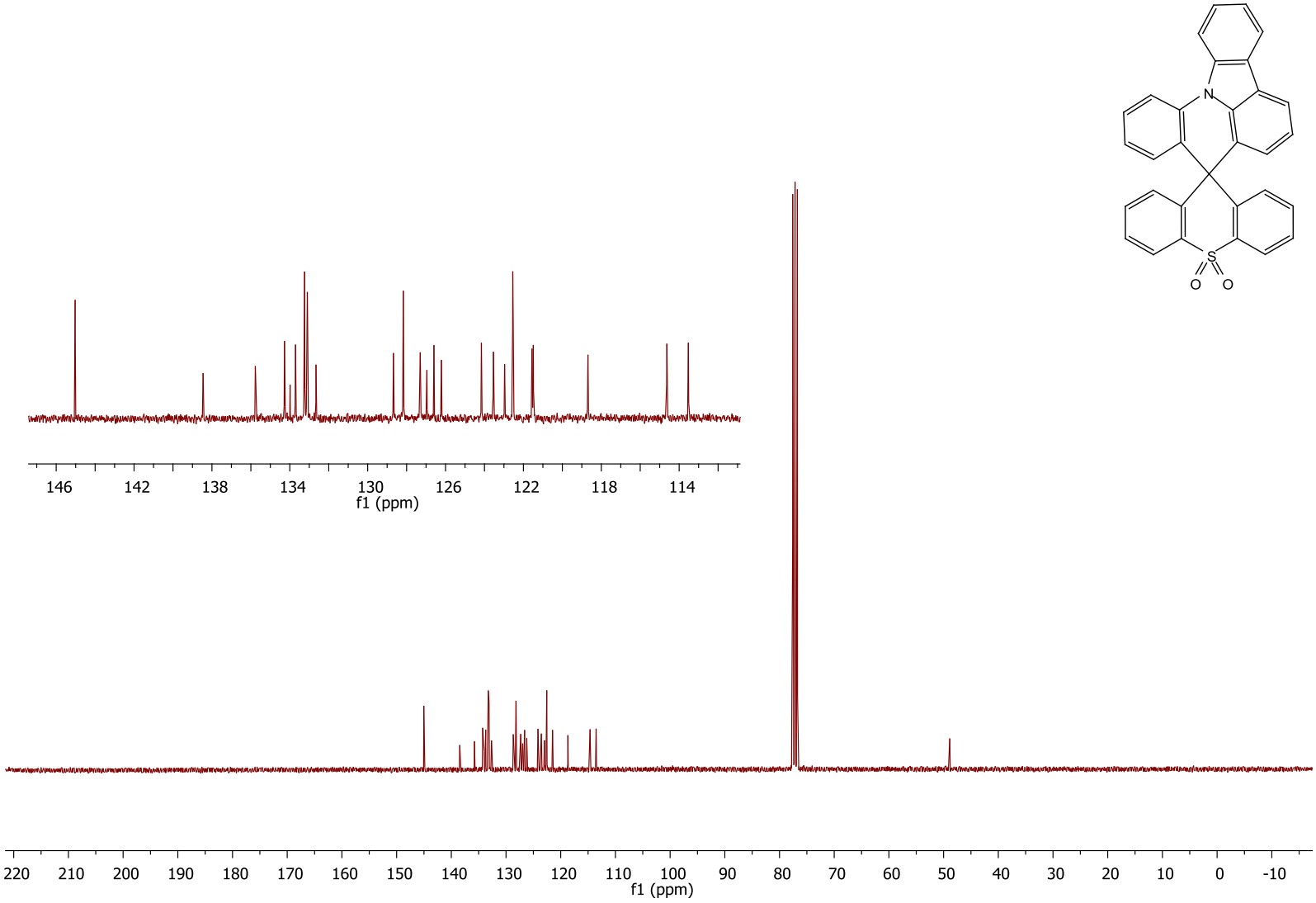

DEPT-**(SIA-TXO$_2$)**-$CDCl_3$

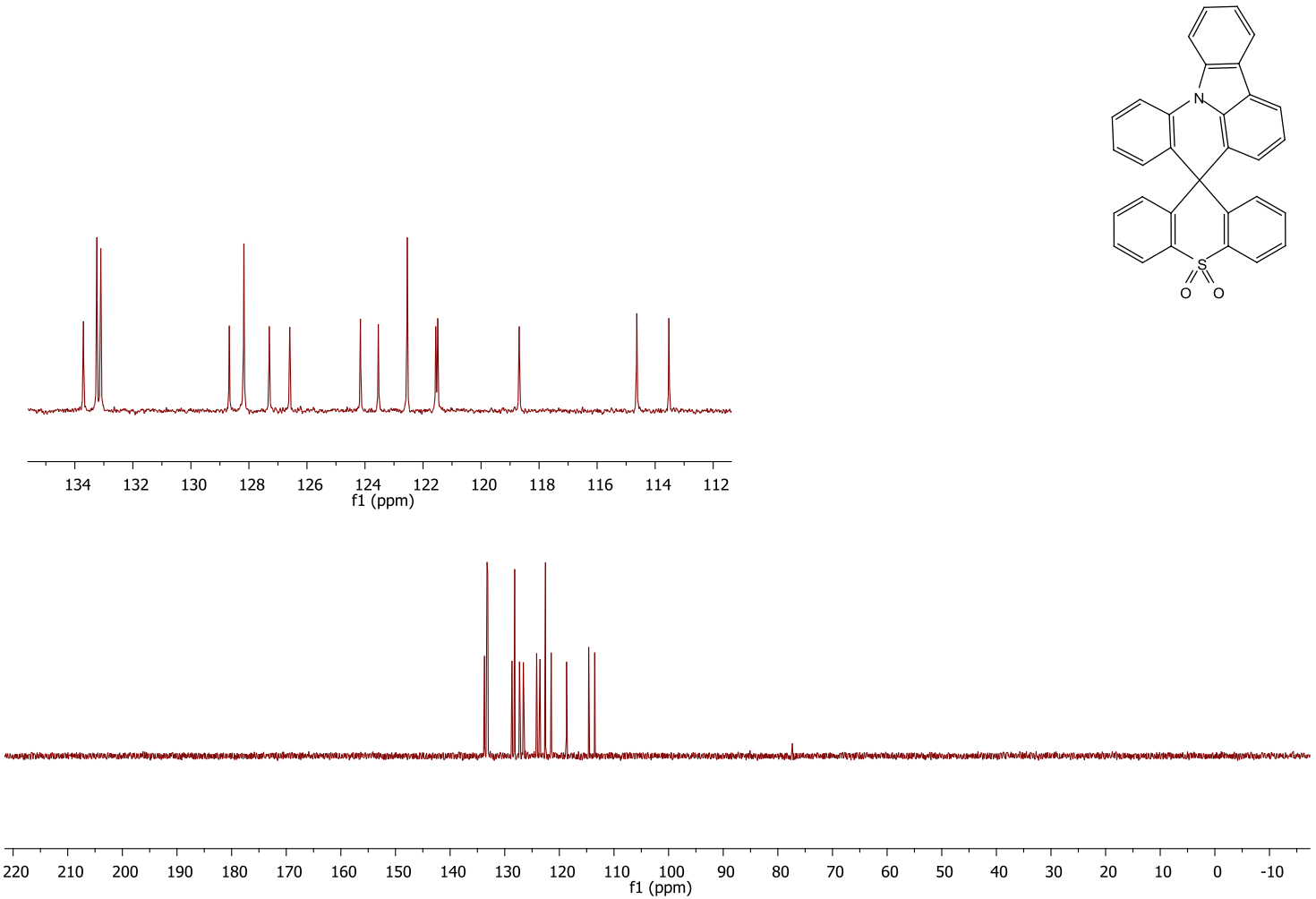

2D NMR STUDIES

COSY-**(SIA-F)**-CD_2Cl_2

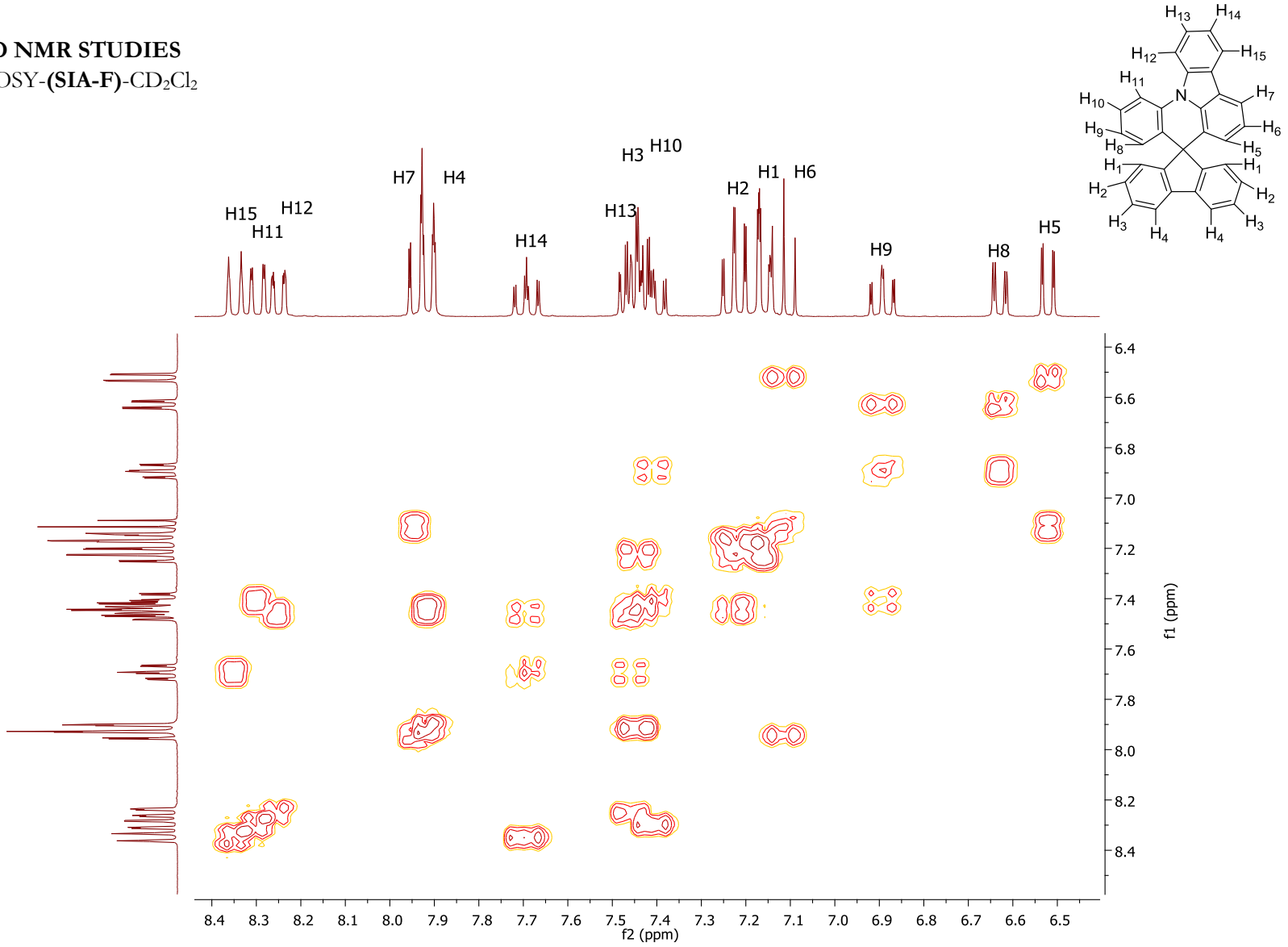

HSQC-**(SIA-F)**-CD_2Cl_2

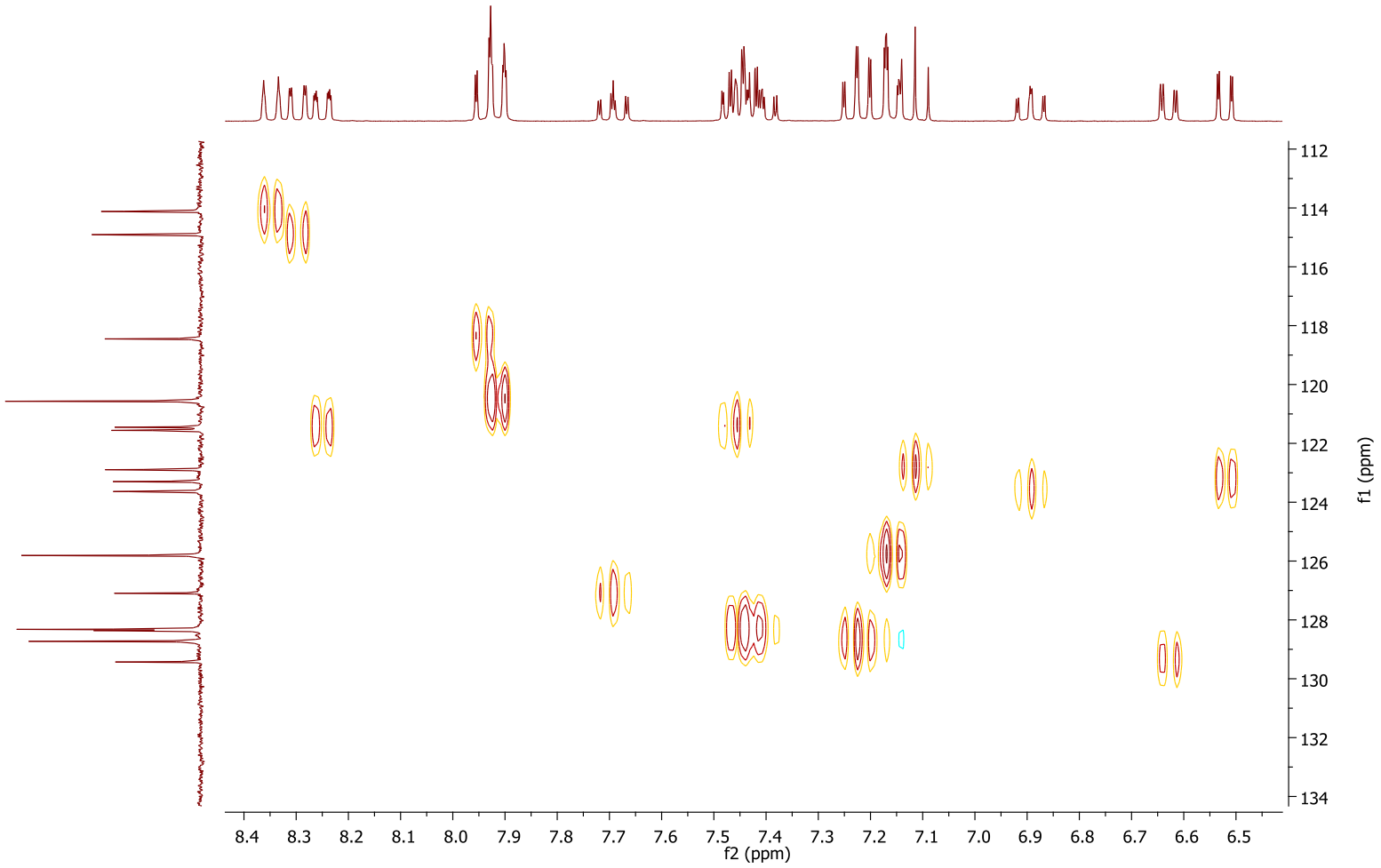

HMBC-**(SIA-F)**-CD_2Cl_2

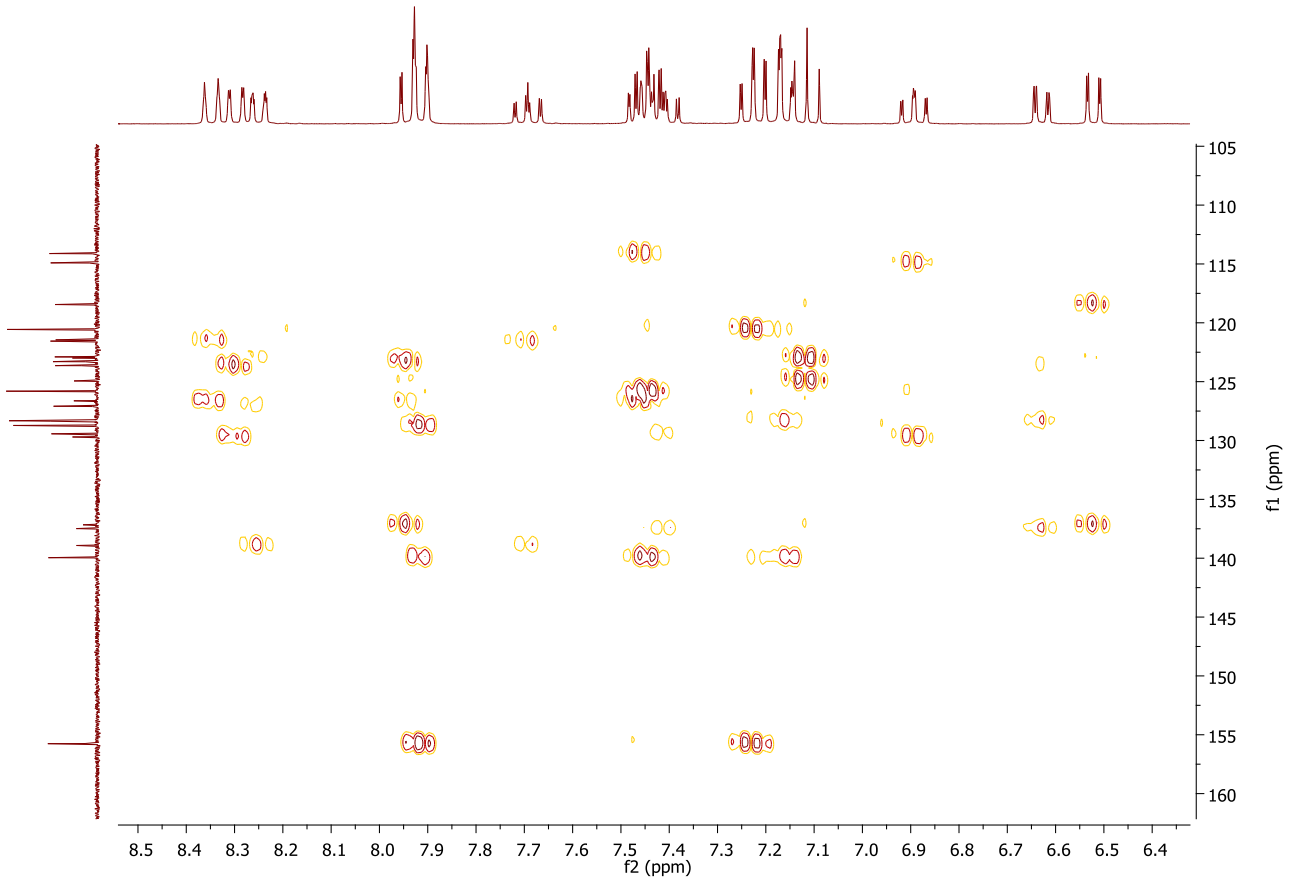

COSY-**(SIA-DAF)**-CD_2Cl_2

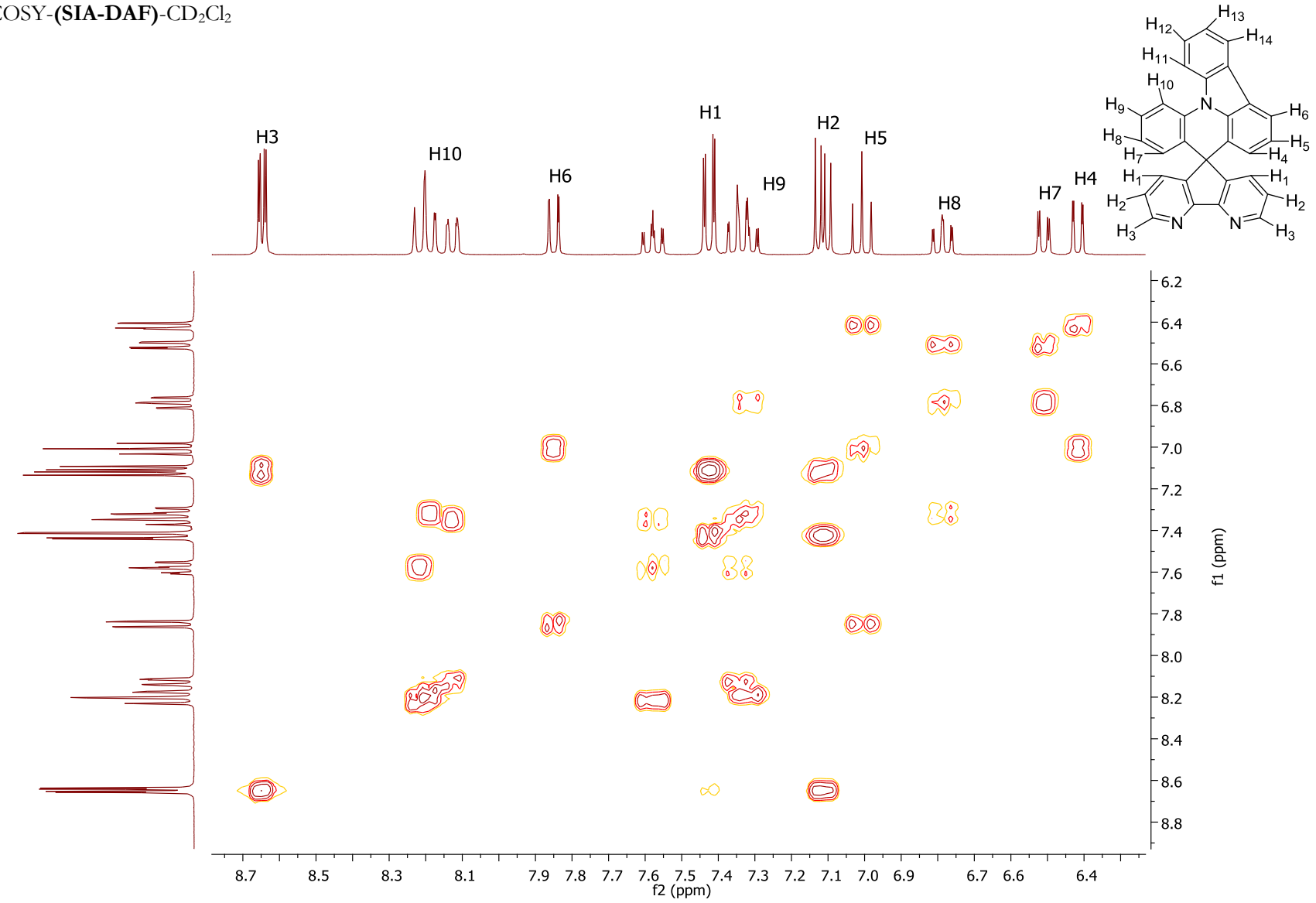

HSQC-**(SIA-DAF)**-CD_2Cl_2

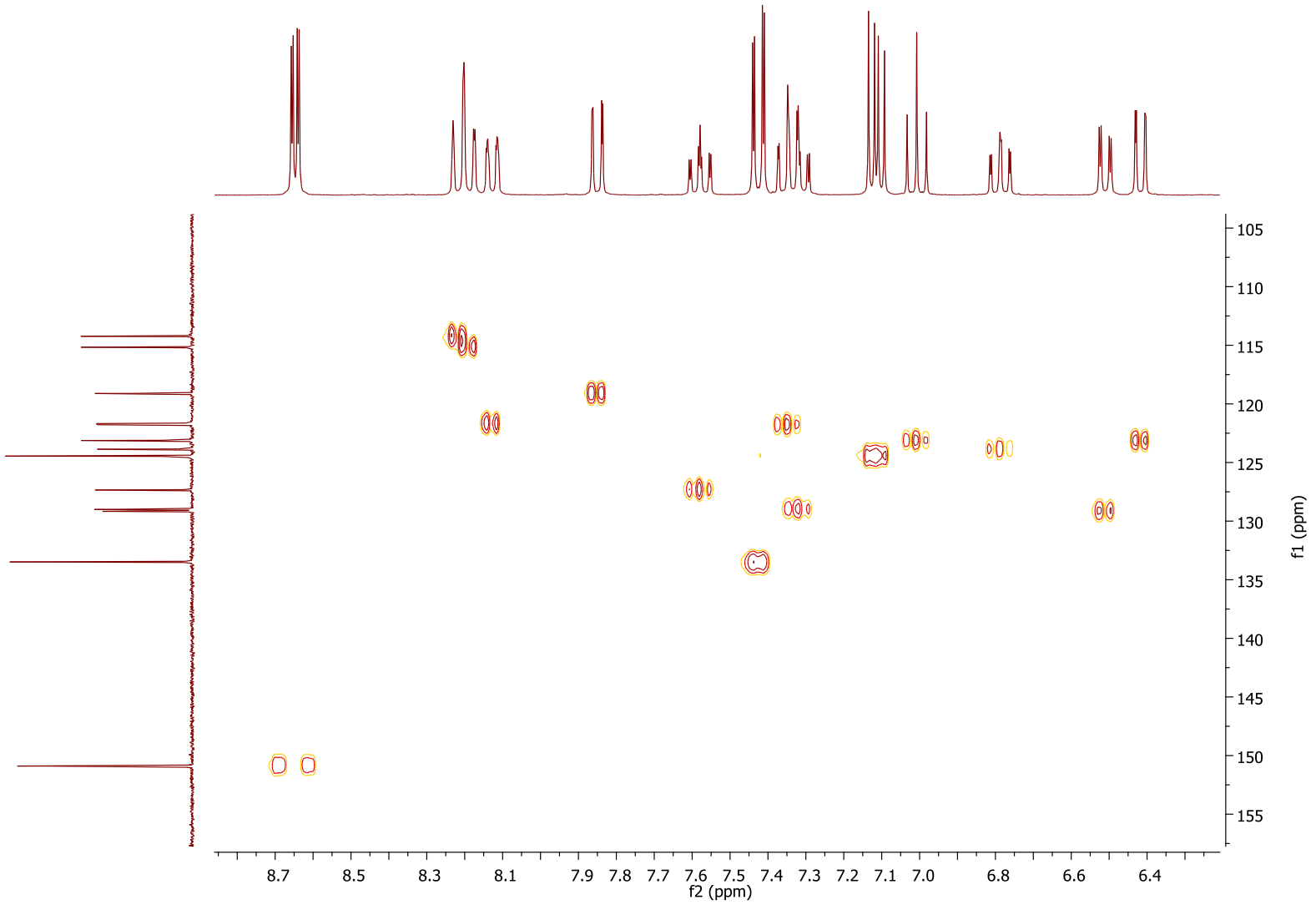

HMBC-**(SIA-DAF)**-CD_2Cl_2

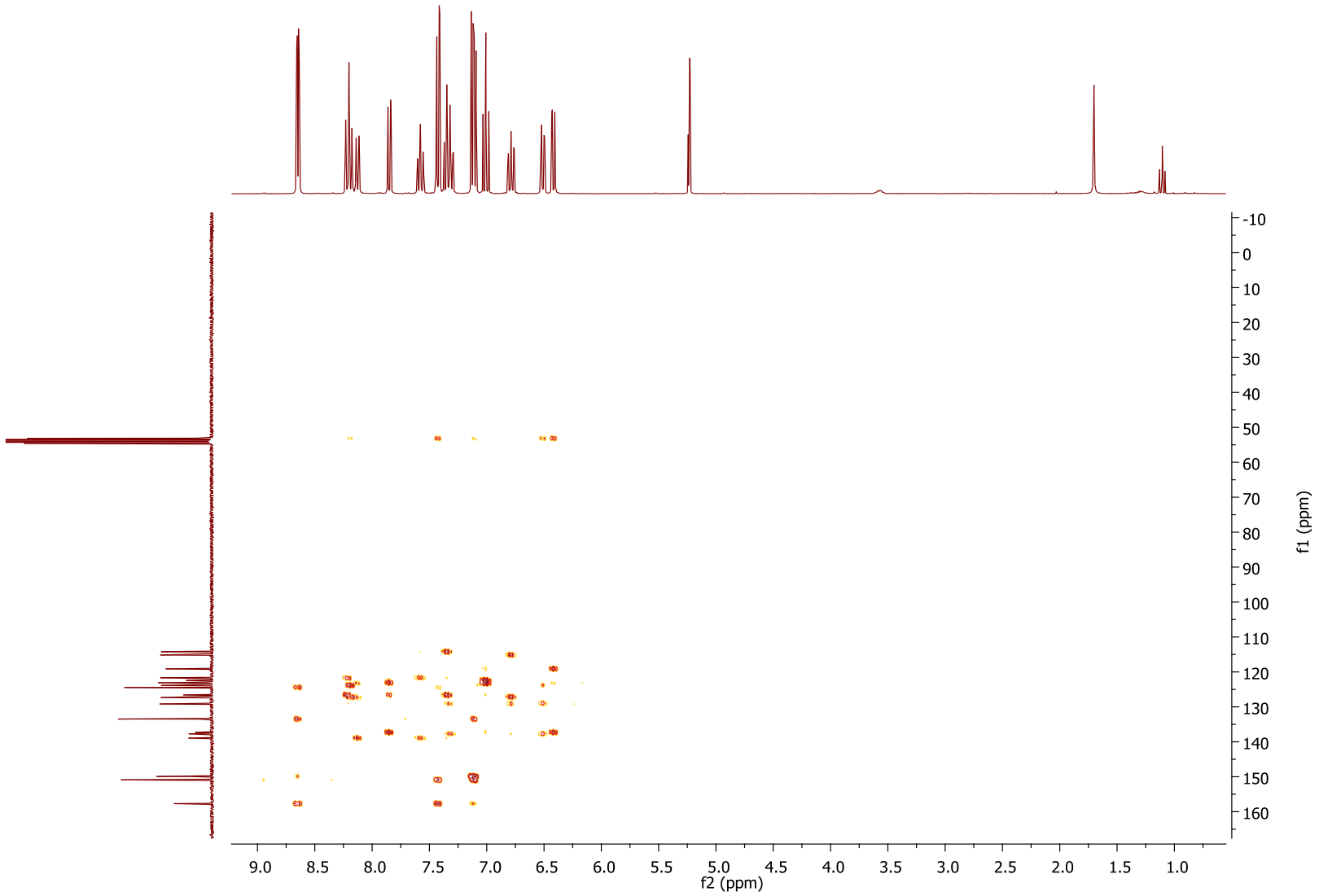

COSY-**(SIA-TXO$_2$)**-$CDCl_3$

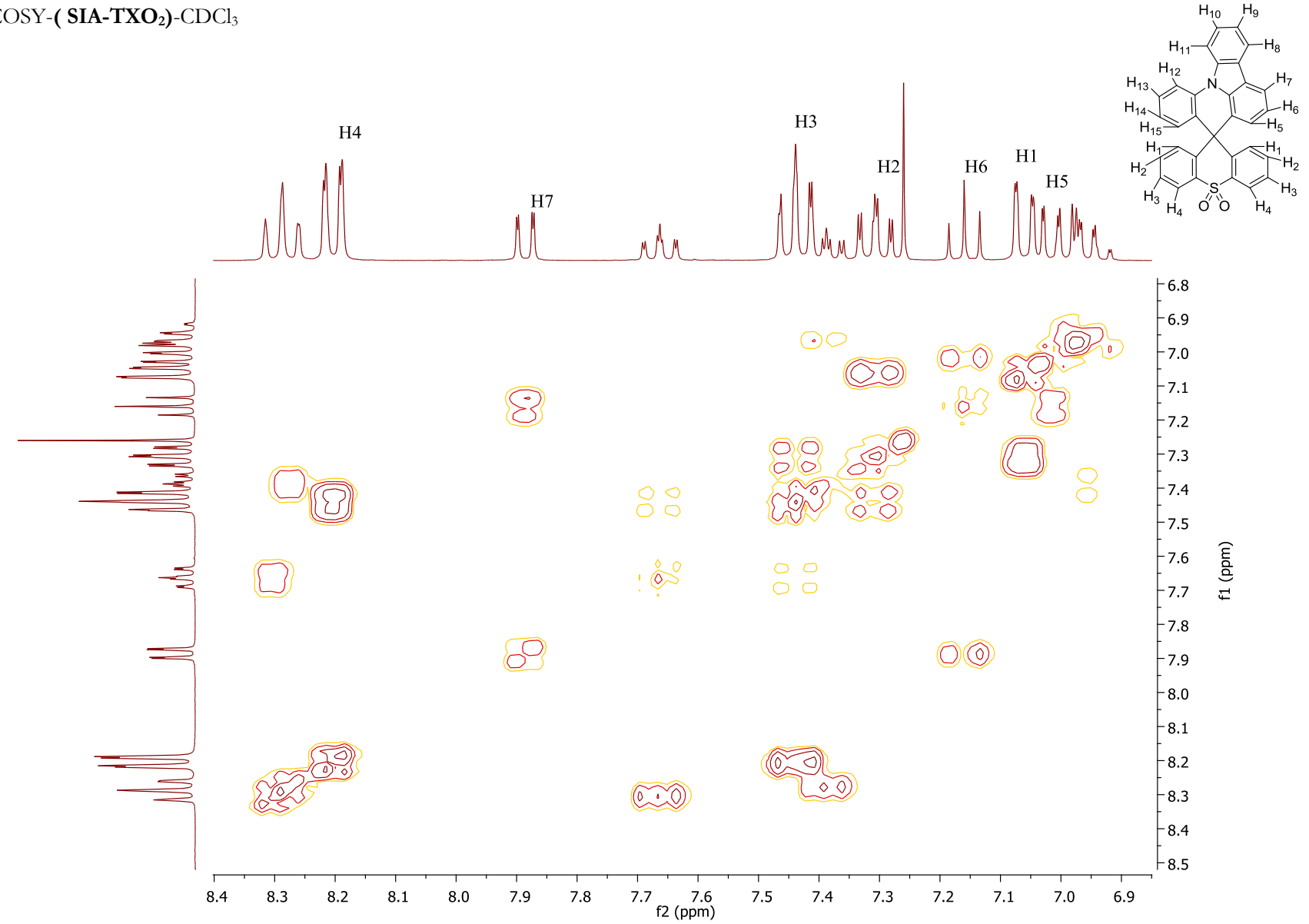

HSQC-(**SIA-TXO$_2$**)-$CDCl_3$

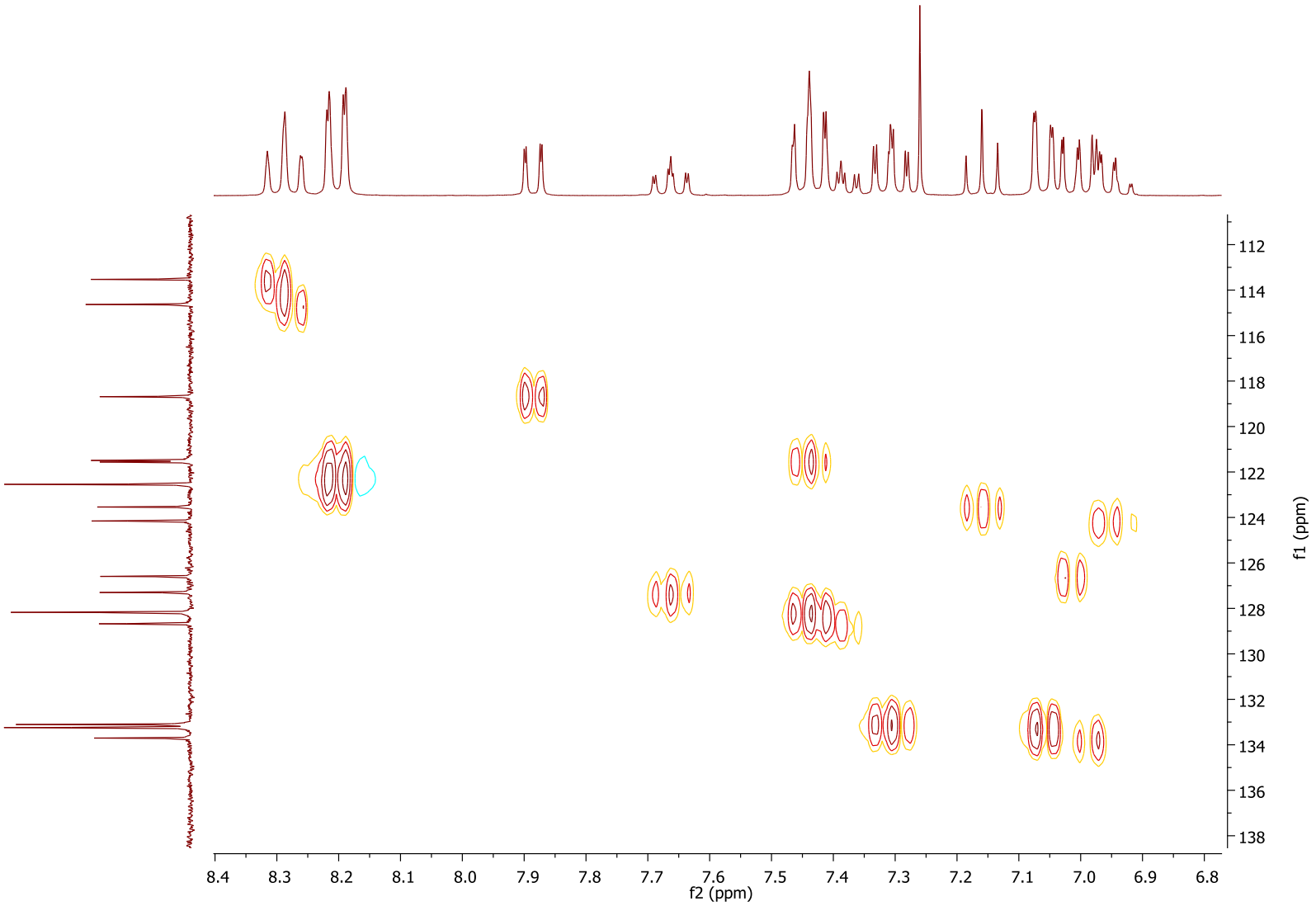

HMBC-(**SIA-TXO$_2$**)-$CDCl_3$

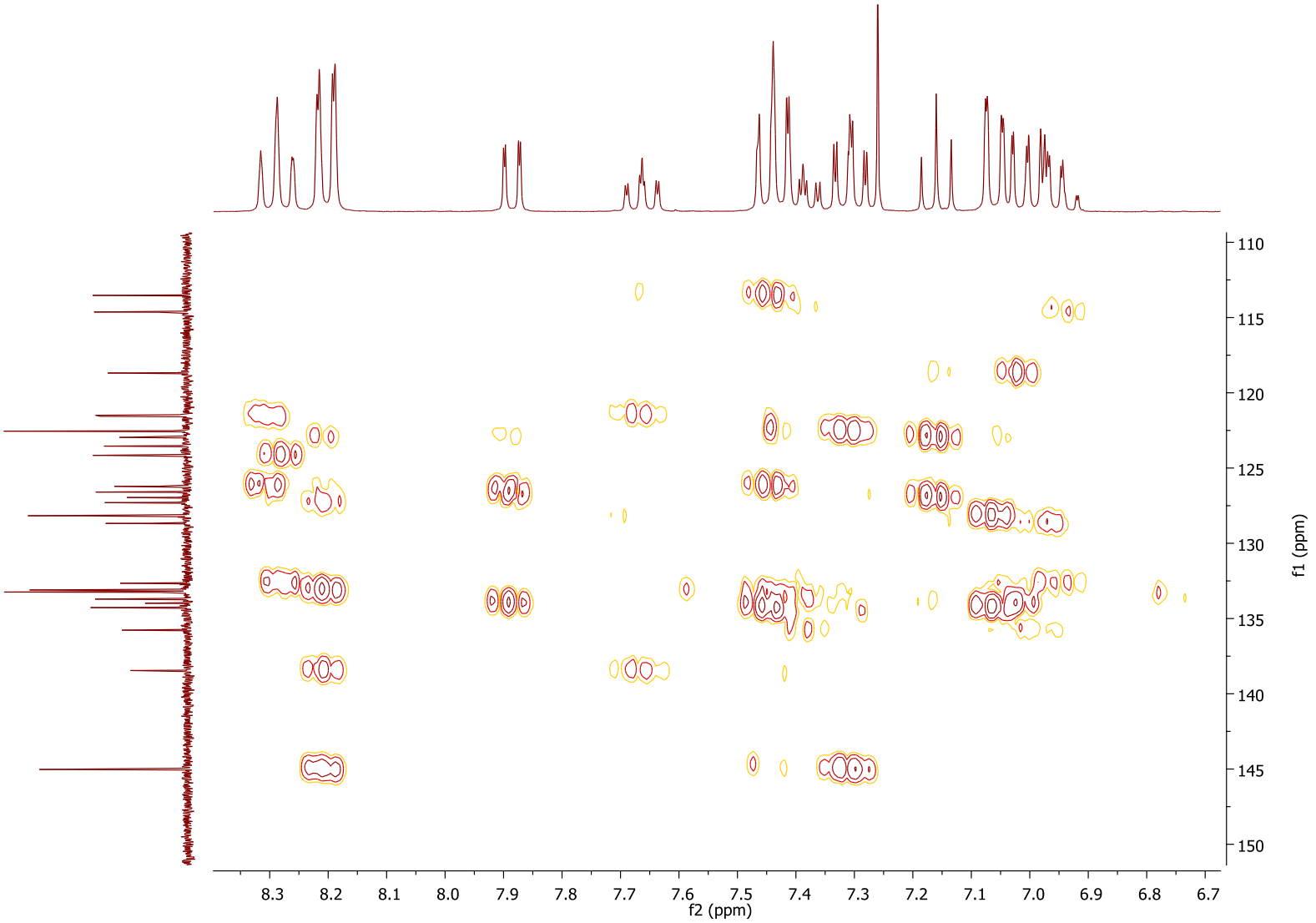

1. A. Altomare, M. C. Burla, M. Camalli, G. Cascarano, C. Giacovazzo, A. Guagliardi, A. G. G. Moliterni, G. Polidori and R. Spagna, *J. Appl. Cryst.*, 1999, 32, 115-119.
2. L. J. Farrugia, *J. Appl. Cryst.*, 2012, 45, 849-854.
3. E. Lippert, *Zeitschrift für Naturforschung*, 1955, 10, 541.
4. Y. Ooshika, *J. Phys. Soc. Jpn.*, 1954, 9, 594.
5. N. Mataga, Y. Kaifu and M. Koizumi, *Bull. Chem. Soc. Jpn.*, 1956, 29, 465-470.
6. A. P. Kulkarni, C. J. Tonzola, A. Babel and S. A. Jenekhe, *Chem. Mater.*, 2004, 16, 4556-4573.
7. P. Hohenberg and W. Kohn, *Phys. Rev.*, 1964, 136, B864-B871.
8. J.-L. Calais, *Int. J. Quantum Chem.*, 1993, 47, 101.
9. A. D. Becke, *Phys. Rev.*, 1988, 38, 3098-3100.
10. A. D. Becke, *J. Chem. Phys.*, 1993, 98, 1372-1377.
11. A. D. Becke, *J. Chem. Phys.*, 1993, 98, 5648-5652.
12. C. Lee, W. Yang and R. G. Parr, *Phys. Rev. B*, 1988, 37, 785-789.
13. M. J. Frisch, G. W. Trucks, H. B. Schlegel, G. E. Scuseria, M. A. Robb, J. R. Cheeseman, R. Scalmani, G. Barone, B. Mennucci, G. A. Petersson, H. Nakatsuji, M. Caricato, X. Li, H. P. Hratchian, A. F. Izmaylov, J. Bloino, G. Zheng, J. L. Sonnenberg, M. Hada, M. Ehara, K. Toyota, R. Fukuda, J. Hasegawa, M. Ishida, T. Nakajima, Y. Honda, O. Kitao, H. Nakai, T. Vreven, J. A. J. Montgomery, J. E. Peralta, F. Ogliaro, M. Bearpark, J. J. Heyd, E. Brother, K. N. Kudin, V. N. Staroverov, R. Kobayashi, J. Normand, K. Raghavachari, A. Rendell, J. C. Burant, S. S. Iyengar, J. Tomasi, M. Cossi, N. Rega, N. J. Millam, M. Klene, J. E. Knox, J. B. Cross, V. Bakken, C. Adamo, J. Jaramillo, R. Gomperts, R. E. Stratmann, O. C. Yazyev, A. J. Austin, R. Cammi, C. Pomelli, J. W. Ochterski, R. L. Martin, K. Morokuma, V. G. Zakrzewski, G. A. Voth, P. Salvador, J. J. Dannenberg, S. Dapprich, A. D. Daniels, O. Farkas, J. B. Foresman, J. V. Ortiz, J. Cioslowski and D. J. Fox, *Gaussian 09, version B01, Gaussian, Inc., Wallingford, CT, 2009.*, 2009.